Photochemical Hydrogen Atom Transfer Reactions of Binuclear Platinum Complexes

Thesis by

Erica Lyn Harvey

In Partial Fulfillment of the Requirements

for the Degree of

Doctor of Philosophy

California Institute of Technology

Pasadena, California

1990

(Submitted August 23, 1989)

for Bob

the Harveys

and Ho and Lu,

who put up with me, too

Acknowledgments

Many people have helped me during the last four years. At the top of the list is Bob Sweeney, who has engaged in innumerable hours of vibrant scientific (and decidedly unscientific) discussion, fed me, lifted me up when I was ready to quit, and collaborated intimately with me upon more than one occasion. I thank Harry Gray for many meals, stories and new types of alcohol, for insightful comments on my research, for enthusiasm about teaching, and most of all for allowing me to confront my own demons. Harry is also, without doubt, the most complex system I studied at Caltech!

Mike Hopkins helped lure me to Caltech, and Al Stiegman began the project that I pursued here. For helpful, fun discussions about my work I thank Vinny Miskowski, Tony Vlcek, Nick Turro, Andy Myers, Mitchio Okumura, and John Bercaw. The informal inorganic/organometallic seminars were another good source of ideas. I've collaborated with a number of people about NMR: James Yesinowski, Paul Haake (although I never met him!), Dave Wheeler, Dom McGrath, Doug Meinhardt, Eric Anslyn, Paula Watnick, and Tracy Handel. Max Roundhill graciously sent me a copy of an NMR simulation program. Seung-Koo Shin has been very helpful in discussions about bond strengths, and Paul Bernard helped with the low-temperature electrochemistry. I'm forever in debt to Sig, Gabor, Tony, Delmer, Guy, Ray, Jim, Paul, Jess, Tom, Art, and especially Tom Dunn and John Sibert for helping me build vac lines and lamp housings and lecture-bottle cases, keep the hazardous wastes down, fix scary electronic things, and maintain some perspective. Pat, Virginia, Sandra, Beth, Fran, Jas, Chris, Bill, Dan, Don, Louie, Emily, Margaret, Alice, and Connie have also been unfailingly helpful and friendly.

The group: Mike Albin got me out of many computer difficulties, and made me feel like a part of the group when I joined. I thank Catherine for making the Birthday list an ongoing tradition. Miriam showed me how to do almost everything, with great patience, and was a constant friendly presence. Pierre Harvey, Tad Fox and Dave Smith

were also prominent features on my grad school landscape. In the last two years, I have drawn great strength and inspiration from Cindy St. Clair. Ramy, Holden and John have each been sources of great help and also some frustration; I value highly the lessons that they have taught me. I have enjoyed watching the group evolve; Mark and Wayne helped usher in a very pleasant, low-key period that has been very productive. Like Miriam and Janet before me, I pass the torch of being the only photogroup woman on to Julia; I'm sure it will be a lighter weight to bear when Bubba-kitty arrives!

I've had the pleasure of interacting with a large segment of the Caltech community outside my research group. TA'ing introduced me to a collection of very individualistic, fun undergrads; I'd like to thank my Chem 1, Chem 3 and Chem 4 classes for giving me an outlet for the teaching itch, and listening with patience to the weirder ideas. Lisa Giaimo kept me in touch with undergrad life here, and contributed scientifically to this work as a Summer Undergraduate Research Fellow in 1987 (i.e., a serf!). The many friends I have made through the GSC, Affirmative Action Committee, OWC, discussion groups and the WorldWork groups (ne the Space Weapons Study Group) have accompanied me in some of the most embittering and also some of the most uplifting experiences I have known. Also instrumental (hehheh) in keeping me from becoming too single-minded here were the Folk Music Society, recorder groups and the CIT jazz band!

I've had strong support from Wellesley faculty and friends, and several people who are both at the same time. Lots of people from home have also kept an eye on me, especially Lori and Barry. Mim, Dece, Todd and Kurt have watched my progress in the last four years with a mixture of amusement, dismay, and I think sometimes pride; they have been a wonderful touchstone. I give special thanks, finally, to my great Aunt Zudie, who got me through the last few weeks:

Mile by mile, life's a trial

But inch by inch, life's a cinch.

Abstract

This thesis focuses on hydrogen atom (H-atom) transfer reactions of the lowest electronic excited state of the d^8 dimer $[Pt_2(P_2O_5H_2)_4]^{4-}$ (the ground state is abbreviated Pt_2; the lowest excited state is a long-lived triplet, abbreviated $^3Pt_2^*$). Factors that influence initial rates of reaction of the excited state with alcohol and hydrocarbon H-atom donors are examined in Chapter 2. Observation of a large kinetic deuterium isotope effect ($k_H/k_D=4$) for phosphorescence quenching by α-secphenethyl alcohol verifies the importance of bond strength in determining reaction rates. A plot of H-atom abstraction rates versus C-H bond strengths reveals that bond strength is not the sole determinant of abstraction rate, however. Faster rates are observed when an α-hydroxy functionality is present, and the size of the substrate also influences abstraction rates. Chapter 3 features characterization of a diplatinum dihydride complex (Pt_2H_2) that acts as a key intermediate in H-atom transfer reactions. $^3Pt_2^*$ reacts with hydrogen-atom donors to give a complex characterized by strong absorption at 314 nm; NMR (^1H and ^{31}P) and IR spectroscopic studies show that the complex is an axial dihydride (Pt_2H_2). Reactions of Pt_2H_2 include photochemical release of H_2, rapid thermal reduction of O_2, and thermal reduction of HCl to H_2. Chapter 4 describes synthesis and characterization of a derivative of Pt_2 modified by substitution of electron-withdrawing BF_2^+ groups for ligand H^+. The new compound exhibits photophysical properties (phosphorescence lifetime, quantum yield, absorption and emission maxima) virtually identical with those of $^3Pt_2^*$, but dramatically shifted ground-state electrochemical properties (peak potential for oxidation shifted +750 mV). Comparisons of thermal reactivity (preparation of axial dihalide and dihydride complexes) and photochemical reactivity (reductive quenching and H-atom transfer quenching) of the two platinum dimers, detailed in Chapter 5, provide further insight into the factors influencing H-atom transfer in binuclear d^8-d^8 compounds.

Table of Contents

List of Figures

Chapter 1

Chapter 2

Chapter 4

Chapter 5

List of Tables

Chapter 2

Chapter 4

Chapter 5

Chapter 1. Background on Tetrakis(pyrophosphito(2-))diplatinate(II) ("Pt_2")

Introduction

Startlingly intense green luminescence from a synthetic side-product caught the attention of Max Roundhill's group in 1977.[1] The emissive species was first thought to be a monomer reported by a Russian scientist twenty years earlier,[2, 3] but solution of the crystal structure in 1980 revealed the complex to be a platinum dimer with four bridging pyrophosphito ligands.[4, 5] This robust, totally inorganic complex has since been the subject of more than 70 papers! The recent publication of two review articles[6, 7] makes an extensive background section here largely unnecessary; however, information relevant to the present work is presented.

Synthesis and Structure:

Heating to dryness an aqueous solution of potassium tetrachloroplatinate and excess phosphorous acid produces $K_4[Pt_2(P_2O_5H_2)_4]$ (abbreviated K_4Pt_2) in approximately 90% crude yield.[8] A reasonable (but unverified) stoichiometric equation for formation of K_4Pt_2 is shown.

$$2\ K_2PtCl_4 + 8\ H_3PO_3 \xrightarrow{\Delta} K_4[Pt_2(P_2O_5H_2)_4] + 4\ H_2O + 8\ HCl$$

As the potassium, barium or sodium salt, the chartreuse tetraanion dissolves only in H_2O. Metathesis to bis(triphenylphosphine)nitrogen(1+) (PPN), tetra-*n*-butylammonium (TBA) or tetraphenylarsonium (TPA) salts extends solubility to

organic solvents including acetonitrile, dichloromethane, methanol, ethanol, and acetone. The complex is a di-acid in aqueous solution, with pK_{a1}= 2 and pK_{a2}= 7.[9] Degradation occurs in basic media, but the complex is stable in 1 M $HClO_4$.[10]

The structure of $[Pt_2(P_2O_5H_2)_4]^{4-}$ (abbreviated Pt_2) can be visualized as two d^8 ML_4 fragments tied together in a face-to-face, rigorously eclipsed fashion along the z axis. Two idealized views of the complex are shown in Figure 1.1. Four μ-pyrophosphito ligands, viewable as condensed, doubly deprotonated dimers of phosphorous acid, bind the two platinum atoms through eight phosphorous atoms. Sometimes referred to as a "lantern," the essentially D_{4h} structure results in an unoccupied exterior axial site on each platinum atom. The common name "platinum pop" arises from the P-O-P bridging linkages of the ligands. Formal assignment of a 2- charge to each pyrophosphito ligand results in two Pt(II) centers.

A long (2.925 Å) Pt-Pt bond length reflects the lack of a formal bond between the two metal centers (*vide infra*). Phosphorous-oxygen bond lengths range from 1.62 Å for the bridging oxygen to 1.58 and 1.52 Å for the terminal oxygens.[11] Observation of two sets of terminal P-O bond lengths suggests that descriptive resonance structures can be drawn with alternating P=O and POH moieties. The 8 ligand hydrogen atoms have not been located by x-ray or neutron diffraction, but are thought to occupy asymmetric bridging positions between the terminal oxygen atoms on adjacent ligands (O(H)·····O distance = 2.505 Å).[11] The resultant fluted ring of H-bonded oxygen atoms around each axial site probably provides a key component of the stability of the complex.

Molecular Orbital Diagram:

The molecular orbital diagram for the class of face-to-face d^8 dimers with π-acceptor ligands was first formulated in 1975 by Mann, Gordon and Gray.[12] The general approach consists of mixing the orbitals of two identical monomeric square-

Figure 1.1 Two views of $[Pt_2(P_2O_5H_2)_4]^{4-}$ (eight ligand protons not shown)

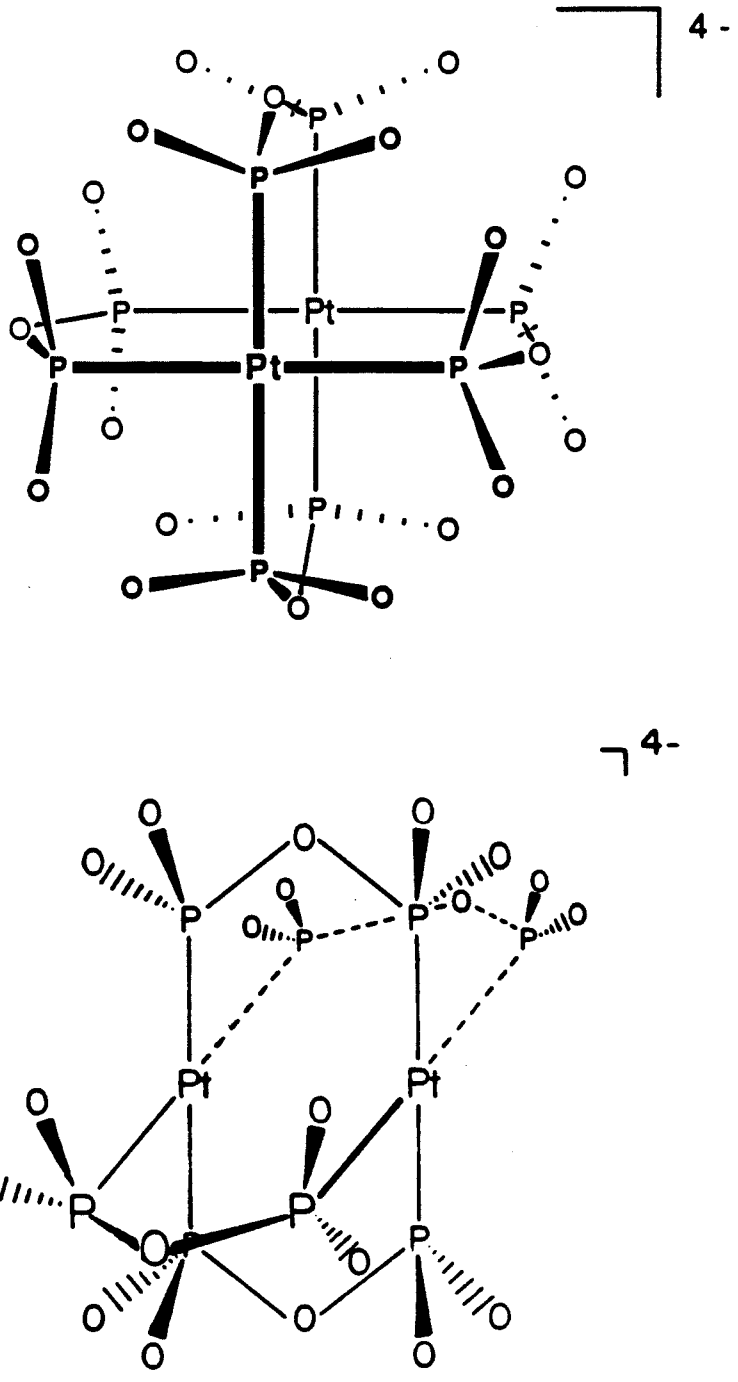

planar fragments along the z-axis (Figure 1.2). The building block, *monomeric* square-planar molecular orbital diagram, shown at the left in Figure 1.2, is meant to be illustrative rather than exact.[13] The orbitals labelled (n+1)s, px, and py, and (n) $d_{x^2-y^2}$ are actually high-energy, antibonding molecular orbitals from sigma combination with the ligands. The torus on (n)d_{z^2} also causes this orbital to be raised somewhat in energy upon combination with the ligands. The (n)d_{xy} and $d_{xz, yz}$ orbitals possess the wrong symmetry to form sigma bonds with the ligands, but they are lowered in energy by π-interactions with empty orbitals in the π-acceptor ligands. Since the degree of π bonding is unknown, the π-symmetry orbitals are arbitrarily placed at slightly bonding levels in Figure 1.2. Similarly, the (n+1)p_z orbital is arbitrarily placed near the $d_{x^2-y^2}$ orbital. Luckily, such uncertainties in the details of metal-ligand bonding do not significantly impact understanding of excited-state chemistry in these dimers. Metal-ligand interactions affect the orbitals involved in higher excited states, but these states effectively decay to the lowest, metal-centered singlet and triplet states on the timescales studied in this work.

The lowest-energy electronic transitions of the dimeric complex are well described by sigma interactions of (n)d_{z^2} and (n+1)p_z orbitals between the two metals. (The letter n denotes the principal quantum number of the orbital.) As shown in Figure 1.3, both types of orbitals have lobes pointing directly into the center of the dimer at the equivalent orbital on the other side; the combination of exact energy match and good spatial overlap leads to a strong interaction. The molecular orbitals formed include a pair of sausage-shaped bonding MO's referred to as dσ and pσ, and a corresponding pair of antibonding dσ^* and pσ^* MO's that contain a node in the middle of the sausage (between the two metals). Orbital occupancy through dσ^* produces a formal metal-metal bond order of zero in the ground state; secondary mixing of dσ with pσ is used to explain the existence of some experimentally observed net bonding stabilization.

Figure 1.2 Molecular orbital diagram for a d^8-d^8 dimer

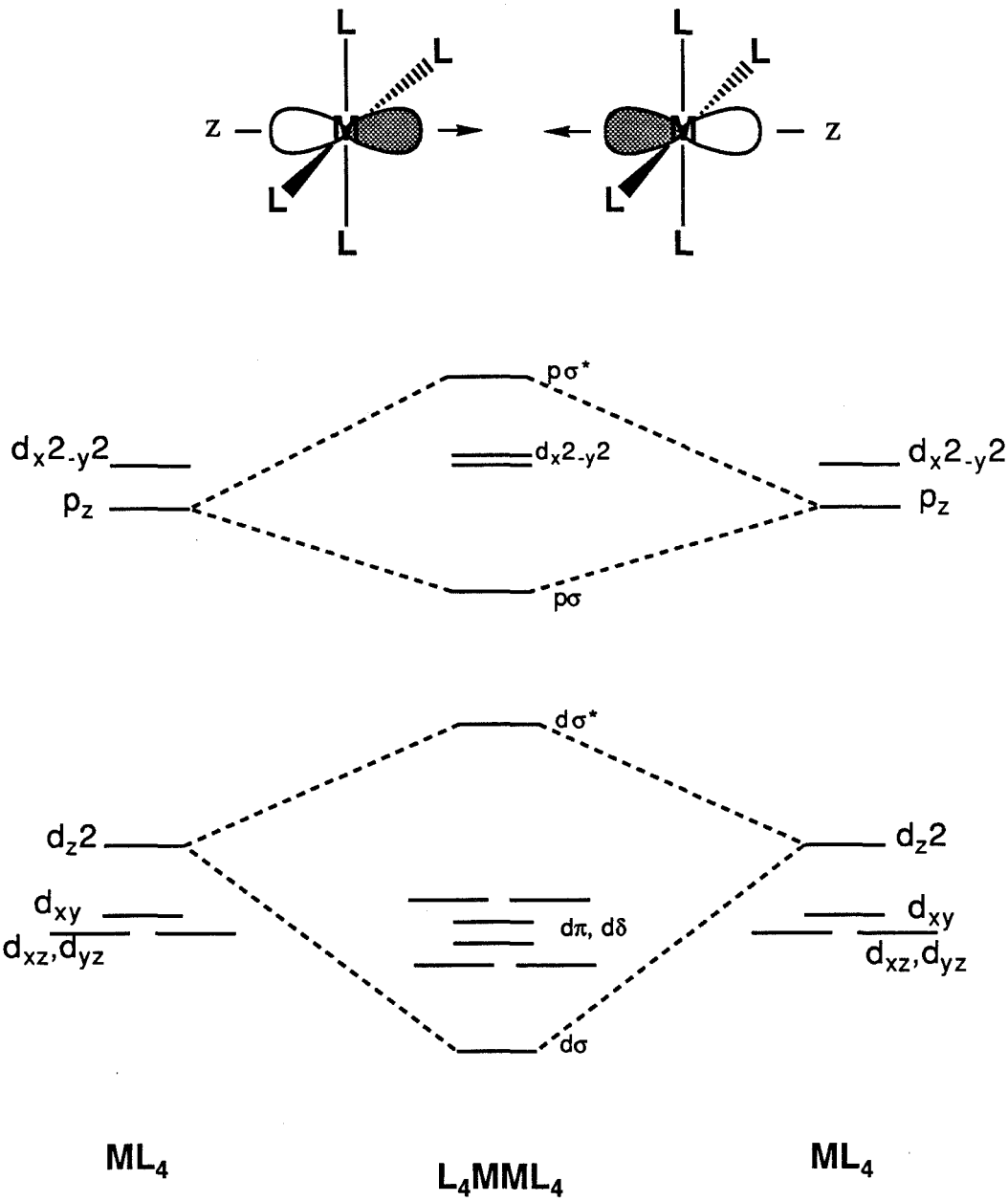

Figure 1.3 Orbitals involved in the lowest electronic transitions of a d^8-d^8 dimer

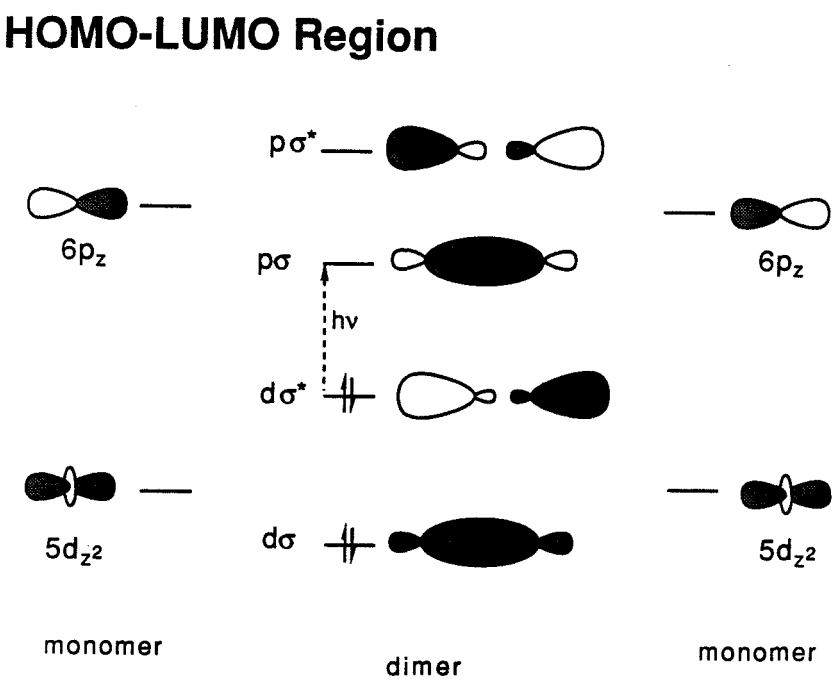

The MO diagram for Pt_2 can be built from a face-to-face interaction of two square-planar ML_4 fragments. The combination of two d^8 Pt(II)'s results in a $p\sigma \leftarrow d\sigma^*$ HOMO-LUMO transition.

Note that the A_{2u} excited state thus created contains a single electron in the $p\sigma$ orbital localized between the Pt centers and in the $d\sigma^*$ orbital pointing out along the z axis.

Basic Photophysics:

The electronic absorption spectrum of the tetra-*n*-butylammonium (TBA) salt of Pt_2 in acetonitrile (Figure 1.4) exhibits an intense band at 372 nm (ε=33,400)and a weak one at 453 nm (ε=155), assigned to the singlet and triplet $d\sigma^*p\sigma$ absorptions $^1A_{1g} \rightarrow {}^1A_{2u}$ and $^1A_{1g} \rightarrow {}^3A_{2u}$, respectively.[14, 15] Excitation into the 372 nm band of a degassed acetonitrile solution of Pt_2 via 355 nm laser light (Nd:YAG) produces long-lived (τ_o=10 μs, λ_{max}=518 nm) green phosphorescence.[16] Fluorescence has also been characterized in the potassium salt in aqueous solution (τ_o<40 ps; λ_{max}= 407 nm).[6] Polarized electronic absorption experiments using TBA_4Pt_2 allowed assignment of the higher-energy spectroscopic transitions at 315, 285, and 246 nm as triplet $d\sigma^* \rightarrow d_{x^2-y^2}$, singlet $d\sigma^* \rightarrow d_{x^2-y^2}$, and triplet $d_{xz,yz} \rightarrow p\sigma$, respectively.[15]

The lowest-energy singlet and triplet electronic transitions promote an electron from a Pt-Pt antibonding $d\sigma^*$ orbital to a bonding $p\sigma$ orbital and formally create a metal-metal bond in the excited state. Comparison of metal-metal vibrational progressions in the low-temperature absorption and emission spectra indicates that the Pt-Pt interaction in the excited state is much stronger than in the ground state,[17] and resonance Raman experiments support this observation.[18] The excited-state Pt-Pt distance is estimated as 2.75 Å, a shrinkage of 0.2 Å from the ground state![19]

Pt_2 is a remarkable chromophore. The phosphorescence lifetime remains essentially constant at 10 μs as the environment is varied from water/ethylene glycol glass at 77 K[20] to room temperature or above in a number of solvents: ethanol, methanol, acetonitrile, water, acid, dimethylformamide, and ethylene glycol. Absorption and emission maxima shift up to 8 nm in different solvents.[21] The bright green phosphorescence emission is observed even in dim roomlight and sunlight; the phosphorescence quantum yield is an unprecedented 50%![10] The light energy added to the compound in the triplet excited state is estimated at 2.5 eV (58 kcal/mol) from the

Figure 1.4 Electronic absorption and emission spectra of $K_4[Pt_2(P_2O_5H_2)_4]$ (from Ref.16)

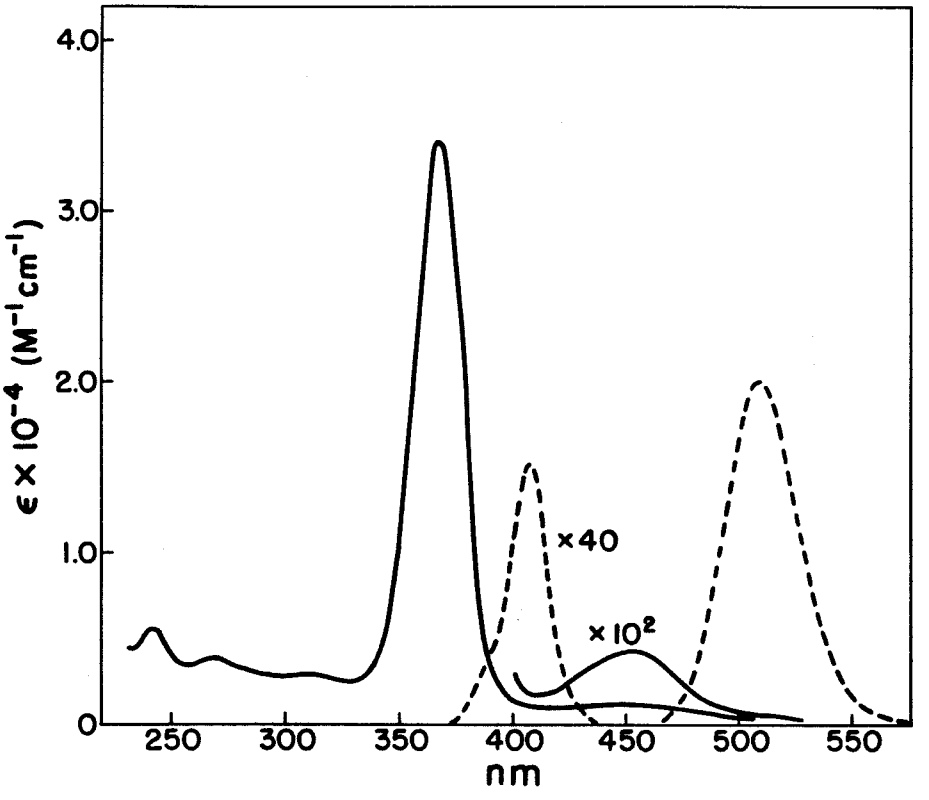

zero-zero spectroscopic transition. Long-term irradiations in degassed acetonitrile do not lead to decomposition of the complex, presumably because the excited state possesses increased bonding. The combination of high energy and long lifetime of the triplet excited state make Pt_2 an attractive candidate for bimolecular photochemical reactions, and a wide range of reactivity has, in fact, been observed from the excited state.

Energy Transfer and Related Quenching Processes:

Substrates with triplet energies lower than that of Pt_2 quench the triplet emission intensity and lifetime of $^3Pt_2^*$.[21] An energy transfer mechanism has been implicated in the isomerization of stilbenes by $^3Pt_2^*$.[22, 23] Terminal olefins are thought to quench the excited state by a combination of energy transfer and addition to the axial site to form a diradical species.[24]

Electron Transfer:

Photochemical promotion of an electron from the highest occupied molecular orbital (HOMO) to the lowest unoccupied molecular orbital (LUMO) generates an excited species that is more powerful as a reductant and as an oxidant than it was in the ground state.[25] (Figure 1.5) The reducing power of the excited state (the excited state's ability to be oxidized) is determined by the energy of the electron that has been promoted from the HOMO to the LUMO. Oxidation of the ground state of a molecule involves removing an electron from the HOMO of the complex. Photochemical promotion of the electron to the LUMO should make the electron easier to remove by the amount of the spectroscopic transition. Similarly, the excited state is a better oxidant than the ground state because putting an electron into the hole left by the promoted electron is more energetically favored (by the amount of the spectroscopic transition) than putting an electron into the LUMO of the ground state.

Figure 1.5 The role of photon energy in creating excited state oxidants and reductants

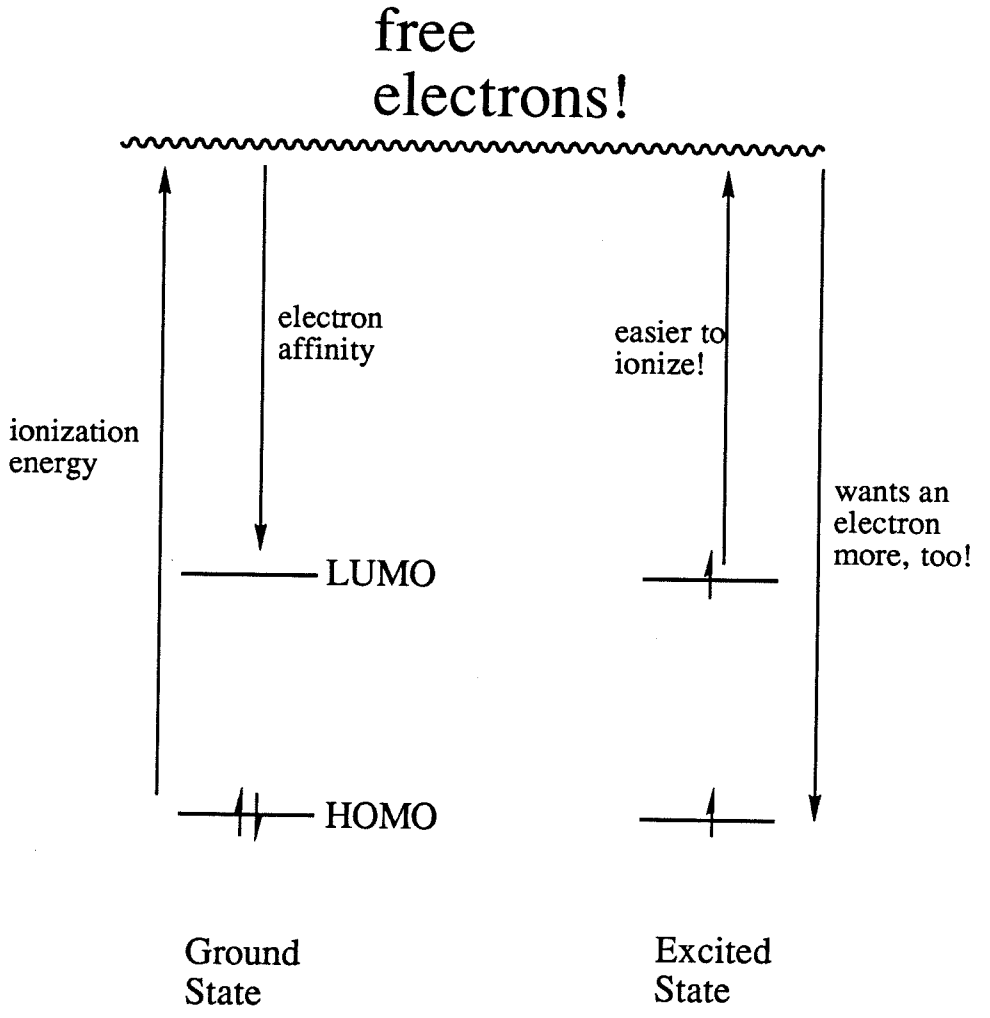

All the electrochemical potentials mentioned in this work refer to the reduction half-reaction between the two species involved. Thus, the ground-state oxidation potential of Pt_2, abbreviated $E^{o(3-/4-)}$, describes the half-reaction shown below.

$$Pt_2^{3-} + e^- \rightarrow Pt_2^{4-}$$

Using this convention, the thermodynamically favored direction for a given electron transfer can be quickly assessed using the Nernst equation, $\Delta G=-nFE^o$. All potentials given are referenced to the normal hydrogen electrode (NHE).

In the ideal situation, measurement of the ground-state reduction and oxidation potentials provides useful predictive information about excited-state redox potentials. Unfortunately, the ground-state electrochemical behavior of Pt_2 is considerably less than ideal. The ground-state electrochemical oxidation of Pt_2 in acetonitrile is irreversible ($E_p^{(3-/4-)} \sim +0.8$ V; E_p denotes the peak potential).[26, 27] Furthermore, while several authors have reported looking for it, the reduction of Pt_2 has not been observed in acetonitrile at any potential between +2.0 and -2.0eV.[26, 27, 28] The reduced Pt_2 species generated by pulse radiolysis in aqueous solution is reported to be extremely short-lived.[29] When an applied potential is oscillated between ±2 V, the characteristic green emission is observed.[28] This electrogenerated chemiluminescence is ascribed to disproportionation of electrochemically-produced Pt_2^{5-} and Pt_2^{3-} species to form one ground-state (Pt_2^{4-}) and one excited-state ($^3Pt_2^*$) molecule. Electrochemiluminescence was also observed by reduction alone at ~-2.8 V, in the presence of tetra-*n*-butylammonium ion. Based on this phenomenon, the ground-state reduction potential of Pt_2 was predicted to occur at ~-2.7 V.[29]

From the rates of excited-state quenching with several substrates of known reduction potentials, the excited-state oxidation potential of Pt_2 in acetonitrile, $E^{o(3-/4-*)}$, has been estimated as ≤-1.0 V vs NHE.[16, 30, 31] The excited state is thus a powerful reductant; it should be able to reduce any substrate with a reduction potential less negative than -1.0 eV vs NHE.[32] Combination of the excited-state energy with the estimated oxidation potential of the ground state gives a predicted value of $E^{(3-/4-*)}$ =-1.7 V.

$Pt_2^{3-} + e^- \rightarrow Pt_2^{4-}$	E_p= +0.8 V (downhill as written)
$Pt_2^{4-} + h\nu \rightarrow Pt_2^{4-*}$	E_{0-0}= -2.5 V ($\Delta G>0$; uphill as written)
$Pt_2^{3-} + e^- \rightarrow Pt_2^{4-*}$	E^o= -1.7 V (uphill as written)

The excited-state reduction potential of Pt_2 has also been estimated by several workers.[10, 21, 28] Quenching experiments were carried out in methanol and acetonitrile with a series of aromatic amine quenchers spanning a range of oxidation potentials. Application of Marcus theory to the data allowed one group[10] to extract a value of the excited-state reduction potential ($E^{o(4-*/5-)}$~1.3 V) and an estimate of the reorganization energy involved in the electron transfer process (λ~1.4 V). Based on the estimated excited-state reduction potential, the ground-state reduction potential $E^{(4-/5-)}$ is expected at ~-1.2 V vs NHE. The lack of observation of any reductive wave is puzzling.

The relationships between the redox potentials of the ground and excited state are compactly illustrated in the modified Latimer diagram (Figure 1.6). Recall that the potential of -1.7 V beside the arrow connecting Pt_2^{4-*} and Pt_2^{3-} refers to the half-reaction written in the energetically uphill, reductive direction.

Figure 1.6 Modified Latimer diagram for $[Pt_2(P_2O_5H_2)_4]^{4-}$

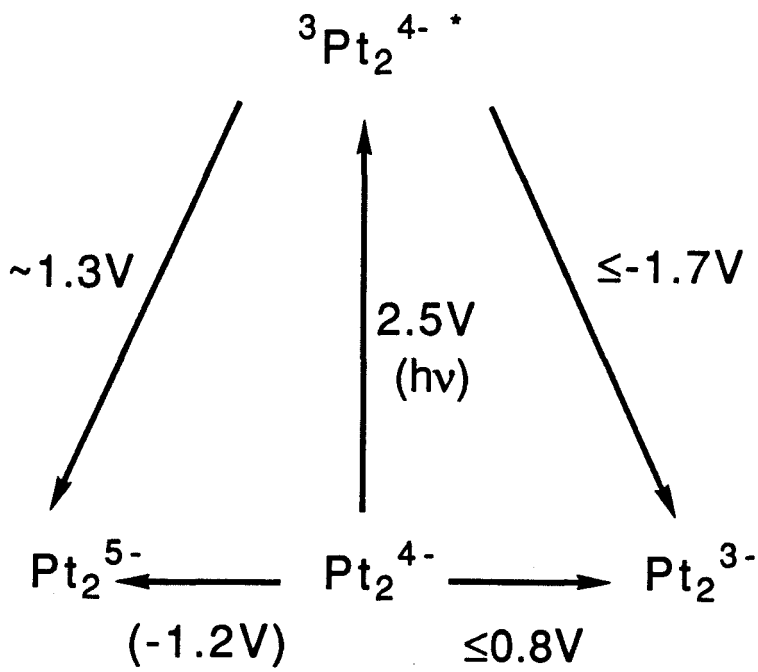

The driving force for electron transfer from Pt_2^{4-*} to an acceptor molecule (A) can be calculated by adding together the two appropriate half-reactions in the direction that produces the desired electron transfer:

$Pt_2^{4-*} \rightarrow Pt_2^{3-} + e^-$	$E_{1/2}$= +1.7 V
$A + e^- \rightarrow A^-$	$E_{1/2}$= -1.6 V (for example)
$Pt_2^{4-*} + A \rightarrow Pt_2^{3-} + A^-$	E = +0.1 V

By the Nernst equation, the net electron transfer in the example shown is thermodynamically downhill.

Halogen Atom Transfer:

A variety of diplatinum(III) complexes containing two axial ligands have been prepared from Pt_2.[6] The dihalide complexes $Pt(III)_2X_2$ (X=Cl, Br, I) are prepared thermally by reaction of Pt_2 with the appropriate X_2, or under oxidizing conditions in the presence of X^- ions.[33] The intense ultraviolet bands observed in the electronic spectra of the Pt_2X_2 complexes have been assigned as ligand-to-metal charge transfer (LMCT) (X→Pt) transitions.[34]

In the presence of alkyl halides, abbreviated RX, Pt_2 photochemically undergoes oxidative addition to produce the axial dihalide complexes.[35] The mechanism of the photochemical transformation was first postulated as electron transfer to RX, followed by X^- dissociation from RX^- and addition to the mixed valence Pt(II)Pt(III) dimer generated by the original electron transfer. This mechanism generated excitement with the suggestion that back electron transfer from a substrate could be inhibited by fast follow-up chemistry at the oxidized site.[36] Subsequent work indicates that the reaction

actually proceeds by an inner-sphere electron transfer (atom transfer) mechanism.[37] Pt_2 can be regenerated photolytically in methanol from Pt_2X_2,[38] forming a catalytic cycle.

Hydrogen-Atom Transfer:

In 1985, Roundhill reported that broad-band photolysis of Pt_2 in isopropanol catalytically yields acetone, with corresponding evolution of H_2.[39] Postulation of the primary photoprocess as H-atom abstraction of the homolytically weak αC-H in isopropanol generated a great deal of interest in the system. Subsequent studies show that this is an exciting two-color photocatalytic process.[36] Narrow-band irradiation into the 372 nm absorption band of the TBA salt of Pt_2 in the presence of isopropanol, benzyl alcohols, and tin and germanium hydrides leads to loss of 372 nm absorption and concomitant formation of an axial dihydride intermediate with a strong UV absorption at 314 nm.[40] Selective photolysis into the new band causes quantitative evolution of Pt_2, as evidenced by reformation of the peak at 372 nm. A variety of researchers have investigated H-atom transfer reactivity with Pt_2; previous work on this subject is described more fully in the introduction to Chapter 2.

Other Similar Compounds:

Because of the promising prospects for achieving useful photochemical transformations with Pt_2, many attempts have been made to synthesize analogues. The structurally and spectroscopically related d^8-d^8 dimer $Ir(tmb)_4$ (abbreviated Ir_2; tmb = 2,5-diisocyano-2,5-dimethylhexane) has been shown to abstract halogen and hydrogen atoms to form Ir_2X_2 or Ir_2H_2.[41] The spectroscopic energy of $^3Ir_2^*$ is about 30 kcal/mole, but several H-atom transfer substrates react faster with $^3Ir_2^*$ than with $^3Pt_2^*$.

Efforts to synthesize other transition-metal complexes with the μ-pyrophosphito ligand have been unfruitful. A platinum dimer with a very similar bridging methylene(bis)phosphonito ligand (abbreviated pcp) has been synthesized.[42] While many of the photophysical properties of $Pt_2(pcp)_4^{4-}$ are unchanged from those of Pt_2, the electron-donating quality of the pcp ligand alters the reactivity. A substantial amount of reactivity with this complex analogous to that seen with Pt_2 has been reported;[22] however, one disadvantage with $Pt_2(pcp)_4^{4-}$ is the reduction in excited-state lifetime to 55ns.[43]

References

1. Sperline, Roger P.; Dickson, Mark K. and Roundhill, D. Max *J. Chem. Soc., Chem. Commun.* 62 (1977). "New Route to the Directed Synthesis of Mixed Metal Chain Oligomers. Identification of a Platinum Complex Having an Intense Emission in the Visible Spectrum in Aqueous Solution."

2. Troitskaya, A. D. *Trudy Kazan. Khim. Tekhnol. Inst. im. S. M. Kirova* **23**, 228 (1957). "Structure of Phosphorous Acid and its Derivatives."

3. Troitskaya, A. D. *Russ. J. Inorg. Chem.* **6**, 585 (1961). "The Structure of Phosphorous Acid and its Derivatives."

4. Pinto, M. A. Filomena Dos Remedios; Sadler, Peter J.; Neidler, Stephen; Sanderson, Mark R.; Subbiah, Arun and Kuroda, Reiko *J. Chem. Soc., Chem. Comm.* 13 (1980). "A Novel Di-Platinum(II) Octaphosphite Complex Showing Metal-Metal Bonding and Intense Luminescence; a Potential Probe for Basic Proteins. X-Ray Crystal and Molecular Structure."

5. Marsh, Richard E. and Herbstein, Frank H. *Acta. Cryst.* **B39**, 280 (1983). "Some Additional Changes in Space Groups of Published Crystal Structures."

6. Roundhill, D. Max; Gray, Harry B. and Che, Chi-Ming *Acc. Chem. Res.* **22**, 55 (1989). "Pyrophosphito-Bridged Diplatinum Chemistry."

7. Zipp, Arden P. *Coord. Chem. Rev.* **84**, 47 (1988). "The Behavior of the Tetra-μ-Pyrophosphito-Diplatinum(II) Ion $Pt_2(P_2O_5H_2)_4^{4-}$ and Related Species."

8. Alexander, K. A.; Bryan, S. A.; Dickson, M. K.; Hedden, D. and Roundhill, D. M. *Inorg. Synth.* **24**, 211 (1986). "Potassium Tetrakis[dihydrogendiphosphito(2-)]-diplatinate(II)."

9. Bryan, Samuel A.; Dickson, Mark K. and Roundhill, D. Max *Inorg. Chem.* **26**, 3878 (1987). "Synthesis, Reactivity, Kinetics, and Photochemical Studies on Tetrakis(μ-pyrophosphito)diplatinate(II) and Dihalotetrakis(μ-pyrophosphito)diplatinate(III) Complexes. Comparison of the Substitution Mechanisms of the Diplatinum(III) Complexes with those of Monomeric Platinum(II) and Platinum(IV) Compounds."

10. Heuer, William B.; Totten, Mark D.; Rodman, Gary S.; Hebert, Eric J.; Tracy, Henry J. and Nagle, Jeffrey K. *J. Am. Chem. Soc.* **106**, 1163 (1984). "Electron-Transfer Reactions and Luminescent Quantum Yield of the Triplet Excited State of Tetrakis[μ-diphosphito(2-)-P,P']diplatinate(II)."

11. Che, Chi-Ming; Herbstein, Frank H.; Schaefer, William P.; Marsh, Richard E. and Gray, Harry B. *J. Am. Chem. Soc.* **105**, 4604 (1983). "Binuclear Platinum Diphosphite Complexes. Crystal Structures of $K_4[Pt_2(pop)_4Br].3H_2O$, a New Linear Chain Semiconductor, and $K_4[Pt_2(pop)_4Cl_2].2H_2O$."

12. Mann, Kent R.; Gordon, J. G. II and Gray, Harry B. *J. Am. Chem. Soc.* **97**, 3553 (1975). "Characterization of Oligomers of Tetrakis(phenyl isocyanide)rhodium(I) in Acetonitrile Solution."

13. Geoffroy, Gregory L.; Wrighton, Mark S.; Hammond, George S. and Gray, Harry B. *J. Am. Chem. Soc.* **96**, 3105 (1974). "Electronic Absorption and Emission Spectral Studies of Square-Planar Rh(I) and Ir(I) Complexes. Evidence for a Charge-Transfer Emitting State."

14. Rice, Steven F. and Gray, Harry B. *J. Am. Chem. Soc.* **105**, 4571 (1983). "Electronic Absorption and Emission Spectra of Binuclear Platinum (II) Complexes. Characterization of the Lowest Singlet and Triplet States of $Pt_2(H_2P_2O_5)_4^{4-}$."

15. Stiegman, Albert E.; Rice, Steven F.; Gray, Harry B. and Miskowski, Vincent M. *Inorg. Chem.* **26**, 1112 (1987). "Electronic Spectroscopy of d^8-d^8 Diplatinum Complexes. $^1A_{2u}(d\sigma^*\rightarrow p\sigma)$, $^3E_u(d_{xy},d_{yz}\rightarrow p\sigma)$, and $^{3,1}B_{2u}(d\sigma^*\rightarrow d_{x^2-y^2})$ Excited States of $Pt_2(P_2O_5H_2)_4^{4-}$."

16. Che, Chi-Ming; Butler, Leslie G. and Gray, Harry B. *J. Am. Chem. Soc.* **103**, 7796-7797 (1981). "Spectroscopic Properties and Redox Chemistry of the Phosphorescent Excited State of $Pt_2(P_2O_5)_4H_8^{4-}$."

17. Fordyce, W. A.; Brummer, J. G. and Crosby, G. A. *J. Am. Chem. Soc.* **103**, 7061 (1981). "Electronic Spectroscopy of a Diplatinum(II) Octaphosphite Complex."

18. Che, Chi-Ming; Butler, Leslie G.; Gray, Harry B.; Crooks, R. M. and Woodruff, William W. *J. Am. Chem. Soc.* **105**, 5492 (1983). "Metal-Metal Interactions in Binuclear Platinum (II) Diphosphite Complexes. Resonance Raman Spectra of the $^1A_{1g}(d\sigma^*)^2$ and $^3A_{2u}(d\sigma^*p\sigma)$ Electronic States of $Pt_2(P_2O_5H_2)_4^{4-}$."

19. Stein, Paul; Dickson, Mark K. and Roundhill, D. Max *J. Am. Chem. Soc.* **105**, 3489 (1983). "Raman and Infrared Spectra of Binuclear Platinum(II) and Platinum(III) Octaphosphite Complexes. A Characterization of the Intermetallic Binding."

20. Markert, J. T.; Clements, D. P.; Corson, M. R. and Nagle, J. K. *Chem. Phys. Lett.* **97**, 175 (1983). "Phosphorescent Lifetime and Quantum Yield Measurements of $K_4Pt_2(H_2P_2O_5)_4$ from 1.6 to 300K."

21. Peterson, John R. and Kalyanasundaram, K. *J. Phys. Chem.* **89**, 2486 (1985). "Energy- and Electron Transfer Processes of the Lowest Triplet Excited State of Tetrakis(diphosphito)diplatinate(II)."

22. Roundhill, D. Max; Shen, Zhong-Ping; King, Christopher and Atherton, Stephen J. *J. Phys. Chem.* **92**, 4088 (1988). "Triplet Excited-State Chemistry of Diplatinum(II) Complexes. Comparative Spectroscopy and Quenching Rate Constants between the Tetrakis(μ-pyrophosphito)diplatinate(II) and the Tetrakis[μ-methylenebis(phosphonito)]diplatinate(II) Tetraanions."

23. Che, Chi-Ming; Lee, Wai-Man; Cho, Kar-Cheong; Harvey, Pierre D. and Gray, Harry B. *J. Phys. Chem.* **93**, 3095 (1989). "Photoreactions of Organic Halides, Alcohols and Olefins with Tetrakis(pyrophosphito)diplatinate(II)."

24. Roundhill, D. Max; Shen, Zhong-Ping and Atherton, Stephen J. *Inorg. Chem.* **26**, 3833 (1987). "Reactivity of the Triplet State of the Tetrakis(μ-pyrophosphito)diplatinate(II) Tetraanion with Alkenes and Alkynes. Comparison with the Energy-Transfer Photosensitizer and Diradical Chemistry of Ketone Triplets."

25. Meyer, Thomas J. *Acc. Chem. Res.* **11**, 94 (1978). "Optical and Thermal Electron Transfer in Metal Complexes."

26. Kim, Joon; Fan, Frank F.; Bard, Allen J.; Che, Chi-Ming and Gray, Harry B. *Chem. Phys. Lett.* **121**, 543 (1985). "Electrogenerated Chemiluminescence. On the Electrogenerated Chemiluminescence (ECL) of Tetrakis(pyrophosphito)diplatinate(II), $Pt_2(P_2O_5H_2)_4^{4-}$."

27. Bryan, Samuel A.; Schmehl, Russell H. and Roundhill, D. Max *J. Am. Chem. Soc.* **108**, 5408 (1986). "Electrochemical Oxidation of the Tetrakis(μ-pyrophosphito-P,P')diplatinum(II) Complex $Pt_2(m\text{-}P_2O_5H_2)_4^{4-}$ Both in the Presence and the Absence of Halide Ions, and Reduction of the Axially Substituted Halodiplatinum(III) Complexes $Pt_2(m\text{-}P_2O_5H_2)_4X_2^{4-}$."

28. Vogler, Arnd and Kunkely, Horst *Agnew.Chem.Int.Ed.Engl.* **23**, 316 (1984). "Electrochemiluminescence of Tetrakis(diphosphonato)diplatinate(II)."

29. Che, Chi-Ming; Atherton, Stephen J.; Butler, Leslie G. and Gray, Harry B. *J. Am. Chem. Soc.* **106**, 5143 (1984). "Generation of Binuclear $(d^8\text{-}d^8)p\sigma$ Platinum and Rhodium Complexes by Pulse Radiolysis."

30. Che, Chi-Ming and Cho, Kar-Cheong *J. Chem. Soc., Chem. Commun.* 133 (1987). "Photoreduction of Nitric Acid by Electronically Excited Diplatinum(II,II) Pyrophosphite, $[Pt_2(P_2O_5H_2)_4]^{4-}$."

31. Hurst, James K.; Thompson, David H. P. and Connolly, John S. *J. Am. Chem. Soc.* **109**, 507 (1987). "Photooxidation of Tetraanionic Sensitizer Ions by Dihexadecyl Phosphate Vesicle-Bound Viologens."

32. A quenching rate of 4.6×10^7 $M^{-1}s^{-1}$ observed with 4-dimethylamino-benzophenone ($E_{1/2}$ = -1.8 V) indicates that the oxidation potential of $^3Pt_2^*$ may be as high as ~-1.8 V in acetonitrile, a value more in line with the predicted value. Zietlow, Miriam H., Ph. D. Dissertation (California Institute of Technology, 1989).

33. Che, Chi-Ming; Schaefer, William P.; Gray, Harry B.; Dickson, Mark K.; Stein, Paul B. and Roundhill, D. Max *J. Am. Chem. Soc.* **104**, 4253 (1982). "Novel Binuclear Platinum (III) Diphosphite Complexes."

34. Che, Chi-Ming; Mak, Thomas C. W.; Miskowski, Vincent M. and Gray, Harry B. *J. Am. Chem. Soc* **108**, 7840 (1986). "Binuclear Platinum (III) Complexes. Preparation, Structure, and $d\sigma d\sigma^*$ Spectrum of $[Bu_4N]_2[Pt_2(P_2O_5H_2)_4(CH_3CN)_2]$."

35. Roundhill, D. Max; Dickson, Mark K. and Atherton, Stephen J. *J. Organomet. Chem.* **335**, 413 (1987). "Thermal and Photochemical Addition of Alkyl and Aryl Halides to Tetrakis(μ-pyrophosphito)diplatinum(II) Tetraanion."

36. Marshall, Janet L.; Steigman, Albert E. and Gray, Harry B. in *Excited States and Reactive Intermediates* (ed. Lever, A.B.P.) (American Chemical Society, Washington, D.C., 1986), pp.166-176.

37. Roundhill, D. Max and Atherton, Stephen J. *Inorg. Chem.* **25**, 4071 (1986). "Bromine Atom Abstraction from Aryl and Alkyl Bromides by the Triplet Excited State of the Tetrakis(μ-pyrophosphito)diplatinate(II) Tetraanion."

38. Che, Chi-Ming; Lee, Wai-Man and Cho, Kar-Cheong *J. Am. Chem. Soc.* **110**, 5407 (1988). "Photochemistry of Platinum(III,III) Pyrophosphite Complexes. Efficient Photochemical Reduction of $[Pt_2(pop)_4X_2]^{4-}$ to $[Pt_2(pop)_4]^{4-}$ in Methanol."

39. Roundhill, D. Max *J. Am. Chem. Soc.* **107**, 4354 (1985). "Excited-State Chemistry of Tetrakis(μ-pyrophosphito)diplatinum(II). Photoinduced Addition of Aryl Bromides and Iodides to the Binuclear Complex and the Photoinduced Catalytic Conversion of Isopropyl Alcohol into Acetone and Hydrogen."

40. Harvey, Erica L.; Stiegman, Albert E.; Vlcek, Antonin, Jr. and Gray, Harry B. *J. Am. Chem. Soc.* **109**, 5233 (1987). "Dihydridotetrakis(pyrophosphito(2-))-diplatinate(III)."

41. Smith, David C., Ph. D. Dissertation (California Institute of Technology, 1989).

42. King, Christopher; Auerbach, Roy A.; Fronczek, Frank R. and Roundhill, D. Max *J. Am. Chem. Soc.* **108**, 5626 (1986). "Synthesis, Structure and Spectroscopy of the Diplatinum(II) Complex $Pt_2(pcp)_4^{4-}$, A $Pt_2(pop)_4^{4-}$ Analogue Having Methylenebis(phosphinic acid) Bridges."

43. King, Christopher; Yin, Yan; McPherson, Gary L. and Roundhill, D. Max *J. Phys. Chem.* **93**, 3451 (1989). "Medium Effects on the Absorption and Emission Spectra and on the Triplet State Lifetimes of the Tetrakis[μ-methylenebis(phosphonito)]diplatinate(II) Chromophore."

Chapter 2. Factors Influencing Rates of H-Atom Abstraction by $^3Pt_2^*$

Introduction

What is H- Atom Abstraction?

The phrase "hydrogen atom abstraction" (or "hydrogen atom transfer") implies that both an electron and a proton are transferred from one species to another, and that no evidence is observed for outer-sphere electron transfer, proton transfer, or hydride transfer. These conditions are often satisfied by showing that electron transfer is not energetically allowed, given the redox potentials of the two species involved, or that H^+ or H^- transfer is not expected from the relative acidities or hydride affinities of the two species involved. Four limiting scenarios can be envisioned within the general requirements of H-atom transfer. Apparent transfer of a hydrogen atom can be accomplished by partial initial transfer of a proton, followed by an electron, from the H-atom donor to the H-atom abstractor. Alternatively, the transfer could involve partial movement of a hydride from the H-atom donor to the H-atom abstractor, followed by electron transfer back to the H-atom donor. An electron could be partially transferred from the H-atom donor to the abstractor species and then a proton could follow. The fourth possibility is partial transfer of an electron to the H-atom donor, in conjunction with transfer of hydride to the H-atom abstractor. A fifth idealized scenario represents a midway point between the four limiting cases: exactly simultaneous transfer of an electron and a proton, i.e., an intact H·, from the H-atom donor to the H-atom abstractor. Each substrate/reagent pair will find a unique combination of the above limiting cases -- all of which qualify as abstraction of a hydrogen atom -- that results in the lowest possible energy pathway for reaction.[1]

The rates of H-atom transfer reactions are determined by the energy needed to reach the transition state, defined as the highest-energy configuration of atoms and electrons along the lowest energy path leading to H-atom transfer. For each hydrogen atom transfer reaction, the transition state will represent a unique distribution of electrons and atoms between the two reactants.

Background on H-atom Transfer in Organic Systems

Elements of the following discussion have been adapted from N. J. Turro's book, *Modern Molecular Photochemistry*.[2] Hydrogen-atom (H-atom) abstraction by organic excited states has been examined in exquisite detail, and this very readable book provides an excellent introduction to the subject, with a number of leading references.

Based on studies with $R_3C\cdot$ as an approximation of π,π^* excited states, and $RO\cdot$ radicals as an approximation of n,π^* excited states, five major factors affecting H-atom transfer reaction rates in organic systems have been identified:[2]

- 1. The strength of the bond being broken.
- 2. The strength of the bond being formed.
- 3. Polar or charge-transfer effects on the energy of the transition state relative to the energy of the reactant.
- 4. Solvent effects on the reagent, substrate, and transition state.
- 5. Steric effects on the approach of the reagent and substrate.

The first two factors listed above usually control the enthalpy change of the H-atom transfer reaction. Because the activation energy for the reaction must be at least as large as any uphill enthalpy changes, the combination of these two factors strongly influences the rates of abstraction. The last three factors usually provide second-order perturbations on the reaction rates. Each factor is discussed below.

•1. To the extent that the transition state for H-atom abstraction involves a concerted transfer of an electron and proton; i.e.; an intact hydrogen atom, the energetic factors influencing the transition state of the atom transfer must include the sum of the energies of all the bonds made and broken during the transfer. Enthalpic effects that are due to the strength of the bond being broken are relatively easy to study, since bond strengths for a variety of closed-shell H-atom donors have been measured.[3] In general, abstraction rates are slower when stronger bonds are being broken.

•2. In n,π^* or π,π^* organic excited states, the absorption of a photon generates an activated diradical species.[4] Bond formation between an H-atom and the electronically excited diradical produces a monoradical species; unfortunately, the C-H or O-H bond energies of interest for such monoradicals are mostly unknown.[5] For a series of reactions with the same excited-state species, however, the strength of the bond being formed remains constant.

The excited-state energy may be considered to contribute to the strength of the bond being formed between the excited diradical and the H-atom. The strength of this bond measured relative to the electronically excited diradical species will be much greater than the strength measured relative to the ground state. Figure 2.1 demonstrates that the two measurements should differ by the amount of the spectroscopic transition between the ground state and the excited diradical. The observation of faster H-atom abstraction rates for organic species with higher-energy electronic excited states indicates that differences in the bond strengths of the O-H or C-H bonds being formed are small compared to the spectroscopic energies. Alternatively, the strengths of the O-H or C-H bonds formed from the ground-state abstractor molecules may parallel the excited-state energies of the abstractor molecules.

Figure 2.1 Diagram of spectroscopic energy contribution to bond formation during H-atom abstraction

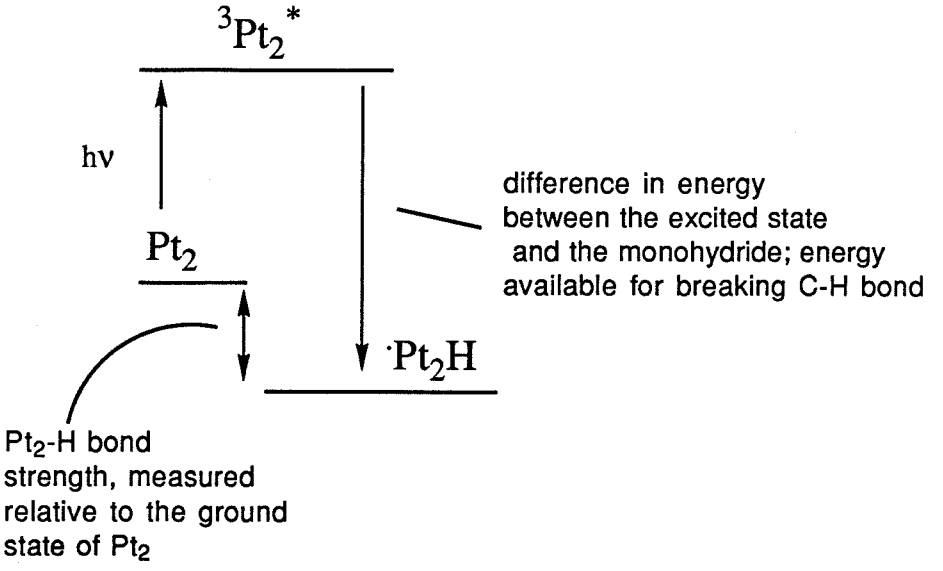

Figure 2.2 Initial orbital interactions for H-atom transfer by the n,π* electronic excited state of a ketone (from Ref.2)

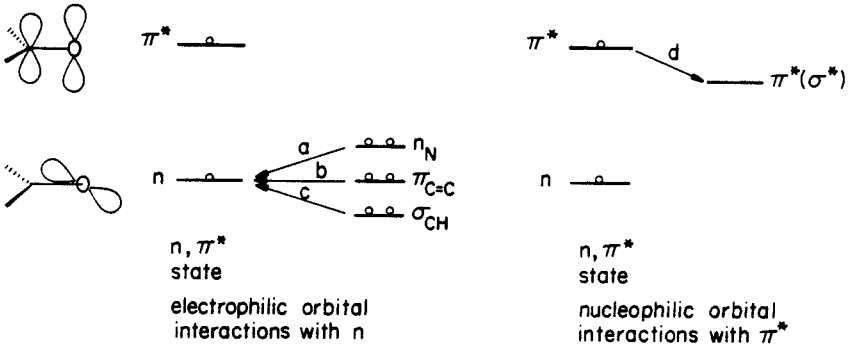

•3. If the transition state for H-atom abstraction involves partial electron transfer in conjunction with proton or hydride transfer, the energetics of the H-atom abstraction transition state must include the appropriate redox potentials of the organic excited state and the H-atom donor, as well as the relative acidities or hydride affinities of the reduced and oxidized species. The initial interactions involved in H-atom transfer reactions can be deduced for organic compounds because comparisons of orbital energy levels between compounds can be made with some certainty. For example, the first interaction in the n,π^* ketone states is thought to be an interaction between filled sigma orbitals of the H-atom donor and the half-empty, oxygen-localized HOMO (or "hole") of the electronically excited abstractor species (Figure 2.2). H-atom donors with electron-rich, relatively high-lying σ orbitals will react faster with n,π^* states than H-atom donors with lower-lying σ orbitals, because the initial electron transferlike interaction will be more energetically favorable in the former case. This is referred to as a "polar effect."

•4. Differences in solvation of the reactants and products affect the overall energetics of the reaction; differences in solvation between the reactants and the transition state affect the rate of the reaction. For example, a transition state with electron transfer character could be stabilized by reaction in a polar solvent, resulting in faster rates.

•5. Steric effects on the approach of the reagent and substrate will be reflected in the change in entropy between the reactants and the transition state. Entropy effects on the rate can be important, since the transition state is expected to be associative. The entropy change of the overall reaction should be small, since two species react to give two products.

Background on H-atom Transfer in Non-Organic Systems

H-atom transfer from organic and organometallic H-atom donors has been observed in several ground-state organometallic systems[6]; notably the metal carbonyl radicals ·$Re(CO)_5$ or ·$Re(CO)_4L$, and ·$Mn(CO)_3L_2$.[7, 8] H-atom abstraction of the αC-H bond in α-secphenethyl alcohol has also been postulated as a reaction pathway for the electrochemically generated rhenium(VI) complex $[Re(py)_4(O)_2]^{2+}$,[9] and the lowest electronic excited state of $[Os(tmc)_4(O)_2]^{2+}$ (tmc= 1,4,8,11-tetramethyl-1,4,8,11-tetra-azacyclotetradecane).[10] Electronically excited atomic mercury can abstract hydrogens from substrates with very strong bonds, including alkanes.[11] A variety of alcohols react with electronically excited uranyl ion, $*UO_2^{2+}$, via an H-atom abstraction pathway.[12, 13, 14] Recently, H-atom transfer has been reported as an important reaction of the $^3A_{2u}$ electronic excited states of the d^8-d^8 dimers Pt_2 (*vide infra*), $Pt_2(pcp)_4^{4-}$ (pcp=methylene(bis)phosphonito),[15] and $Ir_2(tmb)_4^{2+}$ (tmb=2,5-diisocyano-2,5-dimethylhexane).[16]

In the last five years, several researchers have amassed convincing evidence for H-atom abstraction as a reaction pathway for $^3Pt_2^*$. Quenching of the emission intensity and/or lifetime of the triplet excited state of the metal complex is observed with a variety of substrates that have homolytically weak bonds to hydrogen, including alcohols,[15, 17, 18, 19, 20] H_3PO_3,[17] toluene,[19] cyclohexene and cyclohexadiene,[15, 16] and triorganostannanes, -germanes, -silanes.[17, 21, 22] Stern-Volmer kinetics are followed in all cases, indicating a bimolecular reaction between $^3Pt_2^*$ and the substrate as the deactivation pathway. Transient absorptions attributed to Pt_2H· are observed 0.1 μsec after a light pulse in a solution of Pt_2 with various H-atom donors.[15, 17, 18, 20, 23] The expected radical coupling products have been observed after photolyses of Pt_2 with several organic substrates.[17, 19] While quenching of $^3Pt_2^*$ and/or suggestive product formation[15, 17, 18, 19, 20, 22, 24, 25, 26, 27] are observed with many substrates that have activated C-H bonds, quenching of the excited state is slow with

substrates that do not have activated C-H bonds.[19] An inverse correlation of quenching rate with bond strength was observed for a series of substrates R_3EH (E = Sn, Ge, Si).[21, 22] Over a bond-energy difference of ~25 kcal/mol, abstraction rates varied from 10^8 to 10^4 $M^{-1}s^{-1}$. A kinetic isotope effect of 1.7 for quenching with Bu_3SnH and Bu_3SnD was taken as evidence for partial Sn-H bond dissociation in the transition state. This body of evidence indicates that abstraction of a hydrogen atom from an H-atom donor substrate is, in fact, a deactivation pathway for $^3Pt_2^*$. Moreover, a number of substrates can be found for which the quenching rate is a meaningful probe of the H-atom abstraction rate.

Factors Expected to Influence H-atom Transfer in Non-Organic Systems

Little mechanistic information is available about non-organic complexes that exhibit excited-state H-atom transfer reactivity; however, reaction rates are expected to be influenced by the same factors discussed above. The first factor does not depend on the abstractor species, so it will not be affected by the change to an inorganic or organometallic excited state. The strength of the bond formed between the abstractor species and the H-atom is likely to be a complete unknown, as bond energies for inorganic or organometallic radicals are even more rarely measured than those for organic radicals. Furthermore, excited-state energies will not necessarily be effective predictors of H-atom abstraction rates in the non-organic systems, because the bond energies implicitly being compared do not depend solely on the excitation energy. Homolytic metal-hydrogen bond strengths are extremely variable, for example, even for the same metal in different complexes.[28]

Excited-state redox potentials can provide a qualitative assessment of the importance of polar factors; however, absolute orbital energy levels are rarely known in the non-organic systems, so it is difficult to decide what excited state orbitals will interact with the donor orbitals. The initial H^+ or H^- transfer scenarios may not be as

farfetched for non-organic species as they are for the organic systems studied.[29] Solvent effects may appear to be reversed in some inorganic and organometallic systems. For example, where the abstractor excited state is highly charged, an electron transfer-like interaction could actually result in reduced polarity in the transition state, and hence a faster reaction in less polar solvents. Interesting differences in entropy effects can also be envisioned for the inorganic and organometallic excited states.

This chapter discusses the dependence of H-atom transfer rates with $^3Pt_2^*$ on substrate bond strength, sterics and solvent. The importance of polar effects and the strength of the bond being formed, along with a continued consideration of steric contributions, are examined in more detail in Chapter 5.

Experimental

Materials. $[TBA]_4Pt_2$ was prepared from the potassium salt as described previously.[30a] $[PPN]_4Pt_2$ was precipitated by dissolving excess [PPN]Cl in a mixture of water and a minimum of methanol and adding an aqueous solution of $[TBA]_4Pt_2$. Burdick and Jackson high-purity, UV grade acetonitrile was used as received for all experiments. Benzyl alcohol, 1-phenyl-1-ethanol (referred to hereafter as α-secphenethyl alcohol), 1-phenyl-1-propanol, and diphenylmethane were purchased from Aldrich, reagent-grade; 2-methyl-1-phenyl-1-propanol was purchased from Wiley, 97%; and 1-cyclohexylethanol was obtained from Calbiochem. The liquid alcohols and hydrocarbons were purified by distillation under reduced pressure in the presence of sodium metal to remove water and peroxides, and stored under argon, in septum-covered roundbottom flasks, in the dark. The solid quencher was sublimed under vacuum two times immediately prior to use. Purification of ethylbenzene and cumene is detailed elsewhere.[16] Isopropanol and sec-butanol (Adrich Gold Label, 99+%) and toluene (Burdick and Jackson High-Purity Solvent) were used without purification from freshly opened bottles. The perdeuterated compound $PhCD(OD)CD_3$ was synthesized by a Grignard reaction using phenylmagnesium bromide and deuterated acetaldehyde. The monodeuterated alcohol $PhCD(OH)CH_3$ was synthesized by reducing acetophenone with $NaBD_4$ and quenching the reaction with H_2O.

Bulk photolysis. Acetonitrile solutions containing $[TBA]_4Pt_2$ ($3x10^{-4}$ M) were degassed with at least 5 freeze-pump-thaw cycles. Stirred solutions were irradiated in a 1 cm cell, and the absorbance changes were measured in an attached 1mm cell. Cary 17 and Shimadzu UV-260 absorption spectrometers were used. For the irradiation source, a 1000W Hg-Xe lamp with Corning 0-52 cutoff and 7-39 band-pass filter combination provided a 30 nm fwhm transmittance band centered at 370 nm. ^1H NMR and/or GC were used to identify the organic products after photolysis.

Quenching studies. Acetonitrile solutions containing $[TBA]_4Pt_2$ (1-3 $x10^{-4}$ M) plus incrementally varied quencher concentrations were degassed with at least 5 freeze-pump-thaw cycles on a vacuum line with a limiting pressure of ~10^{-5} torr. Quenchers were added directly to the quenching cell (roundbottom flask connected by two arms to 1 mm and 1 cm cuvettes and sealed by teflon vacuum valves) using a syringe of the appropriate volume (between 10 mL and 1 mL); the solution was opened to air for the addition of each quencher aliquot. Excited-state lifetimes (τ) were measured with a Quanta Ray Nd:YAG (8 ns fwhm; 355 nm excitation) laser system described elsewhere.[30b] Kinetic data were analyzed by Stern-Volmer plots of τ_0/τ, $1/\tau$ or $(1/\tau - 1/\tau_0)$ versus quencher concentration. The Stern-Volmer equation describes the dependence of the excited-state lifetime on the quencher concentration when deactivation of the excited state occurs via bimolecular reactions with quencher. Stern-Volmer plots for most quenchers appeared linear within the accuracy of the data points. For α-secphenethyl alcohol, however, a combination of points from several different studies gives a distinctly curved plot at concentrations >0.1 M. (See Appendix 2.2.) The rate reported for this quencher is based on the slope of the line for [Q]<0.1 M, which gave a correlation coefficient of 1.00 for 6 points. Rates slower than 10^4 $M^{-1}s^{-1}$ can be measured only as upper limits by the quenching method. For substrates that quench below this rate, quencher concentrations large enough (>1 M) to perturb the solution medium are needed to see substantial changes in the emission lifetime (~10%). Since the redox potentials and triplet states of the subtrates examined are out of reach of Pt_2, quenching rates are assumed to correspond to H-atom abstraction rates.

NMR. Spectra were obtained on a JEOL FX90Q 90MHz FTNMR spectrometer. Deuterated acetonitrile (Aldrich, 1 mL ampules) was used as the solvent, and residual CHD_2CN (chemical shift = 1.9 ppm) was used as a reference. Samples were not degassed.

Results and Discussion

Table 2.1 and Figure 2.3 show the range of H-atom transfer quenching rate constants for $^3Pt_2^*$ in acetonitrile, correlated with E-H bond strength[31, 32, 33, 34] (E = species bonded to H; the abstractable H is underlined). A trend of slower rates with higher substrate bond strength is apparent in the stannane/germane/silane quencher series.[22] The hydrocarbon substrates clearly do not follow this trend; exceptions to the trend are also evident for some alcohols. The present work focuses on the alcohol and hydrocarbon substrates, because the process of untangling the factors affecting rates is facilitated by comparisons between substrates where only C-H bonds are being broken.

Figure 2.3 Quenching rate constants versus E-H bond energies for H-atom donors (E=Sn, Ge, Si, C)

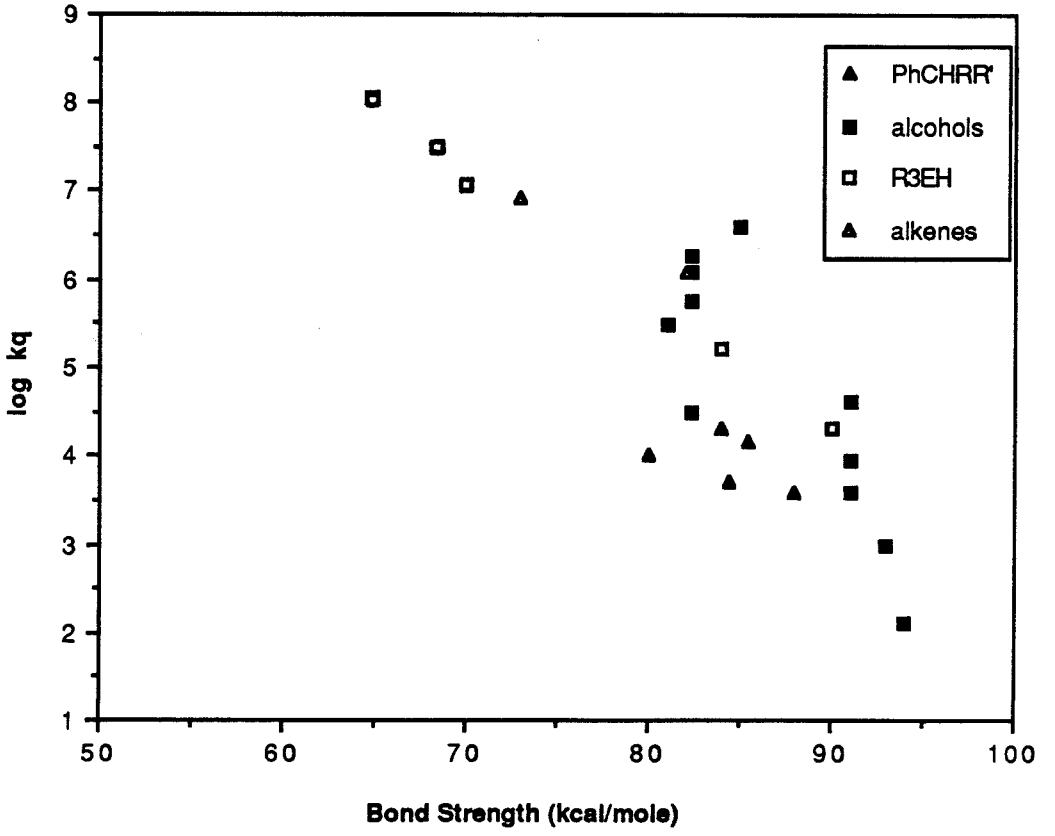

Table 2.1 Rate constants and E-H bond energies (E=Sn, Ge, Si, C) for quenching of $^3[TBA]_4[Pt_2(P_2O_5H_2)_4]^*$ by H-atom donors in CH_3CN

Substrate	Bond Strength (kcal/mole)	Reference	Quenching Rate ($M^{-1}s^{-1}$)	Reference
triphenylmethane	80	32	$<1x10^4$	22
diphenylmethane	84±2	31	$2x10^{4a}$	
cumene	84.4±1.5	31	$5x10^3$	36
ethylbenzene	85.4±1.5	31	$1.4x10^4$	36
toluene	88.0±1	31	$4x10^3$	
benzhydrol	81±4	33	$3x10^5$	42
PhC<u>H</u>(OH)CH_3	82.4±3	31	$1.8x10^6$	
PhC<u>H</u>(OH)CH_2CH_3	82.4±3	33	$1.2x10^6$	
PhC<u>H</u>(OH)$CH(CH_3)_2$	82.4±3	33	$5.6x10^5$	
PhC<u>H</u>(OH)$C(CH_3)_3$	82.4±3	33	$3x10^4$	
benzyl alcohol	85±3	31	$4x10^6$	
cyclohexylmethanol	91±1	33	$4x10^{4a}$	
sec-butanol	91±1	33	$9x10^3$	36
isopropanol	91±1	31	$4x10^3$	
ethanol	93±1	31	10^3	17
methanol	94±2	31	130	
triphenyltin hydride	65±10	34	$1.0x10^8$	21
triphenylgermane	68±10	34	$2.9x10^7$	21
tributyltin hydride	70±5	34	$1.2x10^7$	21
triphenylsilan	84±4	34,31	$1.6x10^5$	21
triethylsilane	90±4	34	$2.0x10^4$	21
cyclohexene	82	31	$1.2x10^6$	16
cyclohexadiene	73	31	$8.2x10^6$	16

a = rate determined by two- or three-point line

Alcohol and hydrocarbon quenching rates are compared in Figure 2.4. $^3Pt_2^*$ is quenched by a variety of alcohols, with rates ranging from $4x10^6$ $M^{-1}s^{-1}$ to <150 $M^{-1}s^{-1}$. H-atom transfer is expected to be the major contributor to the quenching rate, based on a large kinetic isotope effect (*vide infra*) and the observed product formation (Pt_2H_2, H_2, and/or expected aldehyde, ketone, or ketyl coupling products). Furthermore, the oxidation potentials of the alcohol and hydrocarbon substrates examined are too high for outer-sphere electron transfer to $^3Pt_2^*$.[35] In contrast to the reactions with alcohols, very slow rates (~10^4 $M^{-1}s^{-1}$) are observed for all the hydrocarbons studied. Radical coupling products observed after bulk photolysis of Pt_2 with toluene, ethylbenzene and cumene indicate that H-atom transfer does occur with these quenchers.[36] A particularly striking departure from the expected dependence of rate on bond strength is exhibited by triphenylmethane. The tertiary C-H bond is very weak, yet the complex exhibits a level of quenching measurable only as an upper limit. No search has been made for organic coupling products from bulk photolyses with this substrate.

Clearly, quenching rates for $^3Pt_2^*$ with benzyl alcohols are much faster than the rates for hydrocarbons with comparable benzylic C-H bond strengths. This wording implies that the alcohol rates are faster than the "normal" hydrocarbons. The opposite is possible; the hydrocarbon rates may be slower than the "expected" rates exhibited by the alcohols. Some combination of the two situations also may apply. The departure from quenching rate dependence on bond strength indicates that some other factor must be important for $^3Pt_2^*$ reactivity with organic H-atom donors. The list of factors expected to affect H-atom abstraction rates also includes polar effects, solvent effects, and steric effects.[2]

Figure 2.4 Quenching rate constants versus bond energies for alcohol and hydrocarbon H-atom donors

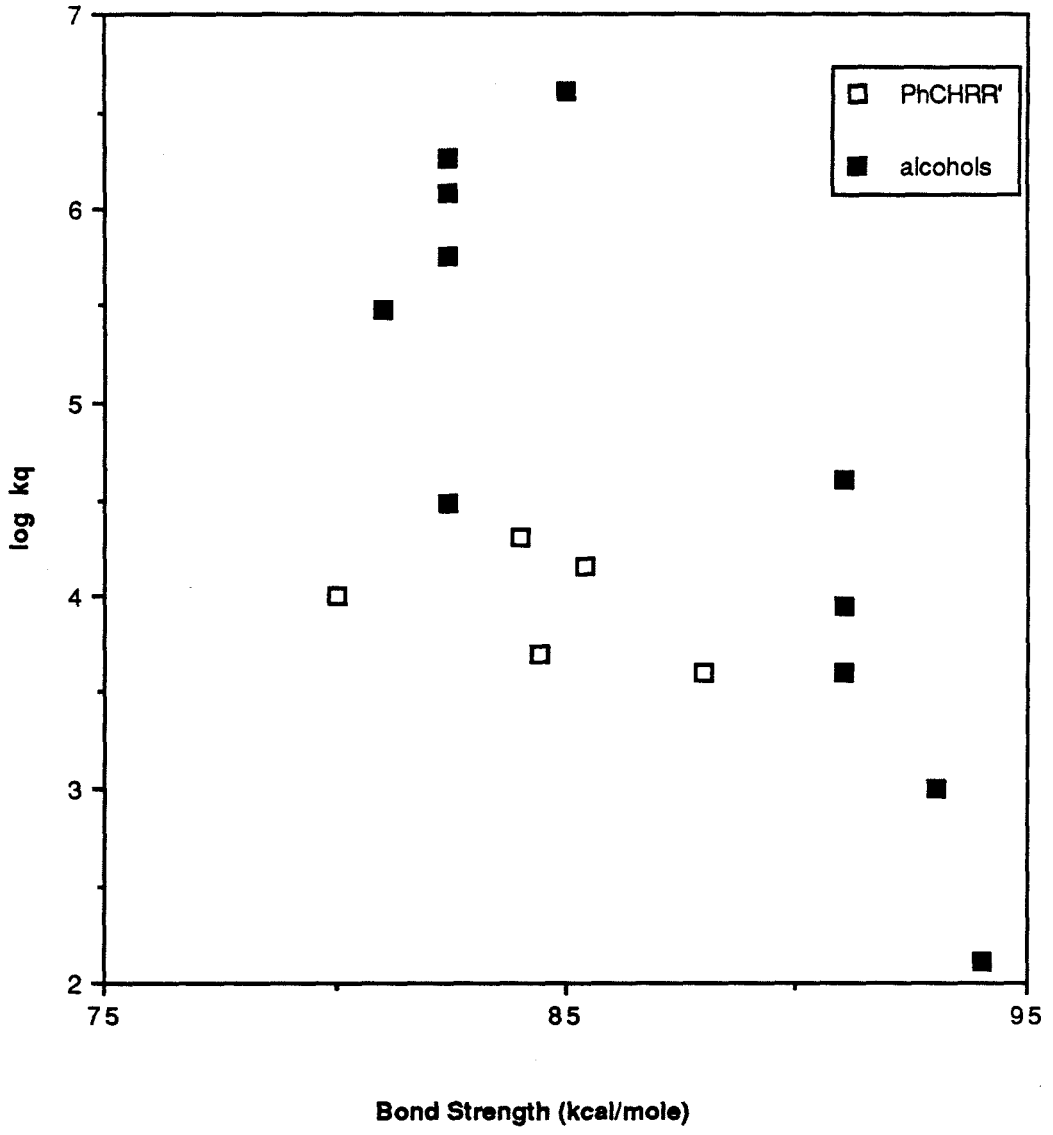

Polar effects

The Pt_2 excited state can be viewed as an excited radical species that will interact with empty σ^* substrate orbitals; alternatively, the half-empty $d\sigma^*$ orbital can be visualized as an oxidizing "hole" that will interact with electron-rich substrates (Figure 2.5). The hydrocarbons are easier to oxidize than the alcohols, yet they react slower with $^3Pt_2^*$; this observation is inconsistent with a polar effect involving initial electron transfer from the substrate to the metal excited state. A large kinetic deuterium isotope effect ($k_H/k_D=4$) observed for quenching of $^3Pt_2^*$ with $PhCH(OH)CH_3$ and $PhCD(OD)CD_3$ or $PhCD(OH)CH_3$ argues against polar effects for the benzyl alcohols. For a pure H-atom transfer to Pt_2^*, the transition state occurs when the metal complex is stabilized enough by the incipient Pt-H bond and related structural rearrangements to overcome the energy of the C-H bond that is being ruptured. The maximum deuterium isotope effect expected for a linear (Pt-H-C), pure H-atom transfer transition state in the absence of tunnelling is 7.[37] A change from hydrogen to deuterium is not expected to affect the redox potentials of the substrate; but the bond energy difference between the two species is approximately 1 kcal/mol, based on half of the difference in IR bond stretching frequency (i.e., the difference in zero-point energies) for the two bonds of interest. The observed isotope effect suggests that the breaking C-H bond is intimately involved in the transition state for this alcohol, and that electron transfer contributions are relatively unimportant.

Initial proton or hydride transfer is possible, but not likely because the carbonium ions and carbanions formed should be high in energy. Acid/base chemistry with Pt_2 occurs at the ligands[38]; no evidence has been seen for protonation at Pt in the ground or excited state. The hydride affinity of the excited state is unknown.

Figure 2.5 Possible initial orbital interactions involved in a polar transition state for H-atom transfer to $^3[Pt_2(P_2O_5H_2)_4]^{4-*}$

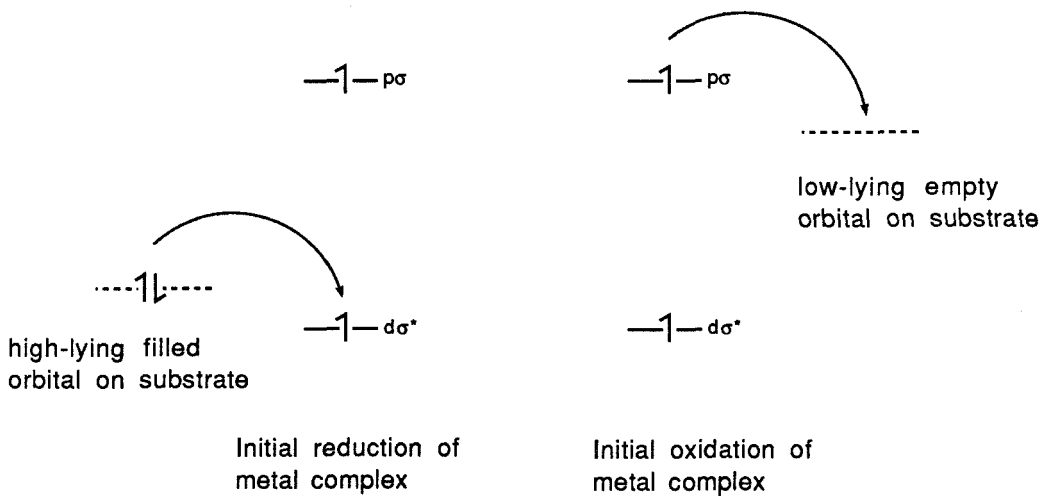

Solvent effects

Interactions with solvent provide another possible source of the non-correspondence of reaction rate with bond strength. Pt_2 is a tetraanion and the quenchers are neutral; since no electron transfer character is expected, interactions of CH_3CN with the separated reactants and the associated transition state should be fairly similar. H-atom transfer rates have been previously reported for a variety of quenchers in four different solvents.[15, 17, 20] Addition of the present work in acetonitrile indicates that there are very definitely some solvent-dependent quenching rates (Table 2.2). Rates in acetonitrile are generally the slowest rates observed. This observation is consistent with coordination of solvent at the axial sites in the excited state that interferes with approach of the substrate. Acetonitrile is expected to coordinate more strongly than water (and presumably methanol as well) on the basis of the observed stabilities for the $Pt(III)_2CH_3CN$ versus $Pt(III)_2H_2O$ complexes.[39, 40]

Table 2.2 H-atom abstraction quenching rates with $^3[TBA]_4[Pt_2(P_2O_5H_2)_4]^*$ for selected H-atom donors in different solvents

Quencher	Acetone	Methanol	CH_3CN	DMSO	H_2O pH 1	H_2O pH 7
isopropanol		1.0×10^5 c	4×10^3		7×10^4 a 1×10^5 d	2×10^4 a
sec-butanol		1.5×10^5 c	9×10^3			
Ph_2CHOH		2.5×10^6 d	3×10^5		8×10^4 a	
$PhCH_2OH$		2.5×10^6 c	4×10^6		3×10^6 a 2×10^7 d	
cyclohexene		1.3×10^6 e	1.2×10^6 b			
Ph_3CH	3×10^3 a		$<10^4$	2×10^5 a 5×10^6 d		
Et_3SiH		4×10^5 a 1.3×10^7 d	2×10^4			
n-Bu_3SnH			1.2×10^7	2×10^5 a 6.3×10^6 d		

a=ref. 17 b=ref. 16 c=ref. 20 d=ref. 15 e=ref. 18

Steric effects

Steric interactions are a very plausible source of the unusual reactivity patterns observed for reactions of $^3Pt_2^*$ with organic substrates. In the triplet excited state of Pt_2 responsible for H-atom transfer reactions, an electron has been promoted from a $d\sigma^*$ orbital whose lobes point in opposite directions out along the Pt-Pt axis to a $p\sigma$ orbital localized between the two Pt's. The 6p orbitals are quite diffuse, so the $p\sigma$ orbital may also have appreciable extension to the axial sites on platinum. Whatever the orbital interactions involved, the C-H bond needs to come in and form a basically linear transition state along the Pt-H-C coordinate. The environment around the axial site of Pt_2 consists of a fluted cup of H-bonded terminal oxygen species from the ligands. This ring of ligands should be both hydrophilic and somehat bulky.

Steric effects one: alcohols versus hydrocarbons

Benzyl alcohol contains phenyl and OH substituents attached to the carbon bearing two abstractable hydrogens, and sports the fastest rate observed for the organic quenchers. Ethylbenzene has approximately the same bond strength, the same number of abstractable hydrogens, and similar steric bulk from the phenyl and methyl substituents, but the rate is slower by two orders of magnitude than that observed for benzyl alcohol. The same apparent acceleration of rates for substrates that contain a hydroxyl group is observed in a comparison of α-secphenethyl alcohol with cumene. It is possible that these comparisons are not entirely fair, because the hydroxyl substituent is not as big as a methyl group. However, the reaction rate with toluene is three orders of magnitude slower than the rate with benzyl alcohol, even though toluene clearly has smaller substituents on the carbon bearing the abstractable hydrogens.

The presence of OH bonds in the alcohols gives rise to the possibility of H-bonding interactions between the substrate and Pt_2 ligands; such interactions may specifically facilitate the approach of alcohol substrates to the hydrophilic axial sites on the metal complex, preparatory to abstraction by $^3Pt_2^*$. Hypothetical docking interactions are shown in Figure 2.6.

Unfortunately, conclusive evidence for interactions between the alcohol and Pt_2 cannot be found through NMR. Previous workers[9, 41] have attributed (implicitly or explicitly) changes in the NMR spectra of alcohols to H-bonding interactions between a metal complex and the alcohol. Addition of acetic acid to a sample of the alcohol produces the same effect, however, suggesting that changes in the NMR signals are due to fast exchange of the hydroxyl proton on the NMR timescale, which could be catalyzed by any acidic substance. (See Appendix 2.1.)

Figure 2.6 Docking interaction between $^3[Pt_2(P_2O_5H_2)_4]^{4-*}$ and alcohol substrates

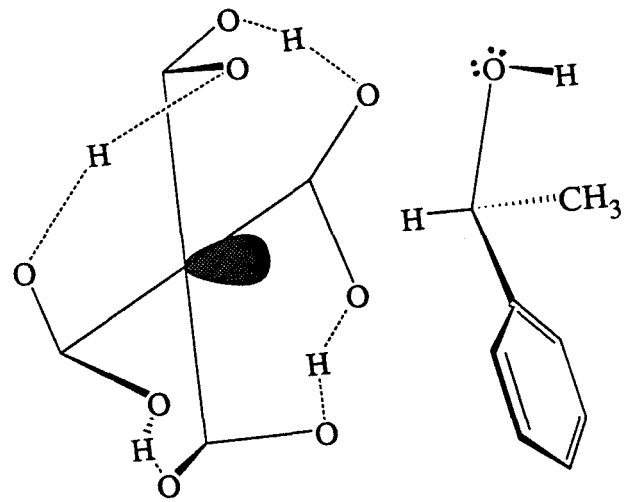

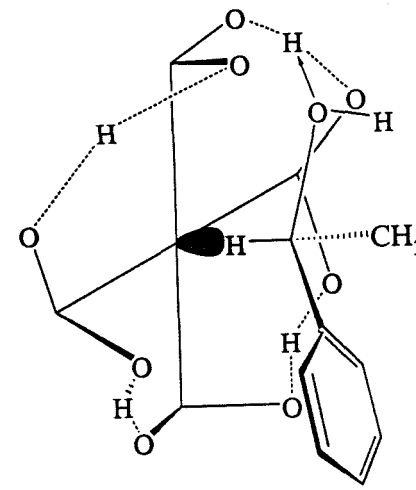

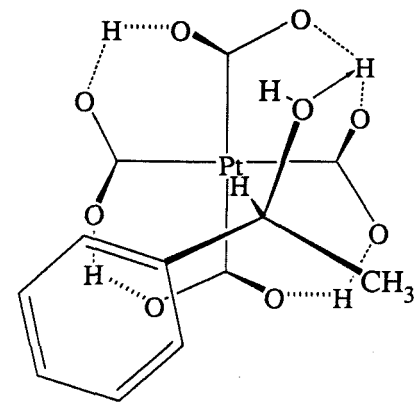

Steric effects two: too little, too big or just right

Slow quenching rates are observed with small aliphatic alcohols. To probe the energetics of the transition state for H-atom transfer, activation parameters for isopropanol were obtained from the results of temperature-dependent quenching studies[42] (Table 2.3). Interestingly, the observation of a small activation enthalpy (2.4 kcal/mole) for isopropanol suggests that the relatively high bond strength for this substrate does not significantly affect the H-atom abstraction rate. The free energy of activation is dominated by a large entropy term ($\Delta S^{\ddagger}$ = -33 e.u.), consistent with a fair amount of organization during the approach to the transition state. For effective H-atom abstraction, the α–CH bond must point toward the Pt_2 axial site, with the three other substituents on carbon pointing back from the axial site like a parachute. For isopropanol this may not be a preferred orientation. The small size of the methyl groups in isopropanol may allow the alcohol to swing freely and orient in ineffectual ways even when the postulated docking H-bond interactions are in place.

Table 2.3 Activation parameters for quenching of the triplet excited state of $[TBA]_4[Pt_2(P_2O_5H_2)_4]$ by isopropanol, benzyl alcohol, and α-secphenethyl alcohol in CH_3CN

Substrate	Pt_2 Quenching Rate ($M^{-1}s^{-1}$)	$\Delta H^{\ddagger}$ kcal/mole	$\Delta S^{\ddagger}$ e.u., cal/mole K
isopropanol $(CH_3)_2CHOH$	$5x10^3$	2.5	-33
benzyl alcohol $PhCH_2OH$	$3.5x10^6$	2.4	-19
α-sec-phenethyl alcohol $PhCHOH(CH_3)$	$1.5x10^6$ (±0.3)	1.6	-26

An increase in quenching rate is observed on going from isopropanol to sec-butanol, even though the αC-H bond-energy difference between the two substrates is expected to be negligible. The quenching rate with cyclohexylmethanol shows the same trend. The effect has been previously reported without explanation;[20] quenching rates measured in methanol were observed to increase in the series isopropanol, sec-butanol, and 2-pentanol. Addition of a bulkier group to the carbon bearing the abstractable hydrogen apparently limits the choice of substituents that can point toward the Pt_2 axial site, and thus lessens the need for reorientation on approach to the transition state. Predictions can be based on this postulate; for example, cyclohexanol is predicted to quench faster than isopropanol, and $\Delta S^{\ddagger}$ is expected to be less negative for cyclohexanol than for isopropanol. The very slow rates observed for quenching with ethanol and methanol probably reflect the higher bond strengths in these substrates, since for methanol any orientation of the docked alcohol should present a C-H bond toward the axial site.

The very similar activation enthalpies for benzyl alcohol and isopropanol (Table 2.3) indicate that bond strength does not control the difference in rates for the two substrates. The faster rate observed for benzyl alcohol is thus consistent with the postulate that a certain amount of bulk on the substrate encourages effective orientation of the alcohol in the transition state. Figure 2.7 demonstrates that addition of too much steric bulk to the substrate can slow the reaction, however. Abstraction rates for a series of benzylic alcohols of the general formula PhCH(OH)R are plotted versus substituent (R) cone angle.[43] The αC-H bond strengths within the series remain essentially constant.[33] Increasing steric bulk on the R substituent allows the alcohol less choice about what group can point in toward the axial site; this steric guidance is expected to ease the ordering requirements of the transition state and result in faster reactions (*vide supra*). Excessive bulkiness apparently causes steric congestion on the approach to the transition state, however, resulting in the observed decrease in rates.

Figure 2.7 Quenching rate constants versus substituent (R) cone angles for a series of alcohols PhCH(OH)R

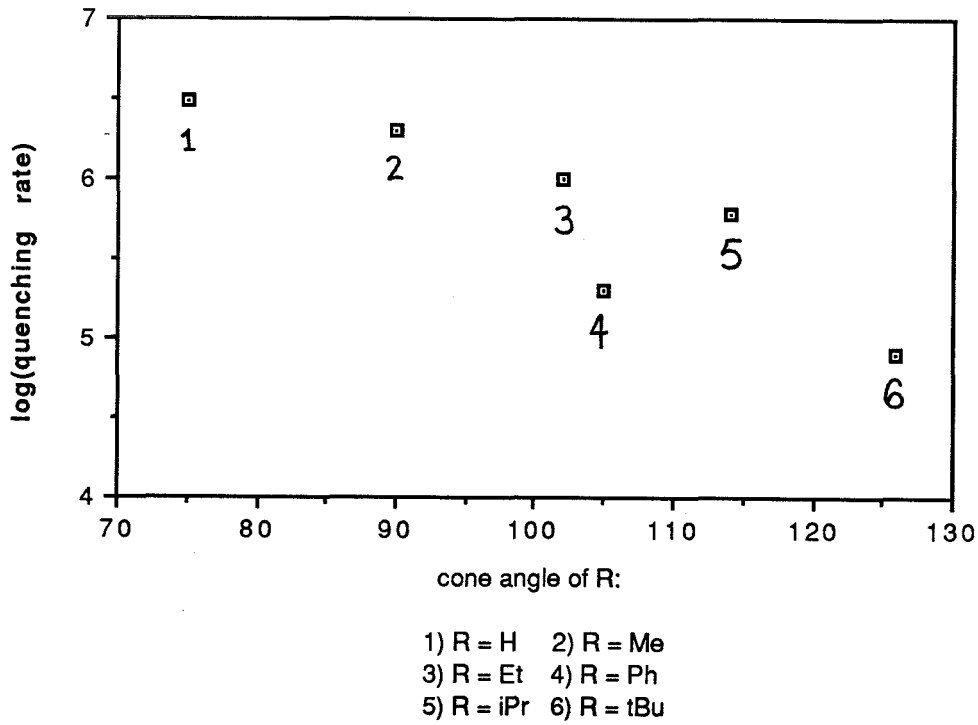

Temperature-dependent studies indicate that the activation entropy controls the quenching rate differences for benzyl alcohol and α-secphenethyl alcohol ($\Delta S^{\ddagger}$ = -16 and -25 e.u., respectively).[44] (See Table 2.3.) The increased negative activation entropy observed upon substitution of a methyl group for a hydrogen atom supports the postulate that there is a certain ideal amount of steric bulk that effectively directs the α–CH toward the axial site, but still allows a close approach for the abstraction step. The less negative value of the activation entropy for benzyl alcohol may also arise from the greater freedom of choice presented by the availability of two abstractable hydrogens for this substrate, as opposed to only a single hydrogen for α-secphenethyl alcohol.

The slow rates with the hydrocarbon substrates are consistent with a general lack of affinity of hydrophobic complexes for the hydrophilic axial site on the metal complex. Across the whole series of hydrocarbons studied, decreasing bond strength is accompanied by increasing steric bulk on the carbon bearing the abstractable hydrogen. For triphenylmethane and diphenylmethane, the general lack of affinity for the axial site apparently combines with steric hindrance caused by the bulky phenyl groups to override the driving force for abstraction caused by the very weak bonds. Within the toluene/cumene/ethylbenzene series, a maximum rate is observed for ethylbenzene. Toluene reacts slowest, indicating that the combination of higher bond strength and general lack of affinity for the axial site overcome the choice of three abstractable hydrogens and the steric situation most reminiscent of the "ideal" found for benzyl alcohol.

Comparison with Organic H-atom Abstractors and Conclusions

An organic analogue of $^3Pt_2^*$ is the $^3n,\pi^*$ excited state of benzophenone.[2] The excited state lifetimes of the two molecules are equivalent; the triplet energy of benzophenone is higher by 11 kcal/mol. Previous work using a series of triorganostannanes, -germanes, and -silanes demonstrated that H-atom transfer quenching rates with $^3Pt_2^*$ qualitatively parallel the rates observed for the same quenchers with electronically excited benzophenone.[22]

The quenching rates of selected alcohol and hydrocarbon substrates with $^3Pt_2^*$ and excited benzophenone,[45, 46] and the ground-state reaction rates of the same substrates with $tBuO\cdot$,[47, 48, 49, 50] are shown in Table 2.4. The inorganic system reacts more selectively than the organic systems with the H-atom transfer substrates studied; while the quenching rates with the organic abstractor species vary by only one or two orders of magnitude, quenching rates with $^3Pt_2^*$ span four orders of magnitude.

Table 2.4 Comparative H-atom abstraction rates for selected substrates with $^3[TBA]_4[Pt_2(P_2O_5H_2)_4]^*$, $^3n,\pi^*$ benzophenone, and *tert*-butoxy radical

Substrate	Quenching Rate with $^3Pt_2^*$ ($M^{-1}s^{-1}$)	Quenching Rate with t-BuO· ($M^{-1}s^{-1}$)	Ref.	Quenching Rate with n,π^* ($M^{-1}s^{-1}$)	Ref.
cumene	$5x10^3$	$8.7x10^5$	49	$5.2x10^5$	50
ethylbenzene	$1.4x10^4$	$1.05x10^6$	49	$5.0x10^5$	50
toluene	$4x10^3$	$2.3x10^5$	49	$1.7x10^5$	50
benzhydrol	$3x10^5$	$6.9x10^6$	49	$4.2x10^7$	50
α-secphenethyl alcohol	$1.8x10^6$	$1.8x10^6$	49		
sec-butanol	$9x10^3$			$1.7x10^6$	50
isopropanol	4x103	$1.8x10^6$	49	$1.3x10^6$	50
ethanol	10^3	$1.1x10^6$	49	$5.6x10^5$	50
methanol	130	$2.9x10^5$	49		

The novel and rather sensitive steric control available for H-atom abstraction using $^3Pt_2^*$ raises the possibility of selective functionalization of organic substrates. The active sites of Pt_2 resemble tulips or magnolias; the excited-state orbitals pointing out from the axial sites are surrounded by a cup of petallike ligands (Figure 2.6). In contrast to the insensitive abstraction reactivity observed for the organic abstractors, $^3Pt_2^*$ demonstrates a refined hunger for hydrogen atoms attached to substrates that are attracted by its hydrophilic petals. Even more discrimination is supplied by the degree of openness of the petals; only substrates that are just the right size are allowed to approach the center of the flower with the correct orientation for quick reaction.

Appendix 2.1. NMR data for alcohols in the presence of Pt_2

Spectra of α-secphenethyl alcohol, α-secphenethylalcohol with added water, and α-secphenethylalcohol with 10^{-3} equivalents of Pt_2 are shown in Figure 2.8(a-c). The chemical shift of the hydroxyl proton varies slightly with the concentration of the alcohol or with the concentration of added water, but the splitting of this peak and the methine peak do not change under such conditions. In the presence of very small amounts of Pt_2 (10^{-5} M), no changes are observed in the NMR spectrum of 0.15 M alcohol. At concentrations $\geq 10^{-4}$ M Pt_2, however, the hydroxyl residue and the residual H_2O singlet broaden into a single low, broad hump. The methine residue, originally a resolved quartet of doublets (from coupling to three methyl protons and the hydroxyl proton), collapses to a sharp quartet. While the spectrum of the alcohol is not affected by addition of [TBA]PF_6, the same changes are observed upon addition of acetic acid (Figure 2.8(d)).

Figure 2.8 ^1H NMR spectra of 0.15 M α-secphenyl alcohol in CD_3CN a) alone b) with 1.1 M H_2O c) with .001 M Pt_2 d) with 0.017 M acetic acid

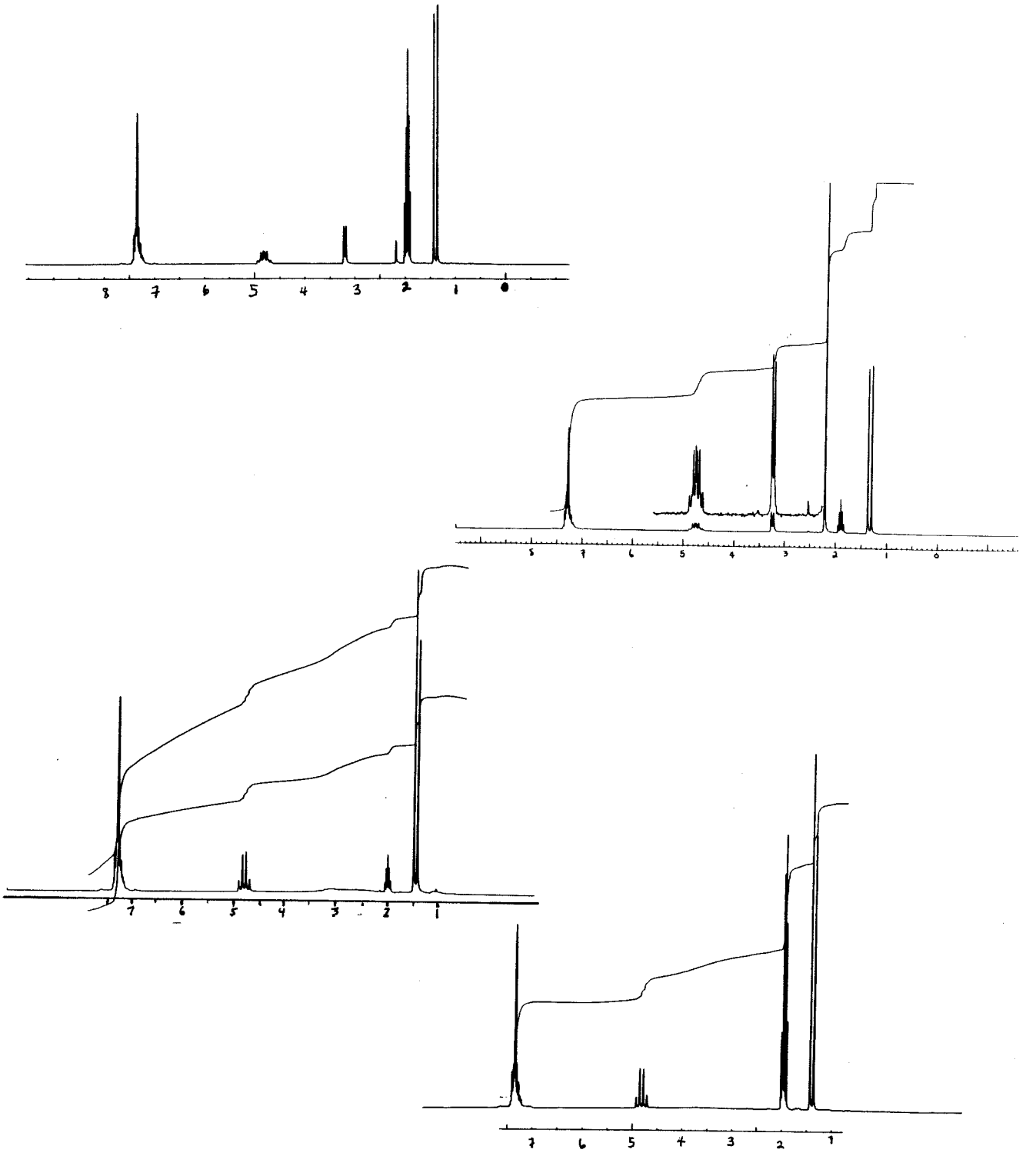

Appendix 2.2. Curved Stern-Volmer plot for α-sec-phenethyl alcohol

Figure 2.9 Stern-Volmer plot for α-secphenethyl alcohol

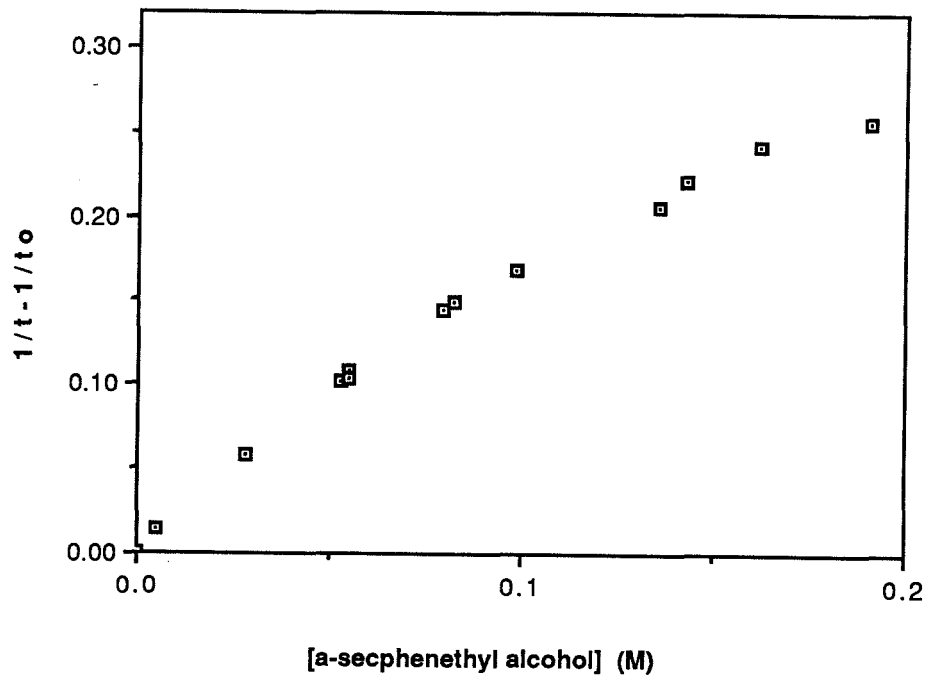

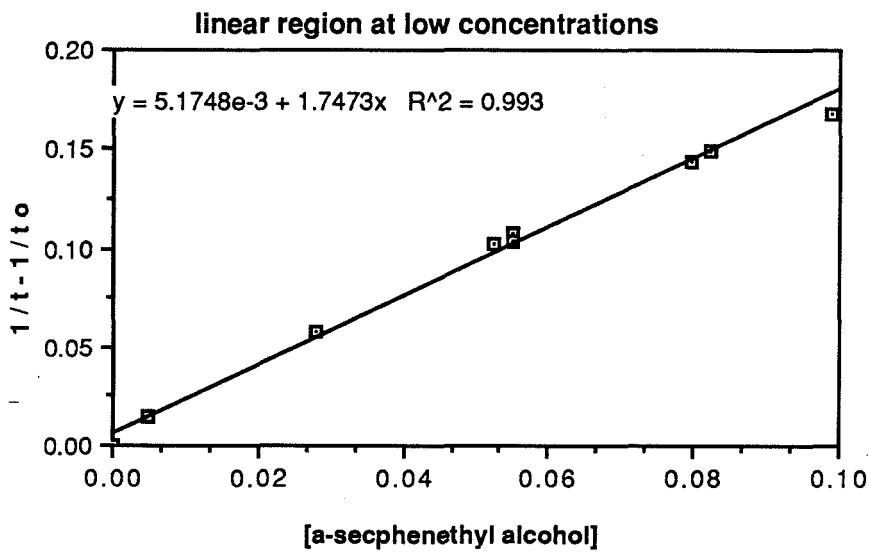

References

1. As timescales at which reactions can be studied get shorter, it should become possible to study the initial interactions of so-called "atom transfer" reactions. The definition of atom transfer can then be modified.

2. Turro, N. J. *Modern Molecular Photochemistry* (Benjamin/Cummings, Menlo Park, NJ, 1978).

3. Golden, David M. and Benson, Sidney W. (1968). "Free-Radical and Molecule Thermochemistry from Studies of Gas-Phase Iodine-Atom Reactions." See also Ref. 31.

4. The lifetime of the diradical excited state indirectly affects H-atom abstraction reactivity. H-atom abstraction must occur fast enough to compete with other deactivation modes for the excited state; Turro (Ref.2) points out that only exothermic H-atom transfers will generally have low enough activation energies to occur faster than other excited state decay processes. The excited state lifetime simply reflects how fast the other deactivation modes are. Longer-lived excited states allow observation of slower H-atom abstraction rates, because even slow H-atom transfers can compete with very slow native deactivation processes.

5. Kerr, J. A. *Chem. Rev.* **66**, 465 (1966). "Bond Dissociation Energies by Kinetic Methods."

6. Tyler, David R. *Prog. Inorg. Chem.* **36**, 125 (1988). "Mechanistic Aspects of Organometallic Radical Reactions."

7. Hanckel, J. M.; Lee, K-W; Rushman, P. and Brown, T. L. *Inorg. Chem.* **25**, 1852 (1986). "Steric and Electronic Effects on Atom Transfer Reactions of $Re(CO)_4L\cdot$ Radicals with Organic Halides and $HSn(n\text{-}C_4H_9)_3$."

8. Lee, Kang-Wook and Brown, Theodore L. *J. Am. Chem. Soc.* **109**, 3269 (1987). "On the Nature of Halogen Atom Transfer Reactions of $Re(CO)_4L$ Radicals."

9. Thorp, H. Holden; Van Houton, J. and Gray, Harry B. *Inorg. Chem.* **28**, 889 (1989). "Excited-State Properties of Dioxorhenium(V). Generation and Reactivity of Dioxorhenium(VI)."

10. Yam, V. W-W.; Che, C-M and Tang, W-T *J. Chem. Soc., Chem. Commun.* 100 (1988). "Metal-Oxo Photooxidants. Photochemical Oxidation of Hydrocarbons by Trans-Dioxo Complexes of Ruthenium(VI) and Osmium(VI)."

11. Brown, Stephen H. and Crabtree, Robert H. *J. Chem. Soc., Chem. Commun.* 970 (1987). "Alkane Functionalisation on a Preparative Scale by Mercury Photosensitisation."

12. Hill, Richard J.; Kemp, Terence J.; Allen, David M. and Cox, Alan *J. Chem. Soc. Faraday Trans. I* **70**, 847 (1974). "Absorption Spectrum, Lifetime and Photoreactivity Towards Alcohols of the Excited State of the Aqueous Uranyl Ion (UO_2^{2+})."

13. Burrows, Hugh D. and Formosinho, Sebastiao J. *J. Chem. Ed.* **55**, 125 (1978). "Uranyl Luminescence Quenching."

14. Matushima, Ryoka *J. Am. Chem. Soc.* **94**, 6010 (1972). "Mechanism of Quenching of the Uranyl Fluorescence by Organic Compounds."

15. Roundhill, D. Max; Shen, Zhong-Ping; King, Christopher and Atherton, Stephen J. *J. Phys. Chem.* **92**, 4088 (1988). "Triplet Excited-State Chemistry of Diplatinum(II) Complexes. Comparative Spectroscopy and Quenching Rate Constants between the Tetrakis(μ-pyrophosphito)diplatinate(II) and the Tetrakis[μ-methylenebis(phosphonito)]diplatinate(II) Tetraanions."

16. Smith, David C., Ph. D. Dissertation (California Institute of Technology, 1989). David Smith showed that both cyclohexadiene and cyclohexene also directly quench the emission of Pt_2, presumably by a combination of pathways including atom transfer, and perhaps addition to the alkene.

17. Roundhill, D. Max; Atherton, Stephen J. and Shen, Zhong-Ping *J. Am. Chem. Soc.* **109**, 6076 (1987). "Hydrogen Atom Abstraction from C-H, P-H, Si-H, and Sn-H Bonds by the Triplet Excited State of the Tetrakis(μ-pyrophosphito)diplatinum(II) Tetraanion. Spectroscopic Observation of the Mixed-Valence Hydride Complex $Pt_2(\mu\text{-}P_2O_5H_2)_4H^{4-}$."

18. Roundhill, D. Max; Shen, Zhong-Ping and Atherton, Stephen J. *Inorg. Chem.* **26**, 3833 (1987). "Reactivity of the Triplet State of the Tetrakis(μ-pyrophosphito)diplatinate(II) Tetraanion with Alkenes and Alkynes. Comparison with the Energy-Transfer Photosensitizer and Diradical Chemistry of Ketone Triplets."

19. Marshall, Janet L.; Steigman, Albert E. and Gray, Harry B. in *Excited States and Reactive Intermediates* (ed. Lever, A.B.P.) (American Chemical Society, Washington, D.C., 1986), pp.166-176.

20. Che, Chi-Ming; Lee, Wai-Man; Cho, Kar-Cheong; Harvey, Pierre D. and Gray, Harry B. *J. Phys. Chem.* **93**, 3095 (1989). "Photoreactions of Organic Halides, Alcohols and Olefins with Tetrakis(pyrophosphito)diplatinate(II)."

21. Vlcek, Antonin, Jr., and Gray, Harry B. *J. Am. Chem. Soc.* **109**, 286 (1987). "Binuclear Platinum(II) Photochemistry. Rates of Hydrogen Atom Transfer from Organometallic Hydrides to Electronically Excited $Pt_2(P_2O_5H_2)_4^{4-}$."

22. Vlcek, Antonin, Jr., and Gray, Harry B. *Inorg. Chem.* **26**, 1997 (1987). "Binuclear Platinum(II) Photochemistry. Reactions of Organometallic Hydrides with Electronically Excited Tetrakis(pyrophosphito)diplatinate(II)."

23. Che, Chi-Ming; Kwong, Hoi-Lun; Cho, Kar-Cheong; Harvey, Pierre D. and Gray, Harry B. *Catalysis Lett.* **1**, 261 (1988). "Photochemical Hydrogen Atom Transfer from Aldehydes to Binuclear Platinum(II)."

24. Roundhill, D. Max *J. Am. Chem. Soc.* **107**, 4354 (1985). "Excited-State Chemistry of Tetrakis(μ-pyrophosphito)diplatinum(II). Photoinduced Addition of Aryl Bromides and Iodides to the Binuclear Complex and the Photoinduced Catalytic Conversion of Isopropyl Alcohol into Acetone and Hydrogen."

25. Harvey, Pierre D. and Gray, Harry B. *New J. Chem.* **11**, 595 (1987). "Photoconversion of Ethanol to Acetaldehyde and Molecular Hydrogen in the Presence of Tetrapyrophosphitodiplatinate (II)."

26. Harvey, Erica L.; Stiegman, Albert E.; Vlcek, Antonin, Jr. and Gray, Harry B. *J. Am. Chem. Soc.* **109**, 5233 (1987). "Dihydridotetrakis(pyrophosphito(2-))-diplatinate(III)."

27. Che, Chi-Ming; Lee, Wai-Man and Cho, Kar-Cheong *J. Am. Chem. Soc.* **110**, 5407 (1988). "Photochemistry of Platinum(III,III) Pyrophosphite Complexes. Efficient Photochemical Reduction of $[Pt_2(pop)_4X_2]^{4-}$ to $[Pt_2(pop)_4]^{4-}$ in Methanol."

28. Pearson, Ralph G. *Chem. Rev.* **85**, 41 (1985). "The Transition-Metal-Hydrogen Bond."

29. Roecker, Lee and Meyer, Thomas J. *J. Am. Chem. Soc.* **109**, 746 (1987). "Hydride Transfer in the Oxidation of Alcohols by $[(bpy)_2(py)Ru(O)]^{2+}$. A k_H/k_D Kinetic Isotope Effect of 50."

30. a) Stiegman, Albert E.; Rice, Steven F.; Gray, Harry B. and Miskowski, Vincent M. *Inorg. Chem.* **26**, 1112 (1987). "Electronic Spectroscopy of d^8-d^8 Diplatinum Complexes. $^1A_{2u}(d\sigma^*\rightarrow p\sigma)$, $^3E_u(d_{xy},d_{yz}\rightarrow p\sigma)$, and $^{3,1}B_{2u}(d\sigma^*\rightarrow d_{x^2-y^2})$ Excited States of $Pt_2(P_2O_5H_2)_4^{4-}$."

b) Nocera, D. G.; Winkler, J. R.; Yocom, K. M.; Bordignon, E. and Gray, H. B. *J. Am. Chem. Soc.* **106**, 5145 (1984). "Kinetics of Intramolecular Electron Transfer from Ru^{II} to Fe^{III} in Ruthenium-Modified Cytrochrome *c*."

31. McMillen, Donald F. and Golden, David M. *Ann. Rev. Phys. Chem.* **33**, 493 (1982). "Hydrocarbon Bond Dissociation Energies."

32. Korcek, S.; Chenier, J. H. B.; Howard, J. A. and Ingold, K. U. *Can. J. Chem.* **50**, 2285 (1972). "Absolute Rate Constants for Hydrocarbon Oxidation. XXI. Activation Energies for Propagation and the Correlation of Propagation Rate Constants with Carbon-Hydrogen Bond Strengths."

33. Benson, S. W.; Cruickshank, F. R.; Golden, D. M.; Haugen, G. R.; O'Neal, H. E.; Rodgers, A. S.; Shaw, R. and Walsh, R. (1968). "Additivity Rules for the Estimation of Thermochemical Properties."

34. The bond energies used to graph the R_3EH (E = Sn, Ge, Si) quenching rates have been measured only for Me_3SiH and Bu_3SnH. See Ref.21 and Jackson, R. A. *J. Organomet. Chem.* **166**, 17-19 (1979). The other energies shown are simply estimates based on interpolation between the two known points; hence the error bars.

35. Bard, A. J., ed. *Encyclopedia of Electrochemistry of the Elements* (Marcel Dekker, New York, 1982). For benzhydrol, α-secphenethyl alcohol and benzyl alcohol, the oxidation wave was reported to be >2.0 V vs Ag/Ag^+. For isopropanol, 2.5 V vs Ag/Ag^+ was reported; toluene, 1.98 V vs SCE, and cumene, 1.87 V vs Ag/Ag^+. The reduction of benzhydrol was reported as -2.90 V vs SCE.

36. Robert Sweeney, work in progress at California Institute of Technology. Experiments to explore the possibilities of photochemical C-H activation in higher bond strength hydrocarbons are currently under way.

37. Melander, Lars and Saunders, William H., Jr. *Reaction Rates of Isotopic Molecules* (Wiley-Interscience, New York, 1980).

38. Bryan, Samuel A.; Dickson, Mark K. and Roundhill, D. Max *Inorg. Chem.* **26**, 3878 (1987). "Synthesis, Reactivity, Kinetics, and Photochemical Studies on Tetrakis(μ-pyrophosphito)diplatinate(II) and Dihalotetrakis(μ-pyrophosphito)diplatinate(III) Complexes. Comparison of the Substitution Mechanisms of the Diplatinum(III) Complexes with those of Monomeric Platinum(II) and Platinum(IV) Compounds."

39. Che, Chi-Ming; Mak, Thomas C. W.; Miskowski, Vincent M. and Gray, Harry B. *J. Am. Chem. Soc* **108**, 7840 (1986). "Binuclear Platinum (III) Complexes. Preparation, Structure, and $d\sigma d\sigma^*$ Spectrum of $[Bu_4N]_2[Pt_2(P_2O_5H_2)_4(CH_3CN)_2]$."

40. Che, Chi-Ming; Butler, Leslie G.; Grunthaner, Paula J. and Gray, Harry B. *Inorg. Chem.* **24**, 4662 (1985). "Chemistry and Spectroscopy of Binuclear Platinum Diphosphite Complexes."

41. Fox, M. A.; Cardona, R. and Gaillard, E. *J. Am. Chem. Soc.* **109**, 6347 (1987). "Photoactivation of Metal Oxide Surfaces: Photocatalyzed Oxidation of Alcohols by Heteropolytungstates."

42. Lisa Giaimo measured the activation parameters for α-secphenethyl alcohol as a Summer Undergraduate Research Fellow in 1987. (Temperature varied from 0-60°C.) Al Stiegman measured the activation parameters for isopropanol and benzyl alcohol.

43. Tolman, Chadwick A. *Chem Rev.* **77**, 313 (1977). "Steric Effects of Phosphorous Ligands in Organometallic Chemistry and Homogeneous Catalysis." The specific cone angles used in this work are reported on p.345.

44. The activation enthalpy is actually a bit smaller for α-secphenethyl alcohol, which has a slightly weaker bond than benzyl alcohol. The experiments were performed by two different researchers, however, so the two observed values are probably indistinguishable within experimental error.

45. Scaiano, Juan C. *J. Photochem.* **2**, 81 (1973). "Intermolecular Photoreductions of Ketones."

46. Pearson, D. E. and Moss, M. Y. *Tet. Lett.* **39**, 3791 (1967). "A Possible Steric Effect in the Photooxidation of Secondary Alcohols by Benzophenone."

47. The ground state tert-butoxy (tBuO·) radical has been used extensively as a model for the n,p* excited state of benzophenone because the electronic appearance of the oxygen in the two molecules is similar; H-atom transfer rates in the two systems also correlate well.

48. Chatgilialoglu, C.; Ingold, K. U.; Lusztyk, J.; Nazran, A. S. and Scaiano, J. C. *Organomet.* **2**, 1332 (1983). "Formation, Decay, and Spectral Characterization of Alkyl- and Aryl-Substituted Carbon-, Silicon-, Germanium-, and Tin-Centered Radicals."

49. Paul, H.; Small, R. D. and Scaiano, J. C. *J. Am. Chem. Soc.* **100**, 4520 (1978). "Hydrogen Abstraction by tert-Butoxy Radicals. A Laser Photolysis and Electron Spin Resonance Study."

50. Scaiano, J. C. *J. Am. Chem. Soc.* **102**, 5399 (1980). "Detection of Trialkylstannyl Radicals Using Laser Flash Photolysis."

Chapter 3. Dihydridotetrakis(pyrophosphito(2-))diplatinate(III)

This chapter is substantially based on Reference 1.[1] Additional details have been supplied, and the supplementary NMR simulation materials have been placed in the discussion section rather than appended at the end.

Introduction

Hydrogen-atom transfer has been established as an important reaction pathway for the $d\sigma^*p\sigma$ triplet excited state of $[Pt_2(P_2O_5H_2)_4]^{4-}$ (Pt_2). Substrates that serve as H-atom donors include alcohols with α(C-H) bonds and triorganosilanes, -germanes, and -stannanes. These substrates all react photochemically with Pt_2 upon 370-nm irradiation to produce the same complex,[2] which is characterized by strong absorption at 314 nm. NMR and IR spectroscopic studies reported here show that the common photoproduct is a binuclear platinum(III) dihydride, $[Pt_2(P_2O_5H_2)_4H_2]^{4-}$ (Pt_2H_2).

Experimental Section

The title compound (Pt_2H_2) is generated by 370-nm narrow-band irradiation of freeze-pump-thaw degassed acetonitrile solutions of $[TBA]_4[Pt_2(P_2O_5H_2)_4]$ containing the hydrogen-atom donor. The extent of the photoreaction and stability of the photoproduct strongly depend on the nature of the substrate; Pt_2H_2 usually decomposes thermally, regenerating Pt_2 by reaction with unreacted substrate as well as with other photoproducts. We have found that Pt_2H_2 is reasonably stable only when generated by photolysis of either Bu_3SnH, $PhCH(OH)CH_2CH_3$, or $PhCH(OH)CH_3$ with Pt_2. The latter

H donor was used in all experiments described here because conversion of Pt_2 to Pt_2H_2 at concentrations as high as 0.04 M was achieved (the half-life of Pt_2H_2 is at least 1.5 weeks in this case). The alcohols were purchased from Aldrich and distilled before use. Acetonitrile (B and J High Purity Solvent) and CD_3CN (Aldrich Gold Label) were used as received. Both ^1H and ^{31}P NMR spectra were obtained on a 400 MHz JNM-GX400 FT NMR spectrometer after direct irradiation of a vacuum-sealed 10-mm NMR tube containing Pt_2 and $PhCH(OH)CH_3$. The IR spectrum was taken on a Beckman IR 4240; for this experiment the photoproduct was generated in a photolysis cell and transferred to the IR cell in a rigorous N_2 atmosphere. A Shimadzu UV-260 spectrometer was used to record the UV-Vis absorption spectra. The composition of the atmosphere above the irradiated solutions before and after reaction with HCl and DCl was analyzed by mass spectrometry; the stoichiometry of release of H_2 during photolysis of the intermediate was measured by Toepler pumping.

Computer simulations were performed by using the Nicolet NMRSIM program at the Southern California Regional NMR Facility at Caltech. Because of the prohibitive number of spins (10-12) in the actual isotopomers, smaller spin systems (<7) were studied extensively and the results were extrapolated where possible. For example, $J_{P\text{-}O\text{-}P}$>42 Hz produces a triplet in the ^1H spectrum of an AA'XX' (A=^1H; X=^{31}P) spin system and a quintet with the same splitting in the ^1H spectrum of an AA'XX'X"X"' spin system. A reasonable extrapolation is to assume that the ^1H spectrum of the actual AA"XX'X"X"'X"''X"''''X''''''X'''''' spin system consists of a nine-line pattern with the same splitting for $J_{P\text{-}O\text{-}P}$ >42 Hz.

The following set of coupling constants was used, although simulations on the smaller spin systems did not require all the values: $^2J_{P\text{-}H}$, 11 Hz; $^3J_{P\text{-}H}$, 3.7 Hz (also could be $^4J_{P\text{-}H}$); $^1J_{Pt\text{-}H}$, 884 Hz; $^2J_{Pt\text{-}H}$, 103 Hz; $^3J_{H\text{-}H}$, 26 Hz; $^2J_{P\text{-}O\text{-}P}$, 45 Hz (any value >42 Hz gives the same result); $^1J_{Pt\text{-}P}$, 2190 Hz; $^1J_{Pt\text{-}Pt}$, 8000 Hz. All

other coupling constants were defined as 0.01 Hz. Very similar systems containing <10 spins have been completely simulated; these simulations indicate that P-P couplings occur through the P-Pt-P and P-Pt-Pt-P linkages as well as through the P-O-P linkage.[3] The magnitudes of the P-P couplings other than via the P-O-P bridge could not be determined in the present work, however.

Results and Discussion

The ^{31}P NMR spectrum of the 314-nm photoproduct (Figure 3.1) consists of an apparent triplet at 27.9 ppm with a splitting of 7.4 Hz (vide infra) and ^{195}Pt satellites (J_{Pt-P}=2200 Hz) spanning ~100 Hz. The spectra measured at 300 and 230 K are identical. The chemical shift and Pt-P coupling are consistent with known[4] binuclear Pt(III) complexes containing axial ligands: Pt_2X_2= $[Pt_2(P_2O_5H_2)_4X_2]^{4-}$; X= Cl, Br, SCN, NO_2. Proton decoupling of the ^{31}P NMR spectrum collapses the central peaks to a singlet.

The ^{1}H NMR spectrum (Figure 3.2) exhibits a complicated symmetric pattern centered at -9.6 ppm, a chemical shift consistent with the presence of terminal hydrido ligands.[5, 6] Analysis of the spectrum suggests an axial structure (H-Pt-Pt-H linkage) in which the presence of chemically equivalent but magnetically inequivalent atoms results in a deceptively simple pattern.[7] Because of the 33.8% natural abundance of NMR-active (I=1/2) ^{195}Pt (*Pt), the spectrum is further complicated by the presence of three isotopomeric forms of Pt_2H_2: H-Pt-Pt-H (44%), H-*Pt-Pt-H (45%) and H-*Pt-*Pt-H (11%).

Figure 3.1 ^{31}P NMR spectrum of the photoproduct generated by 370-nm irradiation (3.5 h) of a 0.043 M $[TBA]_4[Pt_2(P_2O_5H_2)_4]$ and 0.083 M $PhCH(OH)CH_3$ degassed CD_3CN solution

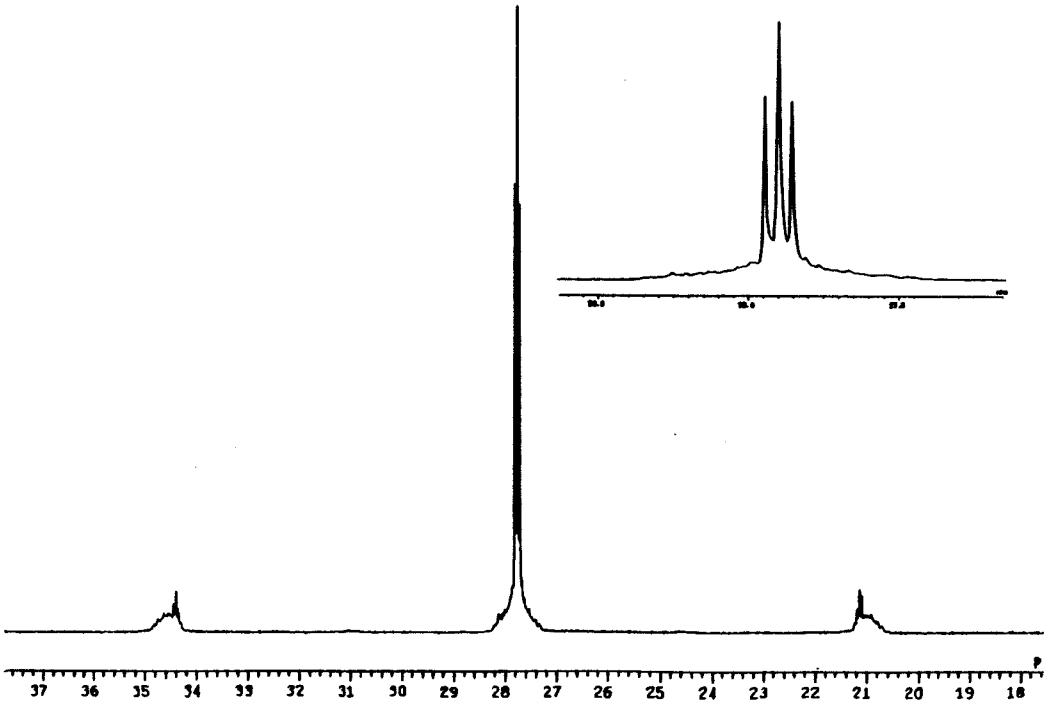

Figure 3.2 ^{1}H NMR spectrum of the photoproduct generated by 370-nm irradiation (1.5 h) of a 0.0081 M $[TBA]_4[Pt_2(P_2O_5H_2)_4]$ and 0.016 M $PhCH(OH)CH_3$ degassed CD_3CN solution

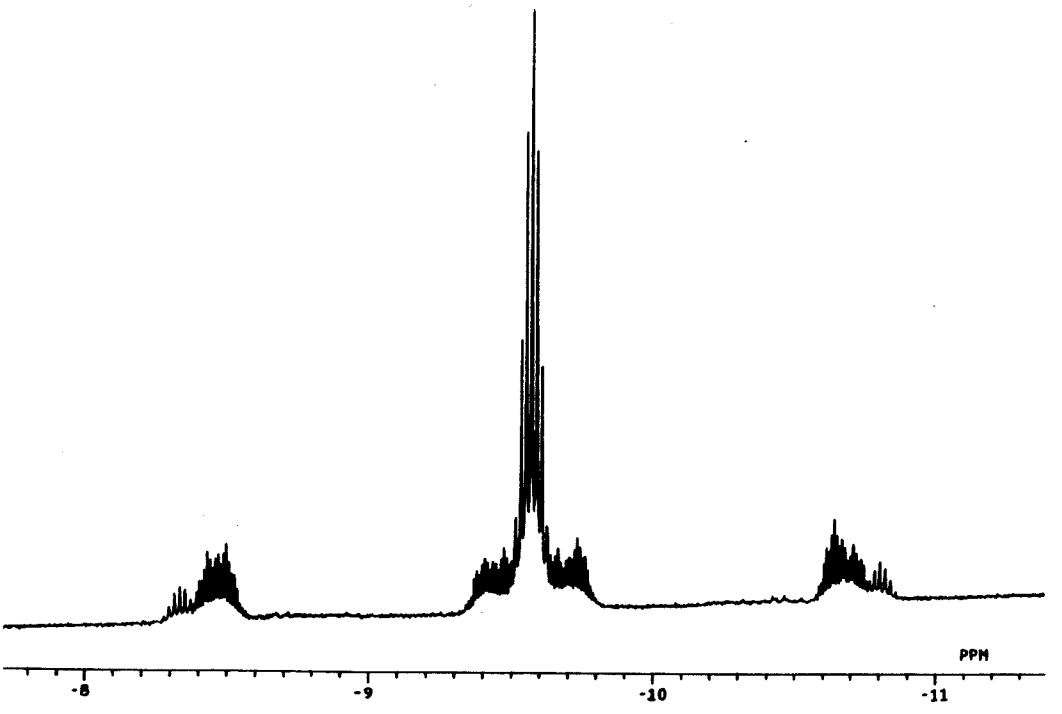

In the simplest symmetric isotopomer (both Pt nuclei are NMR-inactive), all eight ^{31}P atoms have the same chemical shift but can couple to one another via the P-O-P bridges, thereby influencing the ^{1}H spectrum in a manner dependent on the magnitude of the ^{31}P-^{31}P coupling. The two ^{1}H nuclei are similarly chemically equivalent and magnetically inequivalent, so the molecule is an AA'XX'X"X"'X""X"""X""""X"""""" spin system (A, ^{1}H; X, ^{31}P). For large J_{P-O-P}, the ^{31}P nuclei effectively act as an equivalent group to the ^{1}H nuclei, splitting their signal into the observed nine-line pattern in the central peak. (Seven lines are clearly visible; the other two are presumably buried under the satellites to either side.) The apparent splitting of 7.3 Hz agrees with that seen in the ^{31}P NMR spectrum, but simulation of both ^{1}H and ^{31}P spectra on analogous systems containing two (Figures 3.3, 3.5) or four (Figures 3.4, 3.6) ^{31}P atoms has shown that this splitting is actually the average of the ^{31}P-^{1}H couplings, $^{2}J_{P-H}$ = 11.0 and $^{3}J_{P-H}$ = 3.7 Hz.[8]

The small, finely split satellites at the sides of the central peak in the ^{1}H spectrum correspond to $^{2}J_{Pt-H}$ coupling (103 Hz) in the asymmetric isotopomer (spin system AA'XX'X"X"'X""X"""X""""M, M = *Pt). The analogous inner part of the more distant peaks corresponds to $^{1}J_{Pt-H}$ coupling (884 Hz). The apparent doublet character in each of the four multiplets corresponding to the asymmetric molecule is ^{1}H-^{1}H coupling (26 HZ); the further fine splitting arises from $^{1}J_{P-H}$ and $^{3}J_{P-H}$ couplings. This interpretation is supported by the ^{31}P-decoupled spectrum shown in Figure 3.5, which strongly emphasizes the doublet character of these peaks. Only the central phosphorous signal was accessed with the decoupler used; this may account for the apparently incomplete decoupling of the outer satellites. A computer simulation using an AA'XX'X"X"'M system (Figures 3.4 and 3.6) and a remarkably accurate first-order hand simulation using the coupling constants reported above (Figure 3.7) also support the interpretation of the finely split satellite regions of the spectrum.

Figure 3.3 Simulated ^1H NMR spectra of three isotopomeric forms of the hypothetical $Pt_2(POP)H_2$ molecule (4, 5, 6 spins)

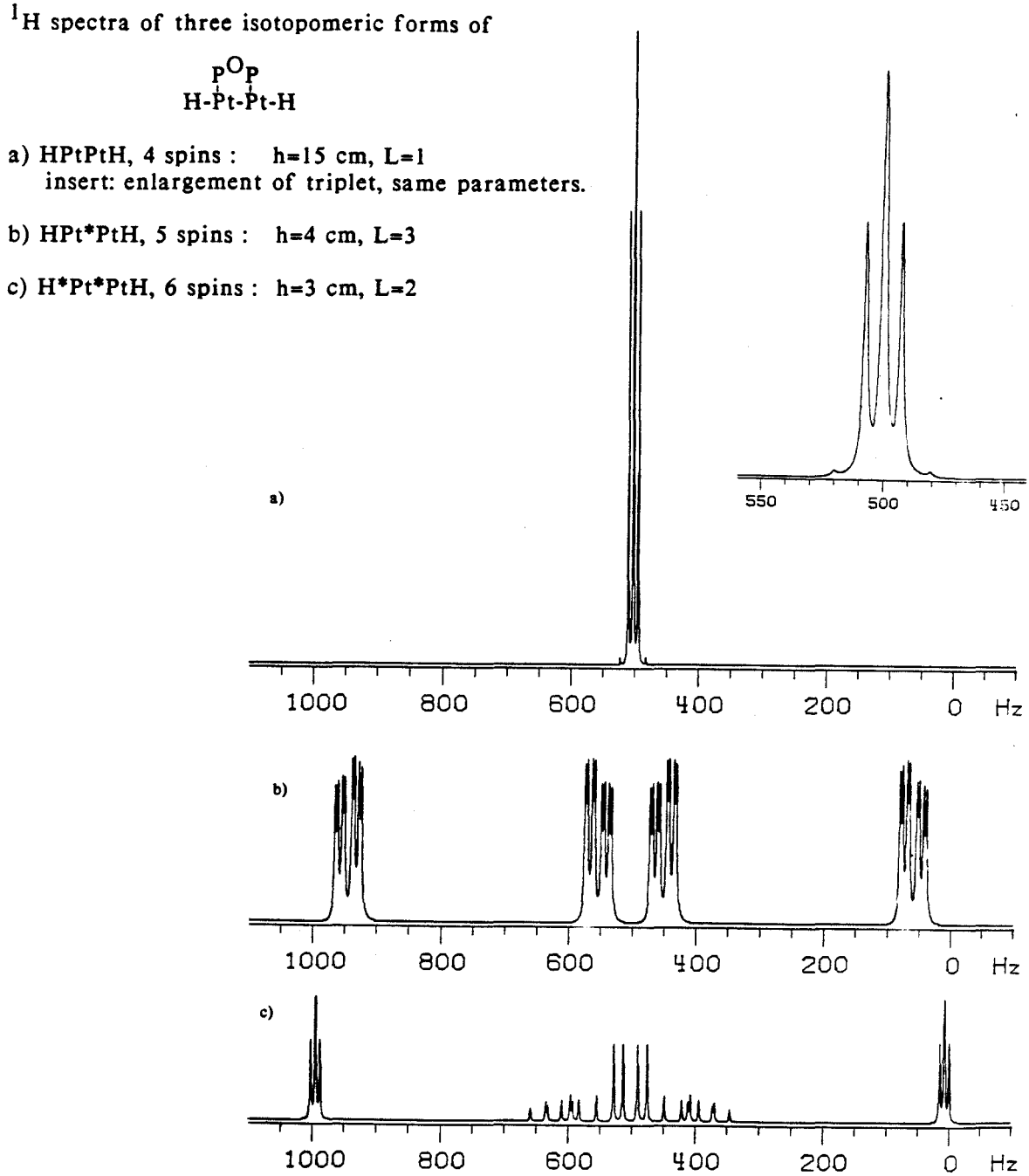

Figure 3.4 Simulated ^1H NMR spectra of two of the isotopomeric forms of the hypothetical $Pt_2(POP)_2H_2$ molecule (6, 7 spins)

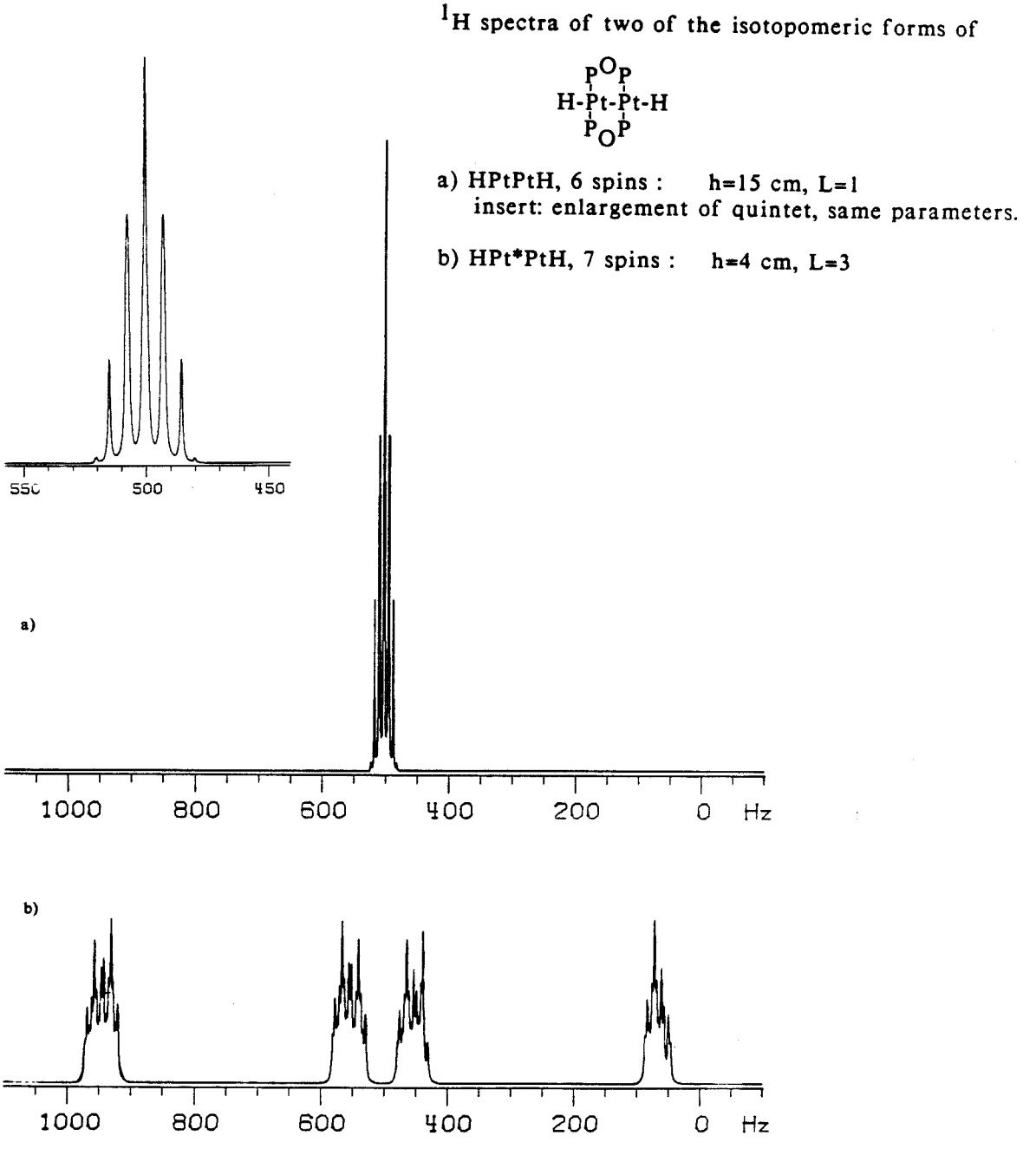

Figure 3.5 Simulated ^{31}P NMR spectra of three isotopomeric forms of the hypothetical $Pt_2(POP)H_2$ molecule (4, 5, 6 spins)

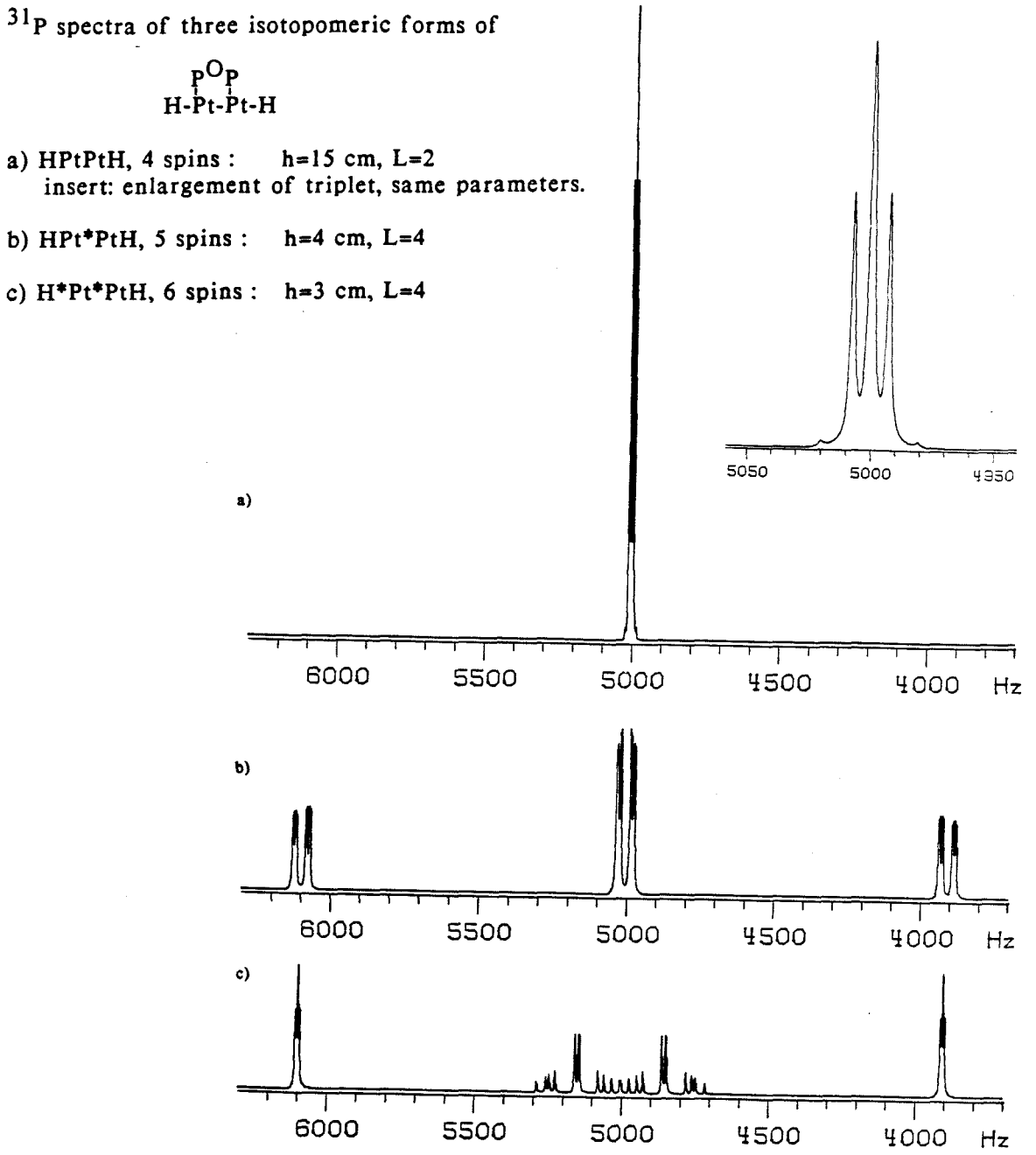

Figure 3.6 Simulated ^{31}P NMR spectra of two of the isotopomeric forms of the hypothetical $Pt_2(POP)_2H_2$ molecule (6, 7 spins)

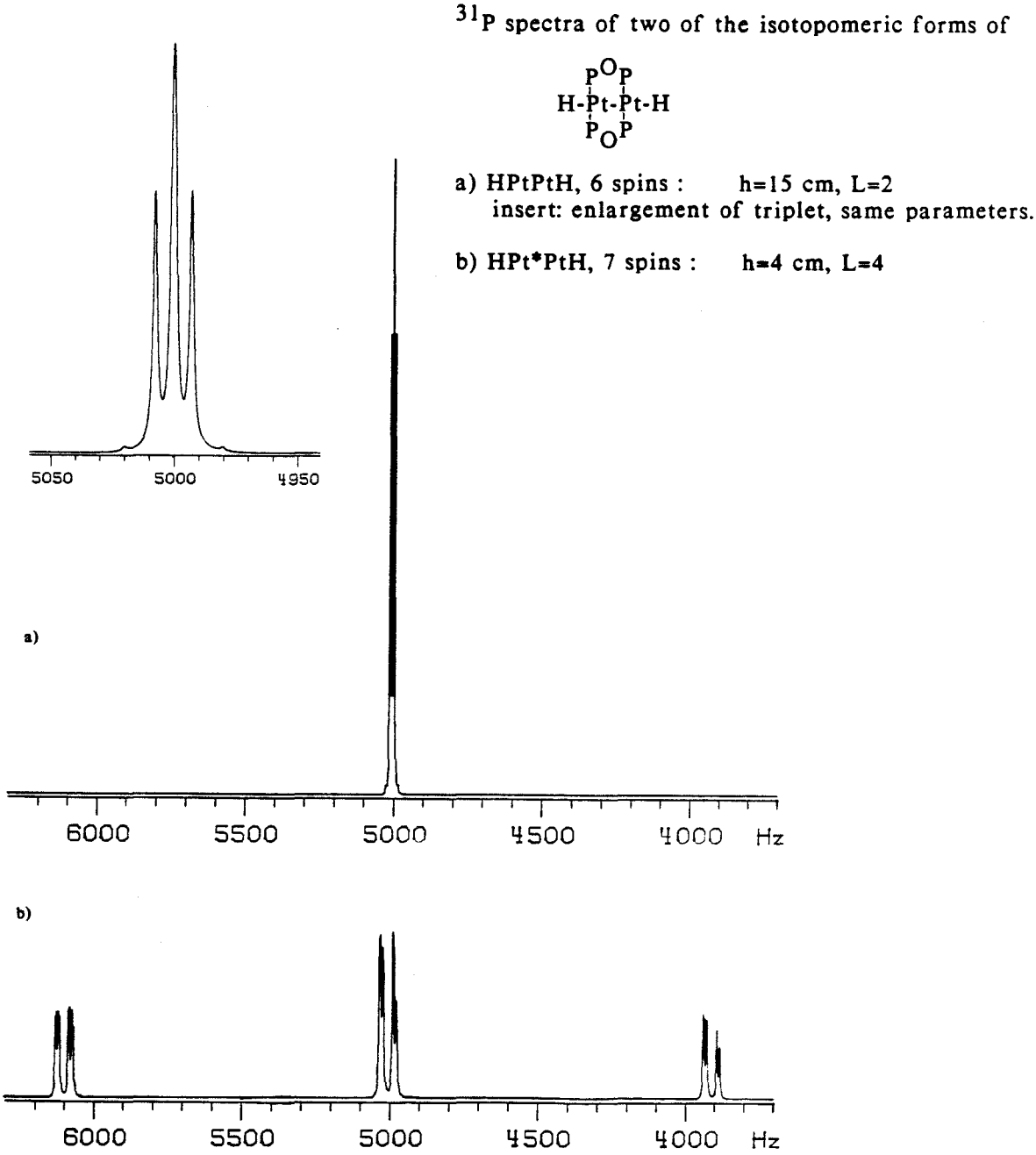

Figure 3.7 Experimental and simulated ^{31}P-decoupled ^{1}H NMR spectra of the photoproduct generated by 370-nm irradiation (3.5 h) of a 0.043 M $[TBA]_4[Pt_2(P_2O_5H_2)_4]$ and 0.083 M $PhCH(OH)CH_3$ degassed CD_3CN solution

There is some noise in the central singlet of the ^{1}H spectrum, and an unexplained peak on the left (*) that has no counterpart on the right. Since it seems doubtful that such an asymmetric element could belong to the spectrum of Pt_2, the peak was ignored.

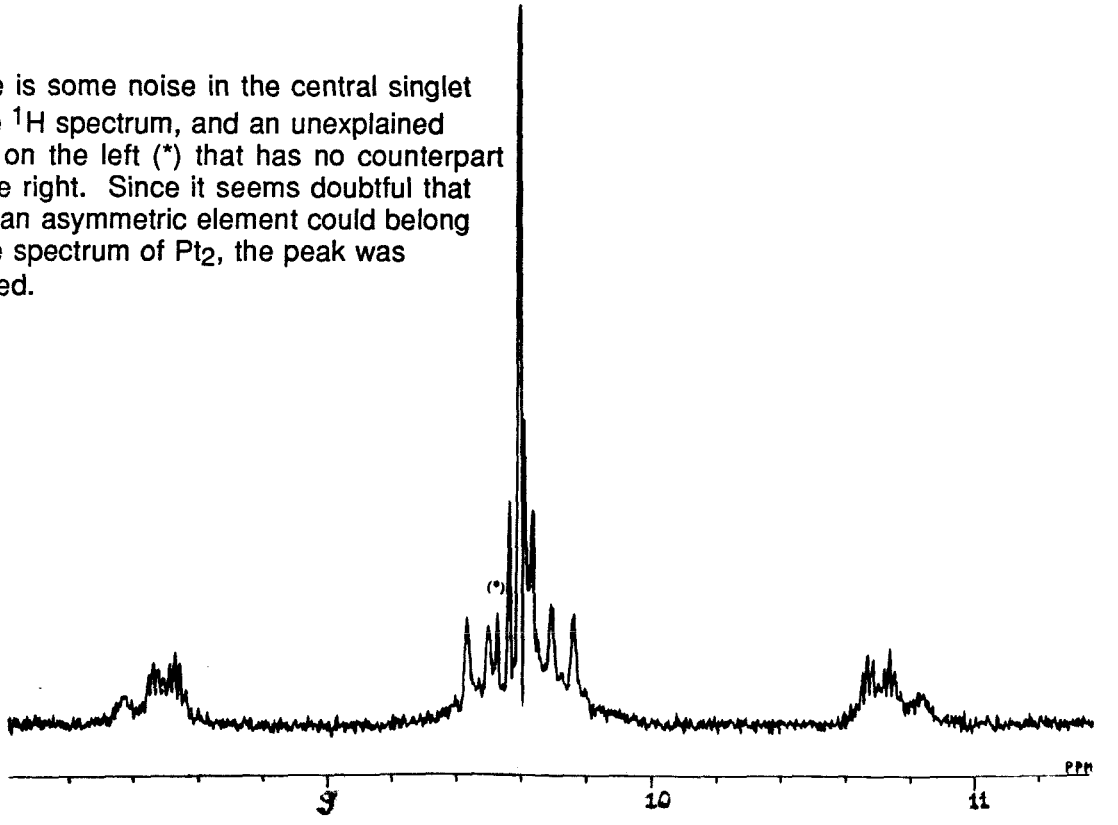

The spectrum shown here is actually a composite of three simulations which together constitute the ^{31}P-decoupled ^{1}H spectrum of Pt_2.

HPtPtH, 2 spins : h=15 cm, L=3

HPt*PtH, 3 spins : h=3 cm, L=3

H*Pt*PtH, 4 spins : h=5 cm, L=3

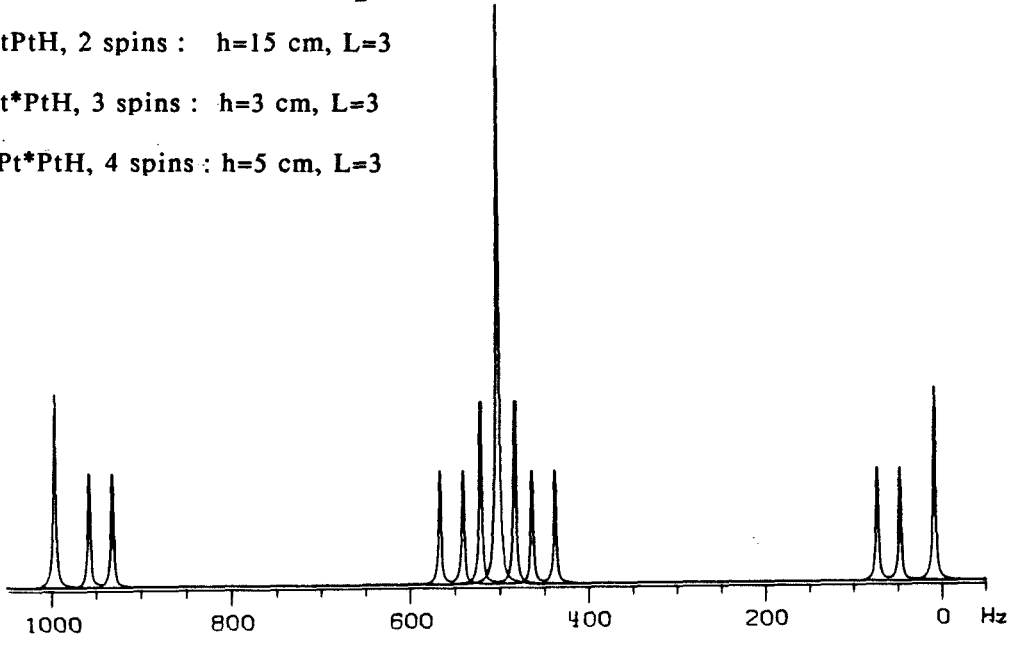

Figure 3.8 Enlargement of the left satellite in Figure 3.2 and first order hand simulation of the same spectral region using the 11-spin asymmetric isotopomer of $[Pt_2(P_2O_5H_2)_4]^{4-}$

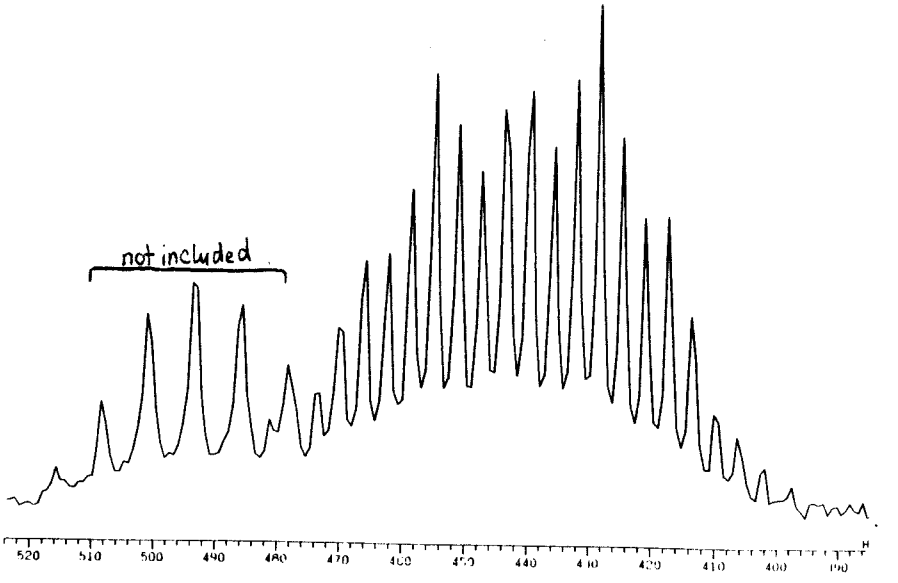

SIMULATION:
NOT TO SAME SCALE AS ABOVE:

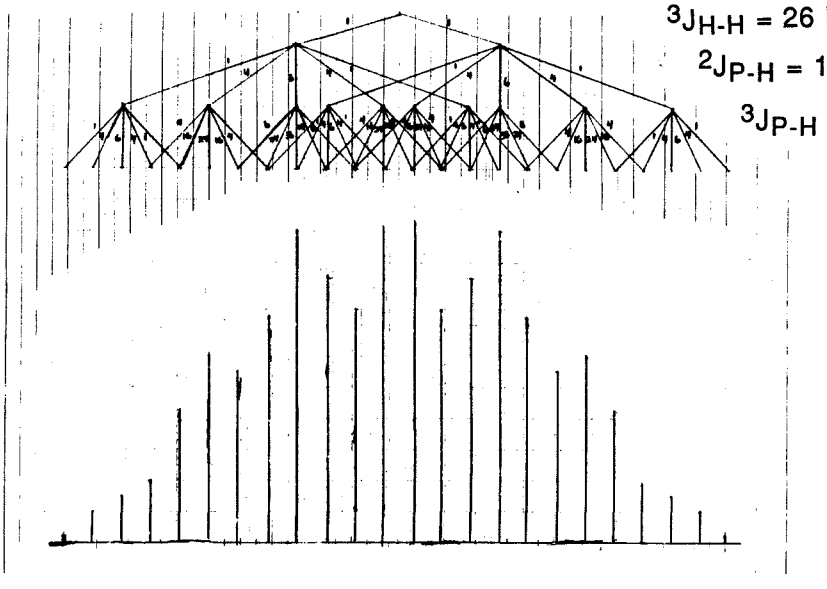

Using the values of $^2J_{Pt-H}$ and $^1J_{Pt-H}$ obtained in the asymmetric isotopomer to simulate the H-*Pt-*Pt-H ^{31}P-decoupled ^1H spectrum produces a four-line pattern with a splitting of 485 Hz between the outer lines and the center for J_{Pt-Pt}>3000 Hz (Figure 3.5). In the actual non-decoupled spectrum, the outermost multiplets occur at 485 Hz from the center and show the same pattern and splitting as the central peak, because of the ^{31}P atoms. The splitting of the inner two lines in the simulated spectrum depends on the value of J_{Pt-Pt}; J_{Pt-Pt} ~8000 Hz reproduces the splitting between two sharp peaks spanning the central singlet in the experimental spectrum and also fits with literature values for Pt-Pt couplings in similar molecules.[3, 9, 10] The overall interpretation of the spectrum is supported by the integration; the outer multiplets should account for 27.5% (22% + 5.5%) of the total integrated intensity of the spectrum, and the experimental value is 30%. Both ^{31}P and ^1H NMR spectra thus provide good evidence for an axial dihydrido structure (Pt_2H_2), which is analogous to other Pt_2X_2 complexes.

A medium-intensity IR band at 1840 cm^{-1}, corresponding to Pt-H stretching,[11] appears after 370-nm irradiation of an acetonitrile solution of Pt_2 with a slight excess of $PhCH(OH)CH_3$. The band disappears when air is allowed into the IR cell. The observed 1840 cm^{-1} Pt-H stretching frequency falls in the terminal M-H range, whereas bridging hydrides are characterized by a much lower Pt-H vibrational frequency.[6, 11]

A recent crystal structure of the related complex Ir_2H_2 exhibits electron density at the axial sites that is attributable to the hydrogen atoms.[12] NMR (δ = -10.6 ppm for Ir-H) and IR (Ir-H stretch = 1940 cm^{-1}) spectra for Ir_2H_2 and Pt_2H_2 are quite similar, providing additional confirmation of the axial nature of the dihydride ligands in Pt_2H_2.

The intense absorption band in the electronic spectrum of Pt_2H_2 at 314 nm (Figure 3.8) has an extinction coefficient equal to that of the $d\sigma^* \rightarrow p\sigma$ transition of Pt_2 ($\sim 3.7 \times 10^4$ $M^{-1}cm^{-1}$). In analogy to other Pt_2X_2 complexes,[4, 13] it is assigned to the allowed $\sigma \rightarrow d\sigma^*$ transition[14] of d^7-d^7 Pt_2H_2. Irradiation (313nm) into the Pt_2H_2 σ-$d\sigma^*$ absorption band quantitatively produces H_2 and Pt_2. (Photochemical reductive elimination is a general reaction of d^7-d^7 M_2X_2 complexes.)[14, 15, 16] Broad-band photolysis of Pt_2 and $PhCD(OD)CD_3$ in CH_3CN produces mainly D_2 and HD, with small amounts of H_2. The gaseous product distribution is consistent with photochemical elimination of D· from Pt_2D_2, followed by radical reactions of D· with acetonitrile.[17]

Other chemical properties of Pt_2H_2 are also consistent with its formulation as a terminal dihydride. It reacts with HCl and DCl to generate H_2 and HD, respectively. Dioxygen reacts with Pt_2H_2 very rapidly with quantitative regeneration of Pt_2. The spectroscopic evidence and the reaction with H^+ point to the formal oxidation state assignment $Pt_2^{III}(H^-)_2$, but the O_2 chemistry indicates that the molecule can also be viewed as a $Pt_2^{II}(H\cdot)_2$ species with the redox centers being the hydrido ligands. The H· groups can be released (and potentially transferred to substrates) either chemically or photochemically in a manner not unlike the alkyl-radical chemistry of certain Co(III) complexes.[18, 19]

Figure 3.9 UV-Vis Absorption spectra recorded a) before and b) after 11 minutes of 370-nm irradiation of a $2x10^{-4}$ M $[TBA]_4[Pt_2(P_2O_5H_2)_4]$ and $2x10^{-3}$ M $PhCH(OH)CH_3$ degassed CH_3CN solution. Inset: Growth of Pt_2H_2 over ten minutes photolysis of $2x10^{-4}$ M $[TBA]_4[Pt_2(P_2O_5H_2)_4]$ with 0.01 M $PhCH(OH)CH_2CH_3$ in degassed CH_3CN.

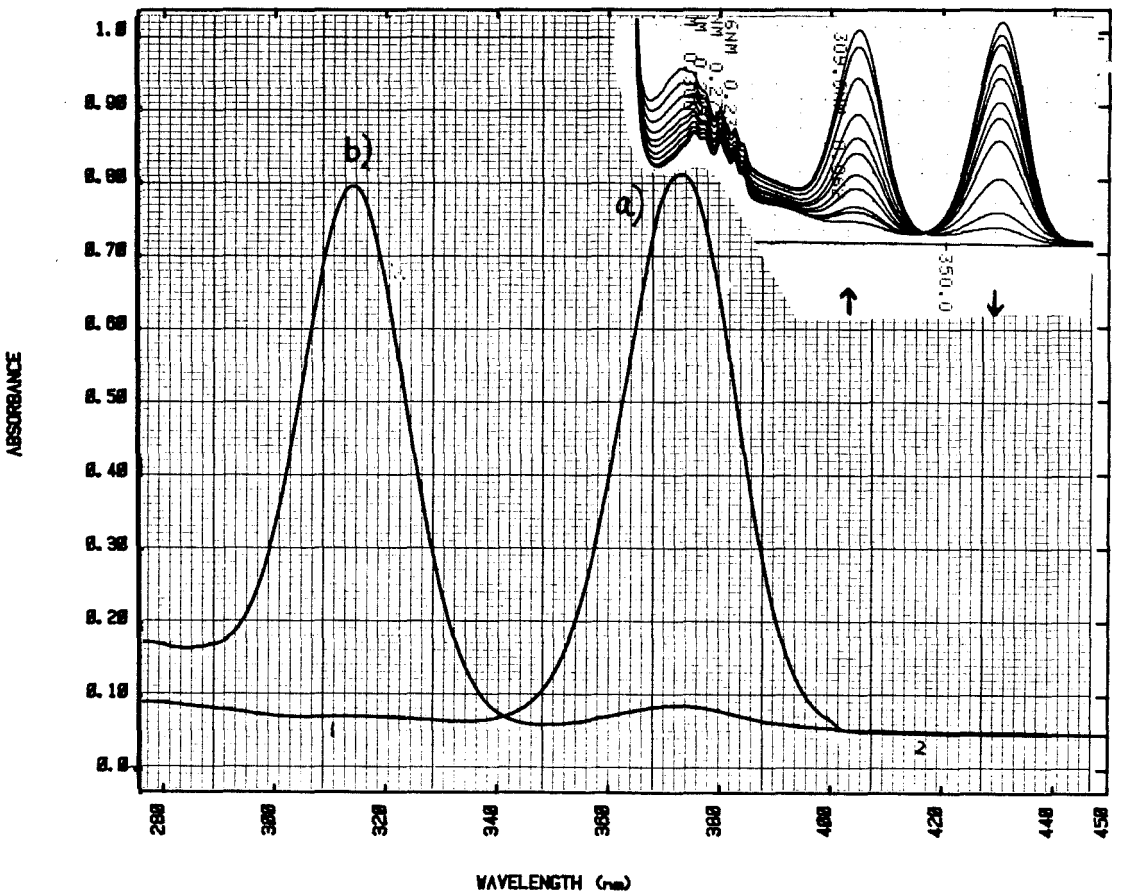

References

1. Harvey, Erica L.; Stiegman, Albert E.; Vlček, Antonin, Jr. and Gray, Harry B. *J. Am. Chem. Soc.* **109**, 5233 (1987). "Dihydridotetrakis(pyrophosphito(2-))-diplatinate(III)."

2. Marshall, Janet L.; Steigman, Albert E. and Gray, Harry B. in *Excited States and Reactive Intermediates* (ed. Lever, A.B.P.) (American Chemical Society, Washington, D.C., 1986), pp.166-176.

3. King, Christopher; Roundhill, D. Max; Dickson, Mark K. and Fronczek, Frank R. *J. Chem. Soc. Dalton Trans.* 2769 (1987). "Diplatinum-(II) and -(III) Complexes with Bridging μ-Diphosphonito-P,P' or μ-Methylenebis(phosphonito)-P,P' Ligands. Synthesis, Structure, and Nuclear Magnetic Resonance Analysis of the "Lantern" Complexes. Crystal Structures of $K_4[Pt^2\{\mu\text{-}CH_2[P(O)OH]_2\}_4].6H_2O$ and $K_4[Pt^2\{\mu\text{-}CH_2[P(O)OH]_2\}_4Cl_2].8H_2O$."

4. Che, Chi-Ming; Butler, Leslie G.; Grunthaner, Paula J. and Gray, Harry B. *Inorg. Chem.* **24**, 4662 (1985). "Chemistry and Spectroscopy of Binuclear Platinum Diphosphite Complexes."

5. Terminal Pt-H complexes exhibit ^1H NMR signals at negative δ values; Pt-H-Pt species usually have $\delta>0$.[6]

6. Ciriano, M.; Green, M.; Howard, J. A. K.; Murray, M.; Spencer, J. L.; Stone, F. G. A. and Tsipis, C. A. *Transition Metal Hydrides* ; Bau, R., ed.; Advances in Chemistry Series 167 (American Chemical Society: Washington, D. C., 1978); pp.111-121.

7. Becker, E. D. , ed. *High Resolution NMR, 2nd ed.* (Academic, Orlando, Fla., 1980); pp.163-167.

8. The $J_{P\text{-}H}$ of 3.7 Hz could arise from coupling via H-Pt-Pt-P (^3J) or H-Pt-P-O-P (^4J).

9. Appleton, T. G.; Hall, J. R. and Neale, D. W. *Inorg. Chim. Acta.* **104**, 19 (1985). "NMR Spectra of Platinum(III) Complexes with Sulfato- and Phosphato-bridges."

10. Harris, R. K. and Mann, B. E. *NMR and the Periodic Table* (Academic, New York, 1978); pp. 256-257.

11. Nakamoto, K. *Infrared and Raman Spectra of Inorganic and Coordination Compounds, 3rd ed.* (Wiley, New York, 1978); pp. 304-305, 381, 396.

12. Smith, David C., Ph. D. Dissertation (California Institute of Technology, 1989).

13. Che, Chi-Ming; Schaefer, William P.; Gray, Harry B.; Dickson, Mark K.; Stein, Paul B. and Roundhill, D. Max *J. Am. Chem. Soc.* **104**, 4253 (1982). "Novel Binuclear Platinum (III) Diphosphite Complexes."

14. Miskowski, V. M.; Smith, T. P.; Loehr, T. M. and Gray, H. B. *J. Am. Chem. Soc.* **107**, 7925 (1985). "Properties of Metal-Metal Single Bonds. Vibrational and Electronic Spectra of Binuclear Rhodium(II) and Iridium(II) Isocyanide Complexes with Comparisons to $Mn_2(CO)_{10}$."

15. Stiegman, A. E.; Miskowski, V. M. and Gray, Harry B. *J. Am. Chem. Soc.* **108**, 2781 (1986). "Metal-Metal Excited State Emission from Binuclear Platinum (III) Complexes."

16. Kurmoo, Mohamedally and Clark, Robin J. H. *Inorg. Chem.* **24**, 4420 (1985). "Spectroscopic Studies on Linear-Chain Semiconductors and Related Species. Vibrational and Resonance Raman Spectroscopy of the Diphosphite Complexes $K_4[Pt_2(pop)_4].2H_2O$, $K_4[Pt_2(pop)_4X_2].2H_2O$,and $K_4[Pt_2(pop)_4X].nH_2O$, X=Cl, Br,I."

17. The H_2 bond (104 kcal/mol) is stronger than the $H\text{-}CH_2CN$ bond (93±2.5 kcal/mol). See Ch.2, Ref.31 and *CRC* Handbook of Chemistry and Physics, 63rd Ed.

18. Halpern, J. B_{12} (Wiley, New York, 1982); pp. 501-542.

19. Halpern, J. *J. Pure Appl. Chem.* **55**, 1059 (1983). "Mechanistic Aspects of Coenzyme B_{12}-Dependent Rearrangements. Organometallics as Free Radical Precursors."

Chapter 4. Synthesis and Characterization of $[Pt_2(P_2O_5)_4H_2(BF_2)_6]^{4-}$ ("BF_2Pt_2")

Introduction/Background

To test the postulate that enhanced H-atom abstraction reactivity of $^3Pt_2$ with alcohol substrates is facilitated by docking H-bonding interactions, an attempt was made to perturb the interligand OH network in the metal complex. Close examination of the H-bonding arrangement around an axial site in Pt_2 reveals four 6-membered rings fused together around a central Pt atom. The arrangement of atoms within each 6-membered ring resembles the arrangement of atoms in the enol tautomer of a β-diketone complex:

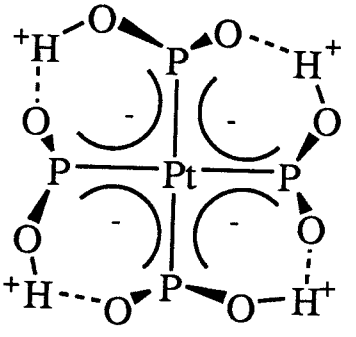

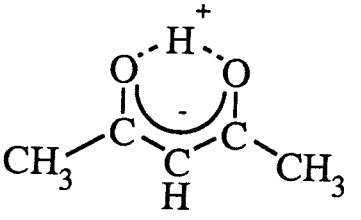

In the deprotonated form, β-diketones serve as bidentate ligands for a rich array of transition and main group elements. For example, a variety of β-diketones and related 3-amino-1-ketones undergo ready substitution of BF_2^+ for the enolic H^+.[1, 2] Synthetic routes involve direct reaction with BF_3 gas or $BF_3{\cdot}OEt_2$. The reaction stoichiometry has been postulated as either

$$BF_3 + x\text{-}H \rightarrow x\text{-}BF_2 + HF$$

or

$$2\ BF_3 + x\text{-}H \rightarrow x\text{-}BF_2 + HBF_4\ .$$

The key to obtaining a bridging difluoroboron moiety seems to be the presence of a moderately acidic proton (pK_a=9 for acetylacetonate)[3] in the vicinity of two atoms with donor electron pairs available for coordination to boron. When no proton is present and/or only one donor atom is present, BF_3 forms Lewis acid/Lewis base adducts like $BF_3{\cdot}NH_3$ or $BF_3{\cdot}OEt_2$.[4]

The first difluoroborato-bridged organic β-diketone was reported in 1905;[5] more recently, the substitution has been introduced into similar 6-membered rings in a number of organometallic and inorganic complexes.[6, 7, 8, 9, 10, 11] Figure 4.1 shows a sampling of such complexes. In many cases the substitution was employed to gain information about the conformation of the H-bonding structure in the original ring.[12, 13]

Reaction of $[TBA]_4Pt_2$ with BF_3 or $BF_3{\cdot}OEt_2$ produces a new compound that bears a striking physical and photophysical resemblance to Pt_2, but is much harder to oxidize. Unfortunately, the structure of the modified species has not been determined by x-ray analysis. A variety of spectroscopic and chemical evidence supports one or all of the structures shown in Figure 4.2; the complex is abbreviated as BF_2Pt_2 .

Figure 4.1 Previously reported inorganic and organometallic complexes containing BF_2^+ substitution

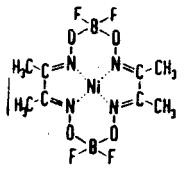

Ref. 11

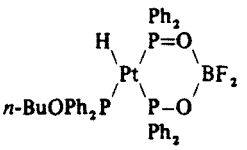

3

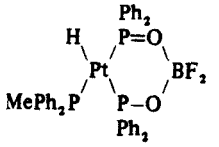

4

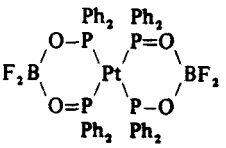

5

Ref. 6

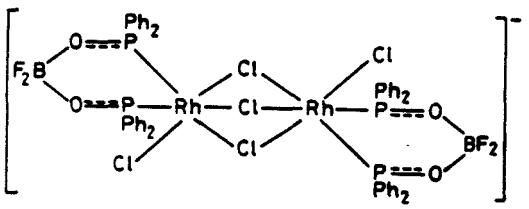

(3)

Ref. 7

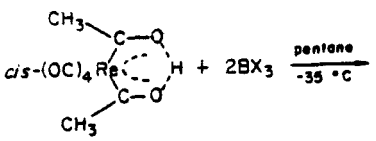

1

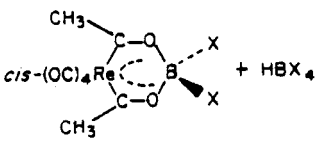

3, X = F
4, X = Cl
5, X = Br
6, X = I

Ref. 8

Figure 4.2 Structure of $[Pt_2(P_2O_5)_4H_2(BF_2)_6]^{4-}$ showing the three most likely arrangements of BF_{2+} substituents

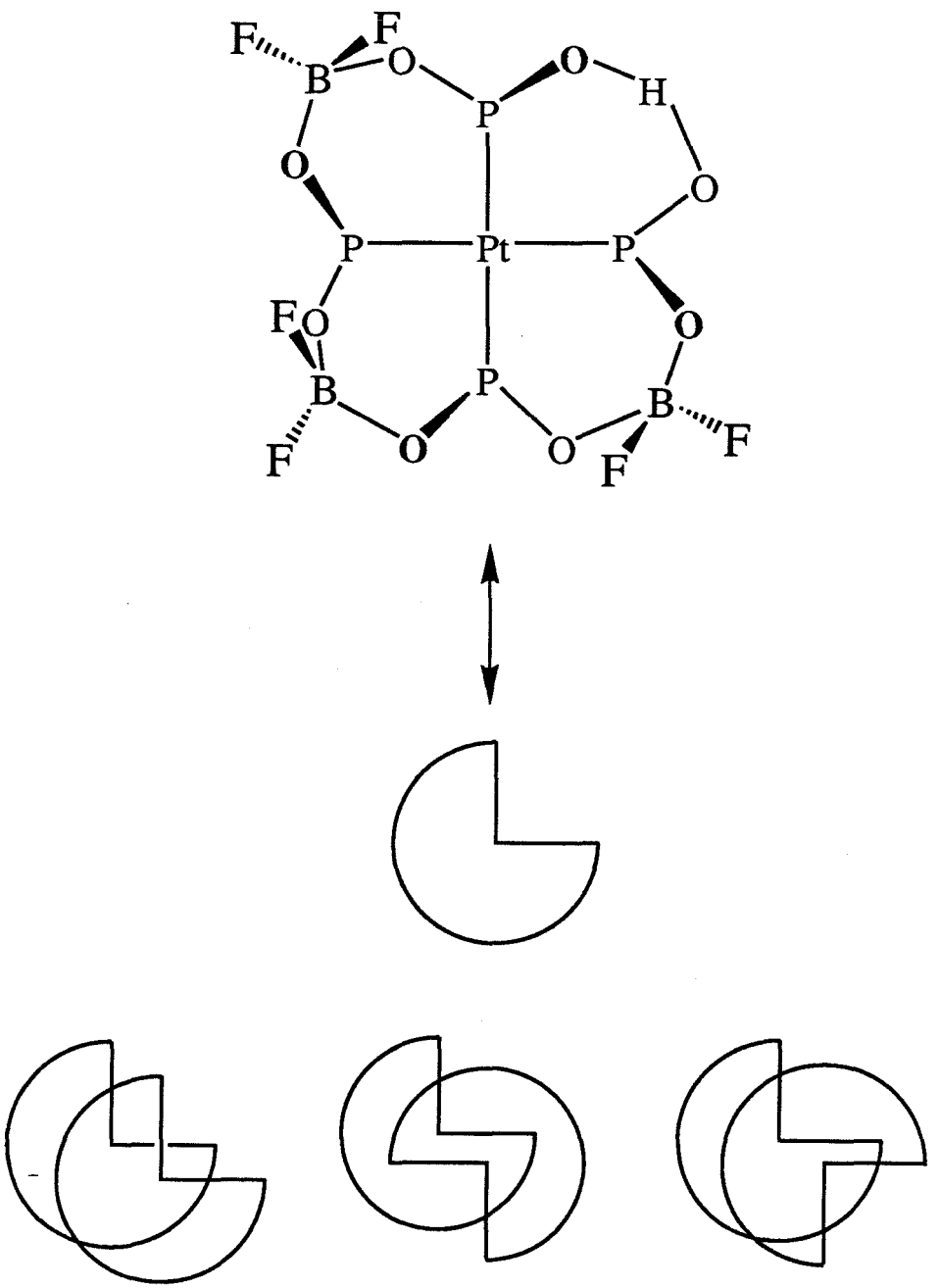

The BF2+ groups may adopt three relative orientations on the front and back faces of the dimer, as shown with these schematic representations.

Experimental:

Syntheses Boron trifluoride is an acidic, corrosive gas that reacts with almost everything.[14] In the first BF_2Pt_2 syntheses, BF_3 gas was bubbled through a mineral oil trap into a solution of 1.0 g $[TBA]_4Pt_2$ in 70 mL CH_2Cl_2, and then through another trap into a kill solution of NaOH in H_2O. Since Pt_2 reacts photochemically with CH_2Cl_2 in room light, the entire operation was carried out in the dark, using a flashlight or red darkroom light at an oblique angle. Argon was flushed through the system for about ten minutes before and after the BF_3 gas, as BF_3 reacts with moisture in the air. The flask containing the $[TBA]_4Pt_2$ solution was cooled in an ice bath during all successful syntheses. The time period during which BF_3 was allowed to flow varied between 1 and 5 minutes, but the flow rate was not monitored. After residual BF_3 was flushed out with Ar, the system was opened to air and new diethyl ether (Fisher, anhydrous) was poured onto the dichloromethane solution. Filtration, followed by copious washings with diethyl ether while the product was on the frit, produced an approximately 30% yield of fine, bright green powder. The remainder of the product usually sat on the bottom of the reaction flask as a viscous yellow oil.

The second approach to the synthesis made use of the easier-to-handle BF_3 etherate reagent (Aldrich). Direct addition of neat BF_3 etherate (0.5 - 3.0 mL) to solid $[TBA]_4Pt_2$ (300mg) under a partial argon blanket in a large, unstoppered test tube resulted in a yellow solution; addition of newly opened diethyl ether caused precipitation of a bright green solid. Crude yields obtained using the $BF_3{\cdot}OEt_2$ reagent were higher (around 70-80%), but the purity of the product was more variable.

Purification was accomplished by dissolution of samples in small amounts of acetonitrile (200mg in 1/2 mL), followed by centrifugation, decantation from the insoluble white impurity, and reprecipitation in diethylether. An approximately 70% yield based on crude product was obtained. Samples treated in this manner exhibit cleaner UV-Vis absorption spectra and higher carbon and hydrogen elemental analysis

ratios than the crude product. Chromatography was not used for purification because disappearance of emission indicated that decomposition occurred when the complex was left on a TLC plate. Attempted recrystallizations by slow evaporation of solvent or layering methods usually gave yellow oils or oily solids, mixed with small amounts of lacy or needlelike whitish crystals. Very small green crystals were obtained by enclosing an open vial containing an acetonitrile solution of BF_2Pt_2 in a larger chamber of toluene.

Instrumentation C, H, N analyses were performed in the analytical facility at Caltech; F, B, P, C, H and Pt were performed by Galbraith Laboratories. Both a Perkin Elmer 1600 series FTIR spectrometer and a Beckman 4240 IR spectrometer were used for the IR spectra. UV-Vis absorption spectra were measured on Shimadzu UV-260 and Cary 17 UV-Vis spectrometers; all spectra were run against air:air baselines.

Emission spectra were recorded on a previously described[15] emission spectrometer; 366 nm excitation light from an Oriel 200W Hg/Xe lamp was selected with a Spex 1670 monochromator and an Oriel 366 nm(#5643) interference filter. Emitted light was sent through a cutoff filter into a Spex 1870 monochromator connected to a Hamamatsu R955 photomultiplier tube and EG and G 182-A lock-in amplifier. Uncorrected spectra were printed out on a chart recorder. The relative phosphorescence quantum yield for $^3BF_2Pt_2^*$ was estimated by matching the absorbances of ~10^{-5} M solutions of BF_2Pt_2 and Pt_2, and comparing the maximum emission intensities for the two compounds. The extinction coefficient of BF_2Pt_2 was estimated with the same sample. Phosphorescence lifetime measurements were carried out using the laser system described in Chapter 2.

Cyclic voltammetry was measured in Burdick and Jackson UV grade acetonitrile, with 0.1M $TBAPF_6$ (recrystallized from ethanol) as the supporting electrolyte. The acetonitrile was taken directly from the bottle without further purification and bubbled

with argon for 15-20 minutes before recording the spectra. A platinum disc working electrode and a platinum wire counterelectrode were used; the reference was a standard calomel electrode in a Luggin capillary, with a Pt wire connection to the non-aqueous solution.[16] The room temperature voltammograms were measured using EG and G PAR electronics, Models 175 (Universal Programmer), 173 (Potentiostat/Galvanostat) and 179 (Digital Coulometer) with a Houston Instruments 2000 X-Y recorder. The low-temperature voltammogram was obtained with a BAS-100 Electrochemical Analyzer hooked up to a Bausch and Lomb Houston Instruments DMP-40 series digital plotter. The supporting electrolyte was 0.1 M [TBA]triflate, and a glassy carbon working electrode and silver wire reference electrode were employed for the low-temperature measurement.

NMR's were carried out in CD_3CN (Aldrich ampules) on a JEOL FX90Q FTNMR spectrometer (^{19}F, ^{31}P) and on a Bruker 500 MHz FTNMR (^{19}F, ^{31}P, ^{195}Pt). Sample concentrations are reported with each spectrum. All NMR spectra are shown with applied field increasing from left to right and frequency decreasing from left to right. The NMR spectrometers automatically assign negative chemical shifts values to all shifts upfield of a reference, so the frequency and chemical shift scales track one another. The convention in ^{19}F NMR, however, is to assign positive numbers to chemical shifts upfield of CCl_3F.[17] So that a narrow frequency window (6000Hz) could be used, the ^{19}F spectra in this thesis were originally referenced to 1% C_6F_6 in C_6D_6, which was measured at +163 vs neat CCl_3F. ^{19}F chemical shifts of spectra shown here have been converted to a reference of neat CCl_3F=0, and the fluorine sign convention followed. Fluorine chemical shifts are reproducible to ±2 ppm between different samples on the same spectrometer, and the precision of the numbers is probably 0.1 ppm within any given spectrum. Shifts of all peaks on the 500 MHz instrument are 4 ppm downfield from those on the 90MHz instrument, for unknown reasons. ^{31}P spectra were referenced to neat H_3PO_4 for the 90MHz instrument and to 85% H_3PO_4 in D_2O for

the 500 MHz instrument. ^{31}P and ^{19}F NMR samples on the FX90Q were first shimmed on ^{2}D, then locked on external ^{7}Li sample so that references in separate tubes could be employed. Standards for the ^{19}F and ^{31}P NMRs were prepared by Wilmad Glass Co. in sealed 5 mm tubes. The ^{195}Pt standard for the $[TBA]_4BF_2Pt_2$ spectrum was $[TBA]_4Pt_2$ in CD_3CN; the latter was standardized against a nearly saturated solution of K_2PtCl_4 in D_2O.

Results and Discussion

Solubility, Stability, Synthesis

The bright green product obtained from reaction of $[TBA]_4Pt_2$ with $BF_3(g)$ or $BF_3{\cdot}OEt_2$ is highly soluble in CH_3CN, soluble in acetone, methanol and ethanol, and slightly soluble in dichloromethane. Unlike $[TBA]_4Pt_2$, however, the modified species is not soluble in water. Over time, the complex reverts to Pt_2 in the presence of protic solvents. In acetonitrile it appears indefinitely stable; a solution that has been sitting in a capped NMR tube for two years is still yellow and emissive, although the UV-Vis and NMR spectra indicate that some impurities have developed. The same tube indicates that the complex is more stable to air oxidation than Pt_2, as Pt_2 solutions tend to turn dark green or blue over a period of weeks or months in undegassed solutions of acetonitrile.

Use of differing excesses of BF_3 reagent during synthesis does not change the physical or photophysical characteristics of the green product; however, use of less than a stoichiometric amount of $BF_3{\cdot}OEt_2$ led to a very sticky solid with absorption bands only slightly shifted from those of Pt_2 (371 nm, 245 nm). Varying amounts of white solid (HBF_4, $B(OH)_3$, other boric acids?) precipitate from concentrated acetonitrile solutions of the product; more precipitate was observed in unpurified samples that were prepared with greater excesses of BF_3 reagent. Such samples sometimes exhibit extra peaks at 334 or 257 nm in the UV-Vis spectrum or appear to be a duller green.

Infrared

IR spectra of K_4Pt_2, $[TBA]_4Pt_2$ and $[TBA]_4BF_2Pt_2$ are shown for comparison in Figure 4.3. Peaks present at 3500 cm^{-1} and 1600 cm^{-1} in the Nujol mull spectra of both K_4Pt_2 and $[TBA]_4Pt_2$ are absent in BF_2Pt_2, consistent with the loss of waters of hydration during synthesis with BF_3, with loss of P-O-H bonds or both. The major fingerprint bands for all three complexes are summarized in Table 4.1. For K_4Pt_2 in fluorolube mull, the band assignments made previously are shown.[18] The broad, strong peak assigned as the PO_2H bend in K_4Pt_2, on the basis of a 300 cm^{-1} shift in the deuterated complex, is dramatically absent from the BF_2Pt_2 spectrum.

Table 4.1 IR data and assignments for $K_4[Pt_2(P_2O_5H_2)_4]$ in nujol mull, and IR data for $[TBA]_4[Pt_2(P_2O_5H_2)_4]$ and $[TBA]_4[Pt_2(P_2O_5)_4H_2(BF_2)_6]$ in nujol mull and dichloromethane solution

Assignment (ref. 18)	Frequency (cm^{-1})					
	K_4Pt_2 fluorolube	K_4Pt_2 nujol	TBA_4Pt_2 nujol	TBA_4Pt_2 CH_2Cl_2	$TBA_4BF_2Pt_2$ nujol	$TBA_4BF_2Pt_2$ CH_2Cl_2
		3491	3420 3339	3658		3682 weak
		1672	1608	1608		1605 weak
		1479 sh	1485 sh	1482 sh	1485 sh 1463	1483 1463 1424
		1384 sh	1384 sh	1381 sh	1380 sh	1381 sh
POH bend	1329	1302 br	1350 br	obscured		
PO_{term} stretch	1085 910	1082 1013 915	1065 str 914,890	1082 917,887	1109 1022,994 923,890	1113 1025,998 925,907
P-O-P stretch	695	704	700	obscured	728	obscured

Figure 4.3 Difference IR spectra of a) $K_4[Pt_2(P_2O_5H_2)_4]$ in nujol mull, b), c) $[TBA]_4[Pt_2(P_2O_5H_2)_4]$ and d), e) $[TBA]_4[Pt_2(P_2O_5)_4H_2(BF_2)_6]$ in nujol mull (b,d) and dichloromethane solution (c,e)

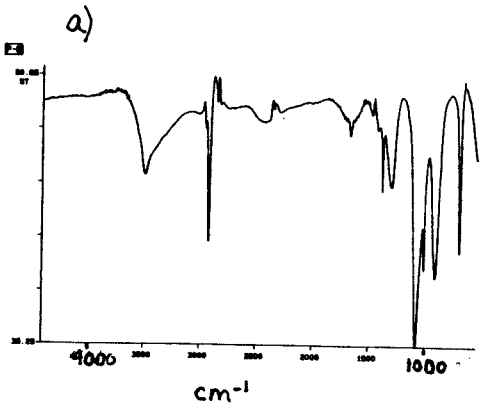

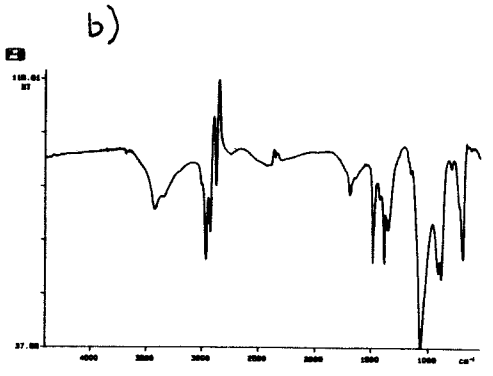

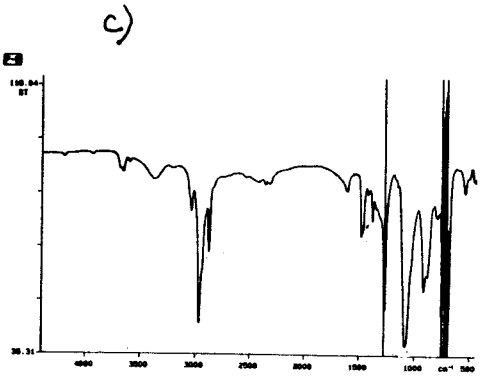

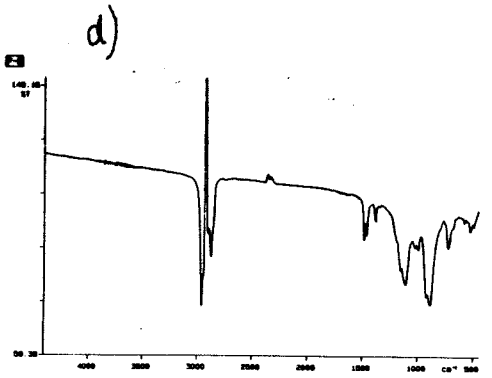

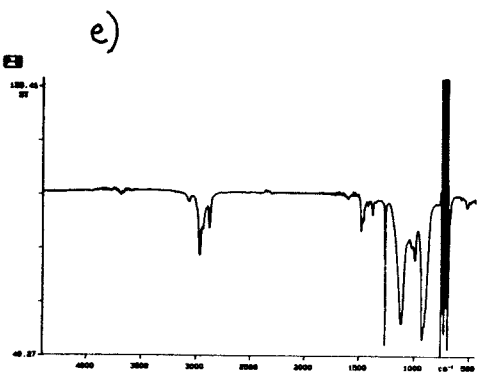

Analytical Results

Chemical analyses (C,H,N,B,F,Pt) are most consistent with the presence of 6 BF_2^+ groups added to the Pt_2 framework. See Table 4.2. Analysis of parent $[TBA]_4Pt_2$ gives reproducibly low values for C and H.[19] A single determination of P and Pt on the $[TBA]_4Pt_2$ sample used to synthesize the first BF_2Pt_2 sample for which analyses are given below indicates that Pt is slightly low and P is high.
The anomalously high phosphorous analyses suggest that some P-containing substance (not seen in the NMR) is the culprit in the low C and H analyses. The P:Pt ratio in Pt_2 of 4.4:1 is nearly identical with that observed in the daughter BF_2Pt_2, suggesting that the phosphorous impurity follows through in the synthesis.

Repeated analyses of different BF_2Pt_2 samples give varying C and H percentages, all lower than calculated for BF_2Pt_2. Presumably this is due in part to the same factors that produce low C and H analyses in the parent Pt_2. The presence of the approximately 1-2% fluoroborated impurity indicated by NMR for the samples analyzed should raise the B and F and lower the other elements. Important ratios to note are the F:B (2.0:1), F:Pt (6.2:1 in both samples analyzed), and B:Pt (3.2:1). These ratios clearly indicate the presence of 6 BF_2 groups, and possibly a small amount of impurity containing B and F. The ratios are not consistent with 4 BF_2^+ or 4 BF_3 groups. While neither BF_2Pt_2 sample analyzes satisfactorily for every element, the combination of values from the two determinations is consistent with the presence of 6 BF_2^+ groups. Both boron and fluorine analyses are simply too low for the complex to be the complex with all eight ligand H^+ moieties replaced by BF_2^+ groups.

A small amount of impurity containing boron and fluorine may be present in the samples used for this work, but electrochemical, photophysical, IR, and NMR data indicate that the samples contain no residual Pt_2. All four techniques allow ready differentiation between the two complexes.

Table 4.2 Compendium of chemical analysis results for $[TBA]_4[Pt_2(P_2O_5H_2)_4]$ and $[TBA]_4[Pt_2(P_2O_5)_4H_2(BF_2)_6]$

Sample	Analysis Source	%C	%H	%N	%P	%Pt	%O	%B	%F
$[(CH_3(CH_2)_3)_4N]_4[Pt_2(P_2O_5H_2)_4]$									
	Calculated	39.79	7.9	2.9	12.8	20.2	16.5		
	Galbraith	42.83	8.28		13.49	19.69			
	Caltech	38.26	7.49	2.88					
$[(CH_3(CH_2)_3)_4N]_4[Pt_2(P_2O_5)_4H_2(BF_2)_6]$									
	Calculated	34.6	6.6	2.5	11.1	17.6	14.4	2.9	10.26
Sample 1	Galbraith	36.32	6.99		11.61	16.62		2.94	10.07
($BF_3 \cdot OEt_2$)	Caltech	33.59	6.28	2.56					
Sample 2	Galbraith					17.76			10.72
($BF_3(g)$)	Caltech	34.04	6.40	2.60					
	Caltech	33.54	6.26	2.46					
	Caltech	34.12	6.29	2.39					
	Caltech	33.9	6.35	2.53					

NMR

^{19}F and ^{31}P spectra have been obtained at 84.25 and 36 MHz (90 MHz for ^{1}H, hereafter referred to as 90 MHz)) and 470 and 202 MHz (500 MHz for ^{1}H, hereafter referred to a 500 MHz) on BF_2Pt_2 samples synthesized using $BF_{3(g)}$. A ^{1}H spectrum was obtained at 90 MHz, and a ^{195}Pt spectrum was obtained on the 500 MHz instrument; but an attempted ^{11}B spectrum was unsuccessful. Spectra of BF_2Pt_2 samples synthesized using $BF_3{\cdot}OEt_2$ have been measured only on the 90 MHz instrument, and only ^{19}F and ^{31}P spectra have been recorded. Representative spectra are shown in Figures 4.4-4.7. The NMR chemical shifts of phosphorous and platinum atoms in the modified complex occur in regions upfield and clearly distinct from Pt_2.[20] Both spectra are more complicated than those of Pt_2, but elements of similarity exist.

Parent Pt_2 contains 8 NMR-active phosphorous atoms (I=1/2) and two platinum atoms (^{195}Pt, 33% abundant, I=1/2); 45% of the dimers will have no NMR-active platinums, 45% will have one NMR-active platinum and 11% will have two NMR-active platinum atoms. The eight ligand hydrogens have not been observed in the ^{1}H NMR, and no evidence for J coupling with these hydrogens has been seen. Both fluorine and boron are NMR-active (^{19}F, 100% abundant, I=1/2; ^{10}B, 18.8% abundant, I=3; ^{11}B, 81.2% abundant, I=3/2), so Pt_2 substituted with 6 BF_2^+ groups represents a combination of 32-, 33- and 34-spin systems, excluding the protons! Several complicating factors exist with this collection of spins. The ^{11}B nucleus has a quadrupole moment, known to cause broadening of peaks in some environments.[17] Fluorine atoms bound to ^{10}B actually have a slightly different chemical shift than those bound to ^{11}B; NMR signals from the 80% of the fluorine nuclei that are bound to ^{11}B appear upfield of the ^{10}B-bound fluorine signals.[1] Fluorines bound to either boron nucleus can exhibit complex splitting patterns if coupling to boron is resolvable.[21]

^{19}F NMR

The chemical shift range of the relatively broad, main part of the ^{19}F NMR spectrum (131-138ppm) (Figure 4.4) falls in the region of BF_2^+ shifts for difluoroborato-β-diketones.[1] The pattern consists of two sets of signals integrating 1:1 whose symmetry misleadingly suggests a coupling pattern. However, a chemical shift difference of ~6 ppm observed on both the 90 MHz and 500 MHz instruments indicates that the signals actually arise from chemically inequivalent nuclei. The pattern suggests two very different and equally likely F environments, consistent with a F_a, F_b situation. The distribution of peaks within each broadly defined F_a or F_b region indicates one ($BF_3{\cdot}OEt_2$ syntheses) or several (BF_3(g) syntheses) microenvironments for the fluorines. Relative integrations of signals assigned to the different microenvironments suggest that they are not equally likely, but they are found in the same relative proportions in the F_a and F_b signals. In the 500 MHz spectrum, each "microenvironment" signal resolves to two peaks of the same height, separated by approximately 60-65 Hz. The latter splitting is consistent with F_a-F_b coupling. A 60-65 Hz peak separation is also observed in the 90 MHz spectra of samples from both synthetic methods.

The ^{19}F NMR also reveals a set of sharp lines in the 150-153 ppm region characteristic of BF_4^- or coordinated BF_3.[22] Integration of spectra obtained using different pulse delays and samples gives areas for these sharp lines of between 1 and 10% of the total fluorine signal. The small relative amount of BF_3-like signal argues against a single molecule containing a mixture of BF_2^+ and BF_3 substituents. The peaks are more probably due to an impurity; $BF_3{\cdot}CH_3CN$,[23, 24] residual $BF_3{\cdot}OEt_2$, or the white solid described earlier are all possibilities. Interestingly, spectra of one sample before and after removal of some white impurity gave identical integrations of ~1% for the impurity signal.

Figure 4.4 ^{19}F NMR spectra of $[TBA]_4[Pt_2(P_2O_5)_4H_2(BF_2)_6]$

a) at 84.25 MHz, 0.04 M solution in CD_3CN

b) at 470 MHz, 0.02 M solution in CD_3CN

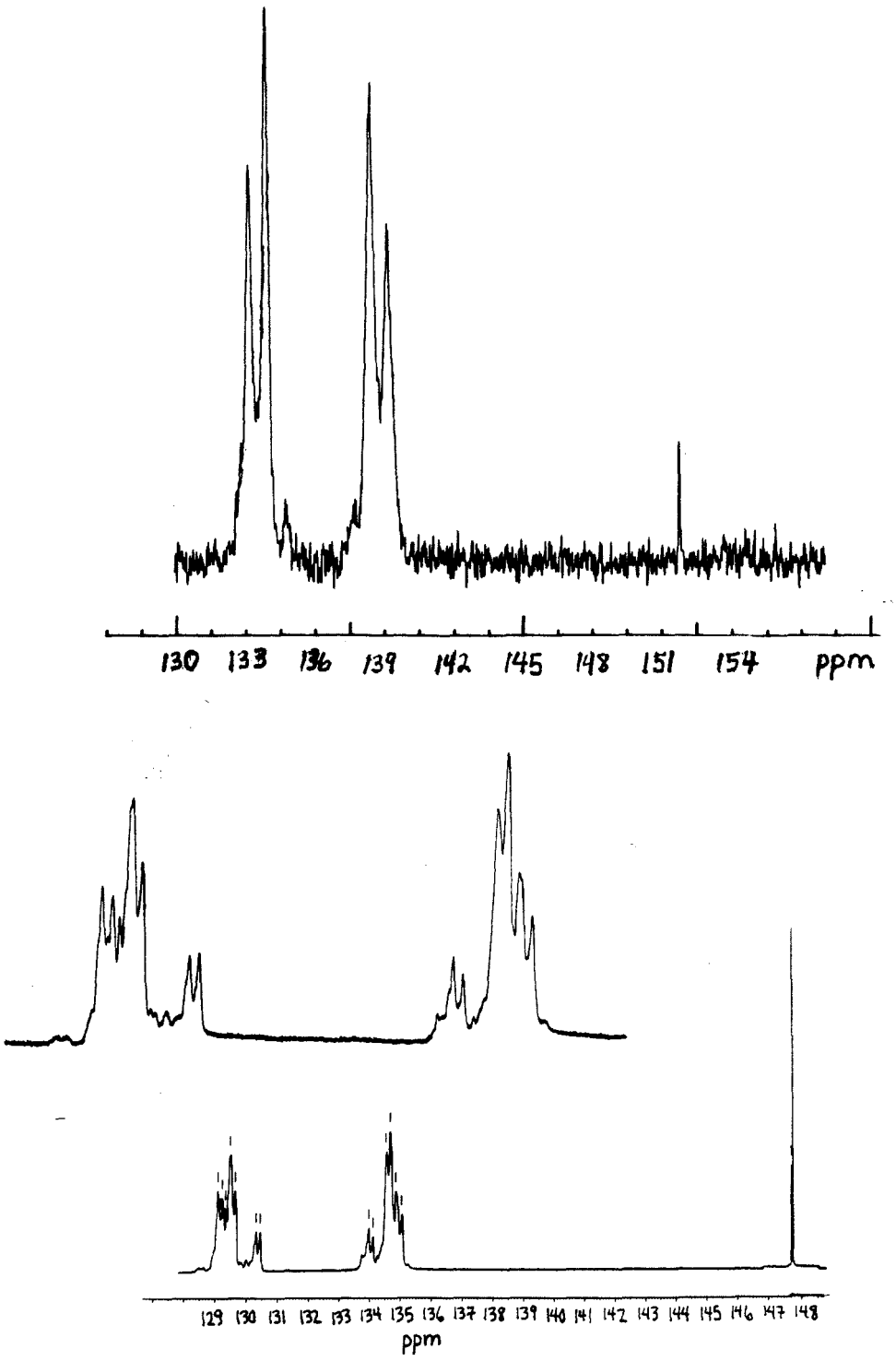

The fluorine NMR's are particularly suggestive of BF_2^+ substitution. Different ^{19}F chemical shifts are expected for the two fluorines of each BF_2^+ moiety because one fluorine atom is directed toward the axial site and one is directed toward the P-O-P bridge. Comparison of spectra for complexes synthesized differently suggests that reaction with BF_3 gas produces several substitution patterns (see the three structures in the introduction) or freezes out several conformations that do not interconvert in solution, whereas the $BF_3{\cdot}OEt_2$ synthesis is more selective for a single conformation or substitution pattern. By comparison, the BF_2^+-substituted organic β-diketone ^{19}F NMR spectra[1] consist of sharp, two-line signals separated by 25 Hz, arising from the fluorines bound to ^{10}B (20%) and those bound to ^{11}B (80%). Several spectra exhibit resolvable coupling to ^{11}B, resulting in a quartet. The lack of F-F coupling indicates that the two fluorine nuclei appear equivalent on the NMR timescale; i.e., the six-membered ring conformations must interconvert quickly in solution. Unfortunately, ^{19}F spectra for the metalla-β-diketonates and phosphinito complexes have not been reported.

^{31}P NMR

The ^{31}P signal is shifted from 68 ppm for Pt_2 to 58 ppm for Pt_2BF_2, referenced to H_3PO_4. (Figure 4.5) The ^{31}P spectrum of BF_2Pt_2 synthesized with BF_3(g) or $BF_3{\cdot}OEt_2$ consists of three or four Pt_2-like patterns separated by approximately 1 ppm, each with a central peak surrounded by two broad satellites from JPt-P coupling of approximately 3100 Hz. A fluxional process could explain the broadness of the signals, but no striking temperature-dependent changes are observed in 90MHz spectra from -45 to +40°C. An alternative explanation for the broadness is the presence of quadrupolar boron nuclei.

Figure 4.5 ^{31}P NMR spectra of $[TBA]_4[Pt_2(P_2O_5)_4H_2(BF_2)_6]$
a) at 36 MHz, 0.04 M solution in CD_3CN
b) at 202 MHz, 0.01 M solution in CD_3CN

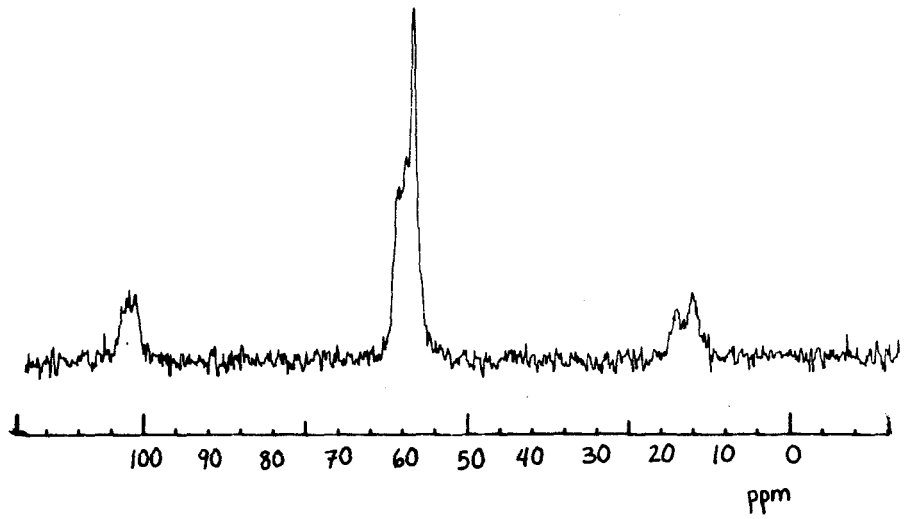

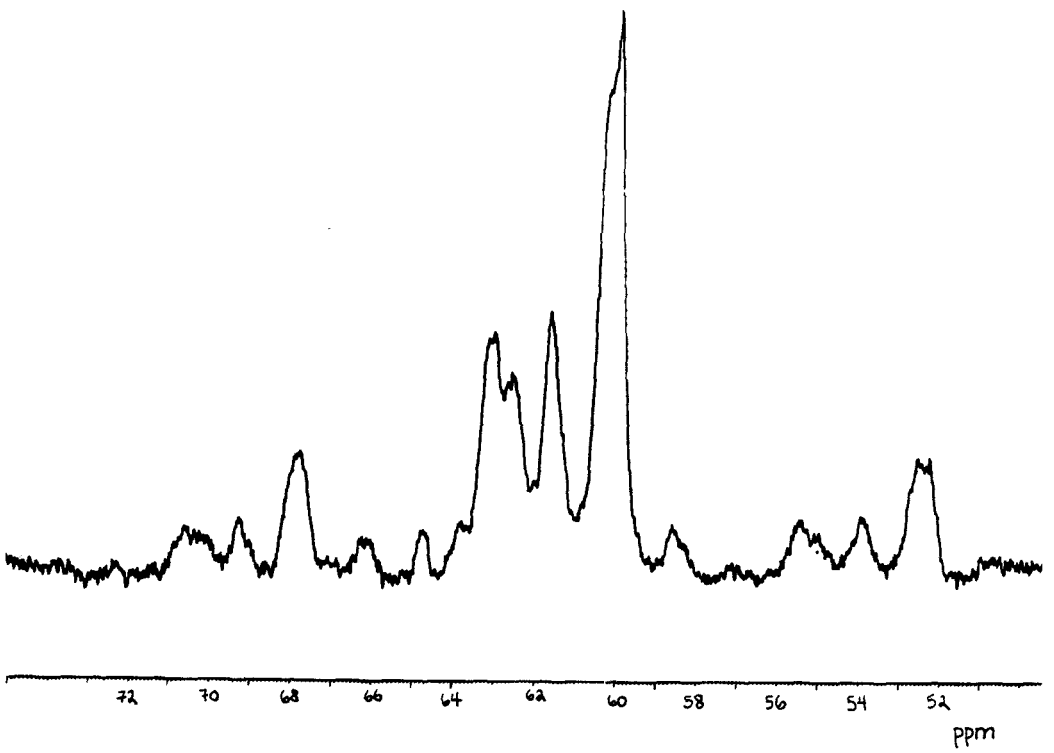

The constancy of the chemical-shift difference between the peaks at different magnetic field strengths indicates the presence of at least three phosphorous environments. The close spacing of the signals (as opposed to ~8 ppm between Pt_2 and BF_2Pt_2 signals) suggests that the phosphorous environments are not highly dissimilar. No matter what the substituents are, structures involving asymmetry between the two ML_4 fragments (e.g., all the substituents on one ML_4 half of the molecule, or more substituents on one side than on the other) should result in very different NMR chemical shifts for phosphorous and/or platinum nuclei on the two sides of the molecule.

^{195}Pt NMR

The ^{195}Pt spectrum of BF_2Pt_2, obtained only with the $BF_3(g)$ synthesis product, is shifted upfield from the spectrum of Pt_2 (Figure 4.6). The Pt_2 pattern, centered at -3567.3 ppm versus K_2PtCl_4 in D_2O, extends symmetrically over a 112 ppm range. The tallest peak of the BF_2Pt_2 pattern is at -3696.6 ppm, and the pattern extends asymmetrically from -3613 to -3755 ppm (142 ppm). The splitting pattern is encouragingly similar to that of Pt_2, but contains many extra peaks. Interpretation is complicated because correction of a large roll in the baseline rendered the relative peak heights questionable. The separation between the tallest peaks ranges from 2700 to 3100 Hz, consistent with the Pt-P couplings seen in the ^{31}P spectrum. The spectrum may consist of overlapping spectra from platinum atoms in slightly different environments; for example, the platinum chemical shift could be sensitive to the chair, boat, or twist-boat conformation of the ring containing BF_2^+'s.

Figure 4.6 ^{195}Pt NMR spectra of $[TBA]_4[Pt_2(P_2O_5)_4H_2(BF_2)_6]$ and $[TBA]_4[Pt_2(P_2O_5H_2)_4]$ at 107 MHz; 0.02, 0.05 M solutions in CD_3CN

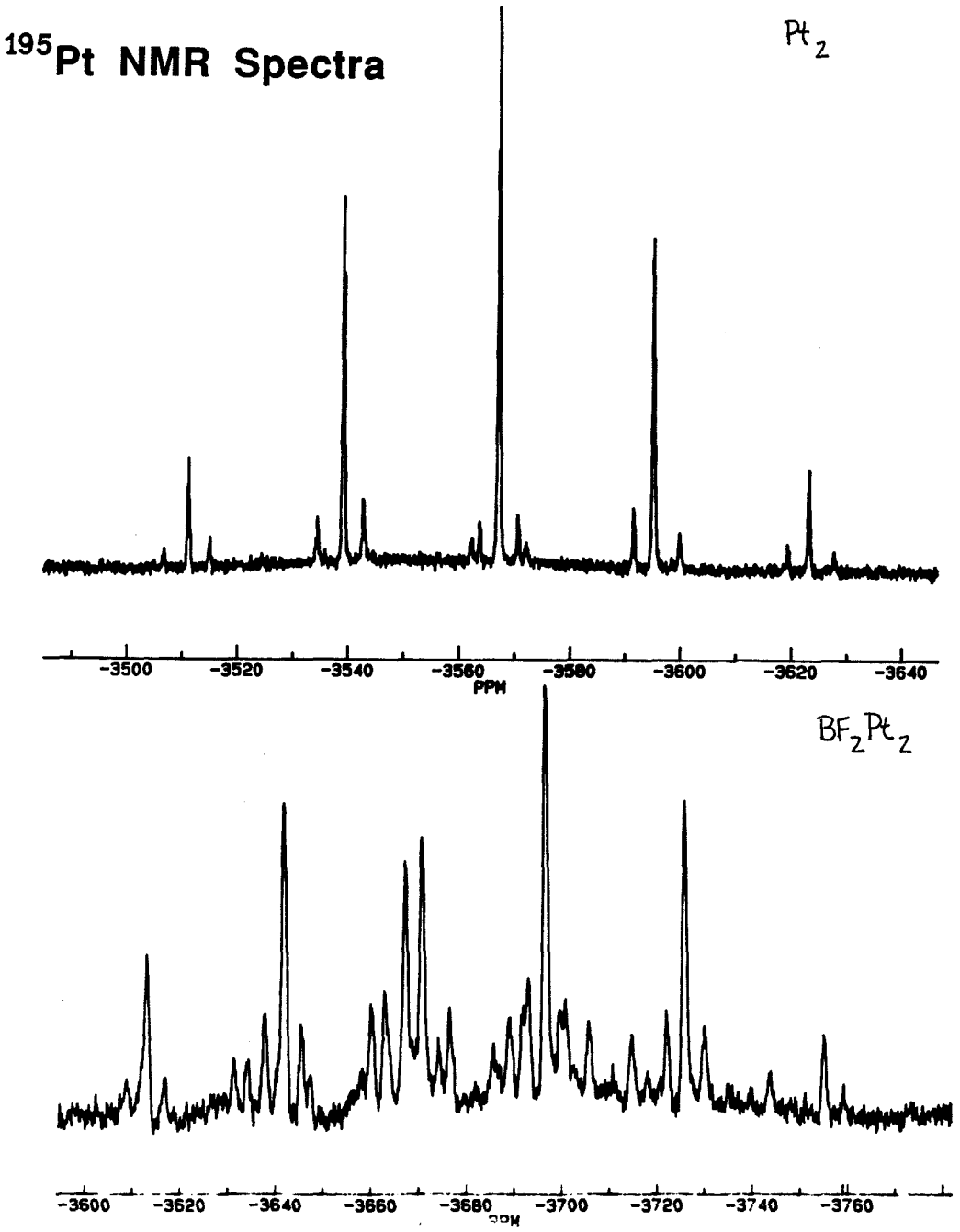

^1H NMR

Proton NMR spectra of $[TBA]_4BF_2Pt_2$ (Figure 4.7) exhibit a broad peak with a sample- or concentration-dependent chemical shift and relative integration in the 3.5-5.0 ppm region. The integration with respect to the TBA counterion protons was higher than expected for 2 ligand protons per metal complex, but such comparisons must be made with caution. The lack of observation of O-H stretches in the IR suggests that the NMR peak is not due to water; in addition, adding water to $[TBA]_4Pt_2$ produces a very broad signal at ~2.5 ppm.

Figure 4.7 ^1H NMR spectra of $[TBA]_4[Pt_2(P_2O_5)_4H_2(BF_2)_6]$ at 90 MHz, 0.04 M and 0.08 M solutions in CD_3CN

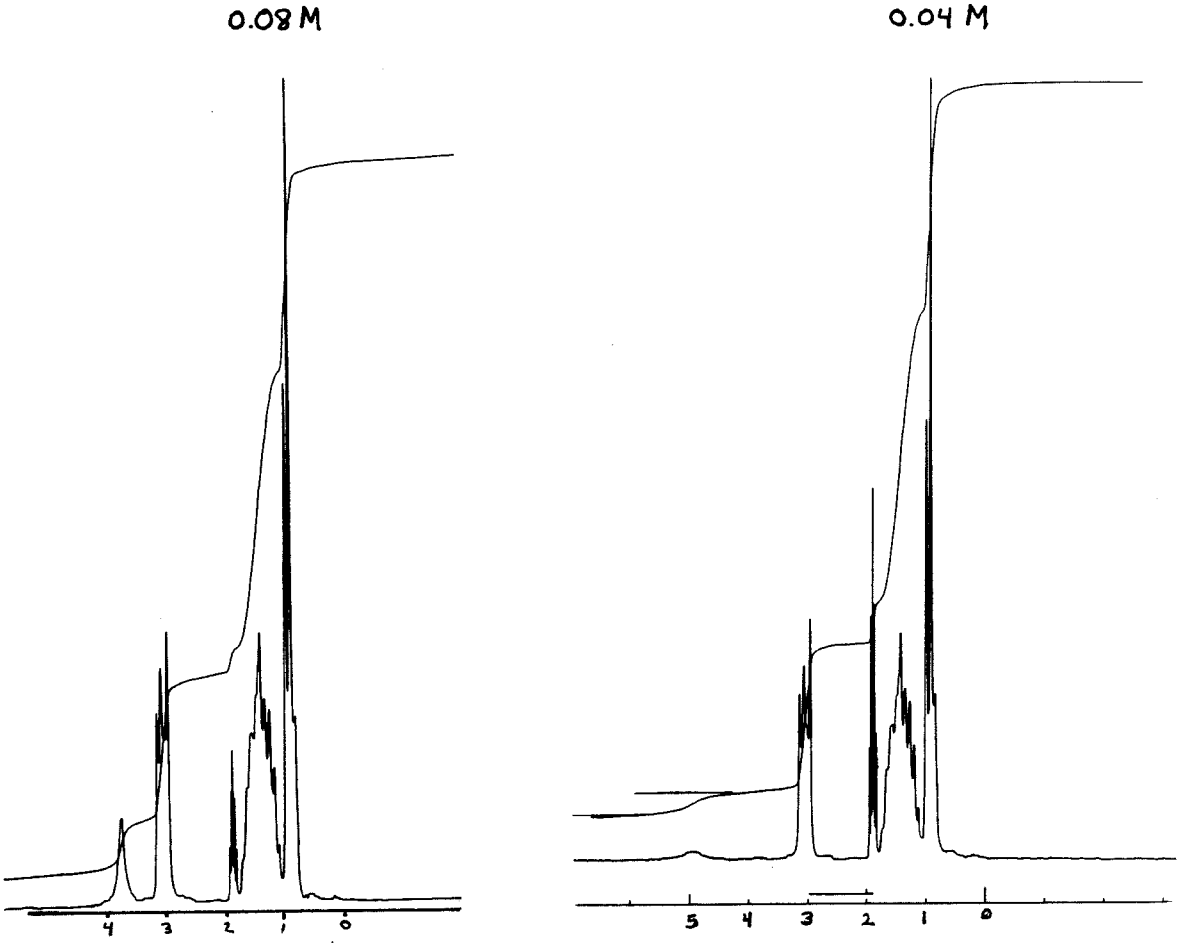

Electrochemistry

As shown in Figure 4.8, the oxidation waves for both Pt_2[25] and BF_2Pt_2 are highly irreversible in CH_3CN; however, the peak potential for oxidation of BF_2Pt_2 in the ground state is shifted +750mV relative to Pt_2. No reduction wave is observed for either complex at room temperature, but a low-temperature cyclic voltammagram of Pt_2 in acetonitrile exhibits a nearly reversible reduction wave at -2.4 V vs Ag wire (peak separation ~100mV) that integrates for approximately the same number of electrons as the irreversible oxidation wave that appears at ~1.0 V vs Ag wire in the low-T spectrum. The single measurement is not definitive; low-temperature electrochemical measurements on both systems merit future investigation. Substitution with electron-withdrawing BF_2^+ groups would be expected to make the complex harder to oxidize, as observed. This effect has been utilized in the metalla-β-diketonates, where substitution with the BF_2^+ group allows synthesis of some manganese complexes that are too sensitive to oxidation to be isolable as the H-bound precursors.[26] The lowered susceptibility of BF_2Pt_2 to air oxidation is also consistent with the observed potential difference between the two complexes.

Photophysics

Photophysical properties of the modified compound (Figure 4.9) are startlingly similar to those of Pt_2, considering the large change in electrochemistry. All electronic absorption bands in BF_2Pt_2 are blue-shifted relative to Pt_2, but the extinction coefficients and band shapes are virtually identical in both compounds. The phosphorescence emission maximum is shifted from 518 nm for Pt_2 to 512 nm for BF_2Pt_2. While the phosphorescence quantum yield is approximately the same in the two compounds (±20%), a large increase is observed in the fluorescence quantum yield of BF_2Pt_2. An excitation spectrum needs to be taken before this peak can be definitively assigned as fluorescence, however. The phosphorescence lifetime of 10 μs for $^3Pt_2^*$ is

Figure 4.8 Cyclic voltammograms of (a) $[TBA]_4[Pt_2(P_2O_5)_4H_2(BF_2)_6]$ and (b) $[TBA]_4[Pt_2(P_2O_5H_2)_4]$ in CH_3CN at room temperature and (c) $[TBA]_4[Pt_2(P_2O_5H_2)_4]$ in CH_3CN at -25 °C

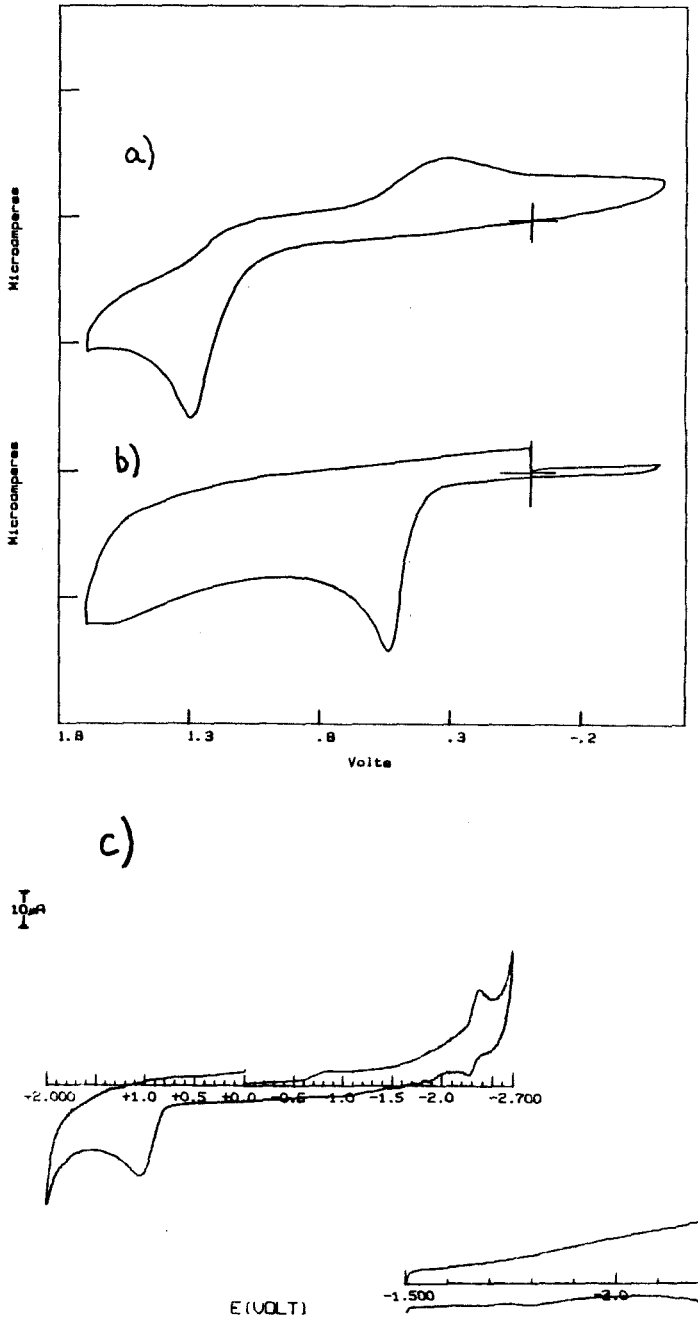

Figure 4.9 Comparative electronic absorption and emission spectra of a) $[TBA]_4[Pt_2(P_2O_5)_4H_2(BF_2)_6]$ and b) $[TBA]_4[Pt_2(P_2O_5H_2)_4]$ in degassed CH_3CN solution at room temperature.

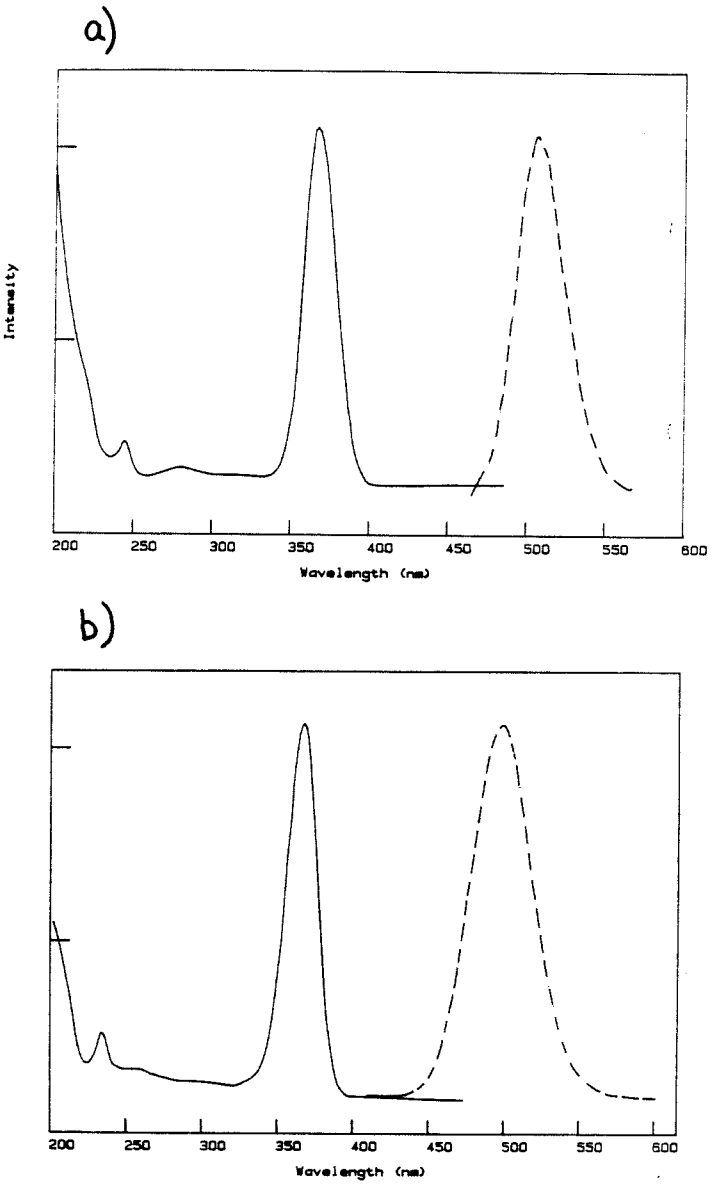

unchanged in the modified complex, indicating that no new vibrational deactivation modes have been introduced. In comparison, the Pt_2 analogue $Pt_2(pcp)_4^{4-}$ (pcp = methylene(bis)pyrophosphito) derivative exhibits slightly red-shifted absorption bands and blue-shifted phosphorescence emission. The lifetime of the triplet state of $Pt_2(pcp)_4^{4-}$ is reduced to 55 ns, however. [27]

Figure 4.10 shows comparative MO levels for the two species. The spacings between levels in the BF_2Pt_2 diagram were obtained by making band assignments for BF_2Pt_2 based on an earlier interpretation of the Pt_2 spectrum.[19] The $d\sigma^*$ HOMO level of BF_2Pt_2 was then placed 0.75 eV lower than that of Pt_2, as indicated by electrochemistry. Qualitatively, the metal-centered orbitals have moved down in energy, consistent with decreased electron density on platinum. The fact that the $d_{x^2-y^2}$ level moves down less than the other metal orbitals reflects the greater ligand field of the BF_2-substituted ligands. Enhancement of the π-accepting ability of the pyrophosphito ligands by the electron-withdrawing BF_2 groups causes stronger backbonding and a shortened Pt-P bond, which in turn results in stronger sigma interactions between the ligand and metal. This well-documented effect[28] overrides the decreased energy of the sigma donor levels of the BF_2-substituted pyrophosphito ligands, and results in a stronger bonding interaction between $d_{x^2-y^2}$ and the ligand orbitals (this produces a higher-lying sigma antibonding "$d_{x^2-y^2}$" orbital). The extra lowering of the π symmetry $d_{xz,yz}$ levels can be rationalized in terms of a better energy match between the metal orbitals and empty π-acceptor ligand orbitals of the BF_2-substituted complex.

Figure 4.10 Relative placement of selected molecular orbitals for $[TBA]_4[Pt_2(P_2O_5H_2)_4]$ and $[TBA]_4[Pt_2(P_2O_5)_4H_2(BF_2)_6]$

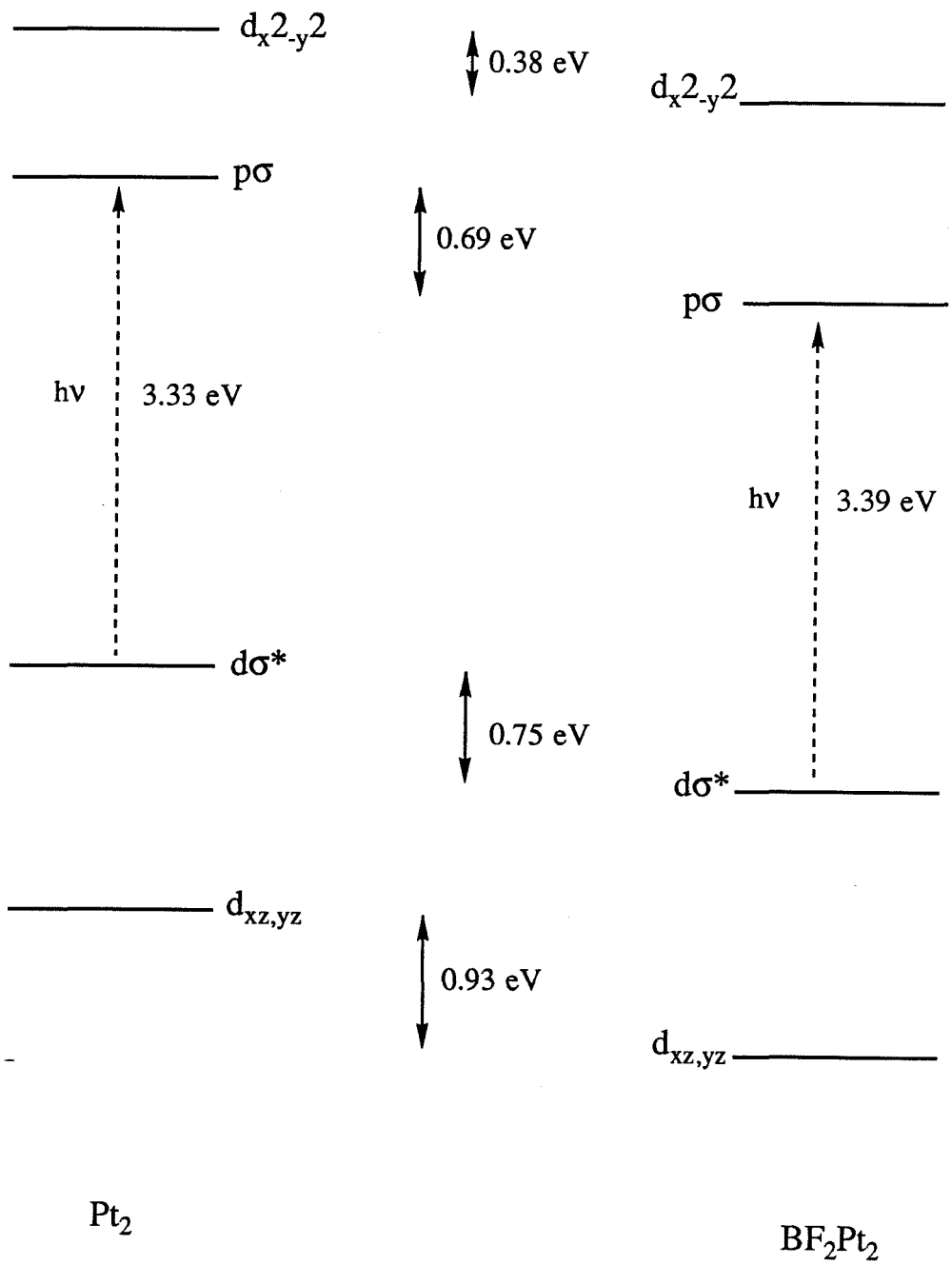

Conclusions

Chemical precedent and ^{19}F NMR evidence indicate BF_2^+ substitution for H^+ in the new molecule, and analytical results are consistent with the presence of 6 BF_2^+. The H-atoms in the parent are presumed to bridge oxygens on neighboring ligands; BF_2^+'s are expected to do the same. The possibility of slow establishment of equilibrium in solutions of the original product between less and more substituted molecules is ruled out by the stable, reproducible shifts observed in the electrochemistry, IR and UV-Vis absorption and emission spectroscopy. The ^{31}P NMR suggests a symmetric arrangement of the 6 substituents between the two Pt fragments. The three structures shown in the introduction emerge as most likely for a complex containing 6 BF_2^+ substituents; any or all could be correct.

The six-membered rings in the ligands of the three possible structures can also exist in several conformations. Fluorine NMR spectra of samples synthesized by different methods indicate that the conformations in the 6 membered rings and/or relative locations of the substituents may be determined during synthesis and remain unaltered over time in solution.

BF_2Pt_2 provides an unprecedented opportunity to study the role played by steric and electronic factors in ground- and excited-state reactivity of the d^8 dimers. The similarities in lifetime, energy, quantum yield and $d\sigma^*p\sigma$ character of the triplet excited states of Pt_2 and BF_2Pt_2 are truly remarkable. The major differences between the two molecules consist of the change in hydrophilicity and steric bulk around the axial sites and the dramatic shift in ground-state oxidation potentials. The ability to change one variable at a time and monitor the experimental outcome is a much sought-after goal in science. The Pt_2/BF_2Pt_2 system provides an unusually close approximation of that situation.

References

1. Brown, N. M. D. and Bladon, Peter *J. Chem. Soc. (A)* 526 (1969). "Spectroscopy and Structure of (1,3-Diketonato)boron Difluorides and Related Compounds."

2. Morgan, G. T. and Tunstall, R. B. *J. Chem. Soc.* 1497 (1932). "Researches on Residual Affinity and Coordination. Part XXI. Boron β-Diketone Difluorides."

3. Vollhardt, Peter C. *Organic Chemistry* (W. H. Freeman & Co., New York, 1987). p. 1014.

4. Massey, A. G. *Advan. Inorg. Chem. Radiochem.* **10**, 1 (1967). "The Halides of Boron."

5. Dilthey, W., Eduardof, F. and Schumacher, F. J. *Justus Liebig's Ann. Chem.* **344**, 300 (1906).

6. Beaulieu, William B.; Rauchfuss, Thomas B. and Roundhill, D. Max *Inorg. Chem.* **14**, 1732 (1975). "Interconversion Reactions between Substituted Phosphinous Acid-Phosphonito Complexes of Platinum(II) and their Capping Reactions with Boron Trifluoride-Diethyl Etherate."

7. Duncan, J. Andrew S.; Stephenson, T. Anthony; Walkinshaw, Malcolm D.; Hedden, David and Roundhill, D. Max *J. Chem. Soc. Dalton. Trans.* 801 (1984). "Rhodium-(I) and -(III) Complexes of Diphenylphosphinous Acid and Secondary Phosphites."

8. Lukehart, C. M. and Warfield, L. T. *Inorg. Chem.* **17**, 201 (1978). "Reactions of Coordinated Molecules. 13. The Reaction of the Rhenium Tetracarbonyl Metalloacetylacetone Complex with Boron Trihalides."

9. Lukehart, Charles M. *Acc. Chem. Res.* **14**, 109 (1981). "Metalla-β-diketones and Their Derivatives."

10. Lukehart, Charles M. *Adv. Organomet. Chem.* **25**, 45 (1986). "Metalla-Derivatives of β-Diketones."

11. Schrauzer, Gerhard N. *Chem. Ber.* 1438 (1962). "Reaktion von Bis-dimethylglyoxim-nickel mit Borverbindungen."

12. Berry, David Eric; Bushnell, Gordon William and Dixon, Keith Roger *Inorg. Chem.* **21**, 957 (1982). "Coordination Chemistry of Bridging PR_2-O Ligands. Crystal and Molecular Structure of Bis(dimethyl phosphito)difluoroborato)platinum(II), $[Pt((P(OMe)_2O)_2BF_2)_2]$."

13. Roundhill, Stephanie G. N. and Roundhill, D. Max *Acta. Cryst.* **B38**, 2479 (1982). "Structure of {[Bis(dimethyl phosphito)difluoroborato]-O,O'}chloro-(triethylphosphine)platinum(II);$PtCl\{[OP(OMe)_2]_2BF_2\}PEt_3$."

14. Booth, Harold S. and Martin, Donald R. *Boron Trifluoride and Its Derivatives* (John Wiley and Sons, Inc., New York, 1949).

15. Rice, S. F., Ph. D. Dissertation (California Institute of Technology, 1982) and Chapter 1, Ref.14.

16. Fox, Lucius S., Ph. D. Dissertation (California Institute of Technology, 1989).

17. Gordon, Arnold J. and Ford, Richard A. *The Chemist's Companion: A Handbook of Practical Data, Techniques, and References* (John Wiley and Sons, Inc., New York, 1972).

18. Stein, Paul; Dickson, Mark K. and Roundhill, D. Max *J. Am. Chem. Soc.* **105**, 3489 (1983). "Raman and Infrared Spectra of Binuclear Platinum(II) and Platinum(III) Octaphosphite Complexes. A Characterization of the Intermetallic Binding."

19. Stiegman, Albert E.; Rice, Steven F.; Gray, Harry B. and Miskowski, Vincent M. *Inorg. Chem.* **26**, 1112 (1987). "Electronic Spectroscopy of d^8-d^8 Diplatinum Complexes. $^1A_{2u}(d\sigma^*\rightarrow p\sigma)$, $^3E_u(d_{xy},d_{yz}\rightarrow p\sigma)$, and $^{3,1}B_{2u}(d\sigma^*\rightarrow d_{x^2-y^2})$ Excited States of $Pt_2(P_2O_5H_2)_4^{4-}$."

20. Pinto, M. A. Filomena Dos Remedios; Sadler, Peter J.; Neidler, Stephen; Sanderson, Mark R.; Subbiah, Arun and Kuroda, Reiko *J. Chem. Soc., Chem. Comm.* 13 (1980). "A Novel Di-Platinum(II) Octaphosphite Complex Showing Metal-Metal Bonding and Intense Luminescence; a Potential Probe for Basic Proteins. X-Ray Crystal and Molecular Structure."

21. Emsley, J. W.; Phillips, L. and Wray, V. *Fluorine Coupling Constants* (Pergamon Press, Oxford, 1977).

22. Dungan, Claude H. and Van Wazer, John R. *Compilation of Reported ^{19}F NMR Chemical Shifts* (Wiley-Interscience, New York, 1970).

23. Bowlus, H. and Nieuwland, J. A. *J. Am. Chem. Soc.* **53**, 3835 (1931). "The Action of Boron Fluoride on Organic Compounds."

24. Hoard, J. L., Geller, S. and Owen, T. B. *Acta. Cryst.* **4**, 405 (1951). "Structures of Molecular Addition Compounds. V. Comparison of Four Related Structures."

25. Kim, Joon; Fan, Frank F.; Bard, Allen J.; Che, Chi-Ming and Gray, Harry B. *Chem. Phys. Lett.* **121**, 543 (1985). "Electrogenerated Chemiluminescence. On the Electrogenerated Chemiluminescence (ECL) of Tetrakis(pyrophosphito)diplatinate(II), $Pt_2(P_2O_5H_2)_4^{4-}$."

26. Lukehart, C. M. and Warfield, L. T. *J. Organomet. Chem.* **187**, 9 (1980). "Reactions of Coordinated Molecules XXIII. The Preparation of Several Metalla-β-diketonate Complexes of Boron."

27. King, Christopher; Yin, Yan; McPherson, Gary L. and Roundhill, D. Max *J. Phys. Chem.* **93**, 3451 (1989). "Medium Effects on the Absorption and Emission Spectra and on the Triplet State Lifetimes of the Tetrakis[μ-methylenebis(phosphonito)]-diplatinate(II) Chromophore."

28. Gray, H. B. *Electrons and Chemical Bonding* (Benjamin, New York, 1964). p. 198.

Chapter 5. Comparative Reactivity of Pt_2 and BF_2Pt_2

Introduction

In analogy to the products of oxidative addition to Pt_2 described in the introductory chapter, a series of $BF_2Pt_2X_2$ (X=Cl, Br, I, H) complexes have been prepared. The products are identified on the basis of the similarity of their electronic absorption spectra to the spectra of the corresponding Pt_2X_2 complexes. Additionally, $BF_2Pt_2Cl_2$ has been characterized by ^{31}P and ^{19}F NMR spectroscopy, and the Pt-H IR bond stretch for $BF_2Pt_2H_2$ has been measured. The second portion of the chapter deals with comparative excited state reactivities of BF_2Pt_2 and Pt_2. Reductive quenching and H-atom transfer quenching results are presented and discussed.

Experimental:

Syntheses The axial dibromide and diiodide derivatives of BF_2Pt_2 were thermally prepared by adding a few drops of bromine or a few crystals of iodine to solutions of 0.10 g $[TBA]_4BF_2Pt_2$ in a minimum (1-5 mL) of acetonitrile.[3] To make $BF_2Pt_2Cl_2$, $Cl_{2(g)}$ was bubbled through a solution of 0.10 g BF_2Pt_2 in 3-4 mL of CH_2Cl_2. The solids were precipitated and washed with diethyl ether. Crude yields were 70% for $BF_2Pt_2I_2$, 55% for $BF_2Pt_2Br_2$ and 78% for $BF_2Pt_2Cl_2$. When dilute solutions of Br_2 in CH_3CN were added to BF_2Pt_2 or Pt_2 in CH_3CN, fairly stable intermediates absorbing at 271 nm and 274 nm, respectively, were observed in the UV-Vis spectra. A complex growth and decay of several intermediates was observed upon addition of dilute I_2 to acetonitrile solutions of Pt_2 and BF_2Pt_2.

Photochemical generation of the axially substituted Pt(III) complexes was performed using 370-nm narrow-band irradiation of freeze-pump-thaw degassed acetonitrile solutions of $[TBA]_4BF_2Pt_2$ containing the hydrogen or halogen atom donor. A photolysis cell was placed in front of a 1000 W lamp (approximately 10^{18} photons/minute) for the stipulated length of time. Temperature was not controlled, but a water filter was employed to absorb IR light from the lamp, and placement of the entire apparatus in a hood ensured constant air flow over the irradiated sample.

Approximately complete conversion of a $2.2x10^{-4}$ M solution of BF_2Pt_2 to $BF_2Pt_2H_2$, as monitored by changes in UV-Vis absorbance, was achieved with a 0.05 M solution of α-secphenethyl alcohol after 7 minutes' photolysis. For the IR experiment, an acetonitrile solution $1.4x10^{-3}$ M in BF_2Pt_2 and $7.2x10^{-3}$ M in α-secphenethyl alcohol reached approximately 60% conversion to the dihydride after 35 minutes photolysis. Irradiation of a solution 0.016 M in 1,2-dibromopropane (Matheson, Coleman, Bell) and $2.2x10^{-4}$ M in $[TBA]_4Pt_2$ produced complete disappearance of the absorbance of the starting platinum complex within 3 minutes. Three new bands appeared at 334, 298, and 272 nm; with continued photolysis the absorbance of the 272 nm band increased and then began to decrease. When the sample was allowed to sit in the dark, the 272 nm band continued to decrease; after 24 hours the spectrum exhibited peaks only at 300 and 336 nm. Irradiation of a 0.017 M 1,2-dichloropropane (Eastman) and $3x10^{-4}$ M $[TBA]_4Pt_2$ solution for a total of two hours produced an increase in the absorbance at 274 nm and an approximately 30% decrease in the absorbance at 366 nm; storage in the dark for 24 hours produced no changes in the spectrum.

Instrumentation NMR data were obtained as described in Chapter 4. UV-Vis absorption spectra were measured on Shimadzu UV-260 and Cary spectrometers; the emission spectrometer is described in Chapter 4. Quenching experiments were carried out using a frequency-tripled, Q-switched Nd:YAG laser at 355 nm; 8 ns fwhm; power

set at .01 W at 10 Hz. The power was measured using an Ophir laser-power meter. Raman shifting of the 355 nm line to ~400 nm was accomplished by passing the focused laser line through a methanol solution. Unfortunately, the 300 cm glass tube used to hold the methanol was not long enough, and the focused laser beam damaged the faces. Other difficulties were encountered in trying to filter out the residual 355 nm light; a very sharp cutoff filter is needed that does not fluoresce or get chewed up by the laser.

Quenching Studies N,N,N'N'-tetramethylphenylenediamine (TMPD), N,N,N',N'-tetramethylbenzidine (TMBD), and triphenylamine (TPA) quenchers were purchased from Aldrich, reagent grade, and purified by sublimation. Diphenylamine was purchased from Matheson, Coleman and Bell, and recrystallized from a hot toluene/pentane mixture. The 10-methylphenothiazine (MPTZ) was obtained from Pfaltz and Bauer; the white, crystalline solid was not purified. The sublimed amines were briefly handled in air during transfer to a storage vial; solutions were made up in volumetric flasks purged with argon. For the intensity-quenching experiment, transfers of TMPD aliquots to the quenching cell were performed in a glove bag under argon. Alcohol and hydrocarbon substrates were prepared as described in Chapter 2.

Pt_2 and BF_2Pt_2 concentrations ranged from 1-3 $x10^{-4}$ M in the lifetime-quenching experiments. For the intensity-quenching experiment with TMPD, the concentration of BF_2Pt_2 was $6x10^{-4}$ M, so that appreciable phosphorescence emission intensity could be seen when the complex was excited into the triplet absorption. An Oriel 436 nm (#5645) interference filter was used to select the excitation line. Quenching data measured using two different samples of BF_2Pt_2 complex fit on the same Stern-Volmer plot; all rates were measured using samples synthesized with $BF_3(g)$, rather than $BF_3{\cdot}OEt_2$. For methanol, the quenching rate was obtained as an upper limit by simply measuring the lifetime in neat quencher. Partial hydrolysis of BF_2Pt_2 to Pt_2 was observed in the UV-Vis spectrum taken after the laser measurement.

Results and Discussion

I. Axially Substituted Binuclear Pt(III) Complexes

Because of the instability of BF_2Pt_2 in H_2O, the non-photochemical syntheses of the dihalide complexes were modified from reported procedures by the use of non-aqueous solvents.[1, 2, 3] Like Pt_2H_2, $BF_2Pt_2H_2$ is readily formed by narrow-band photolysis of BF_2Pt_2 with benzyl alcohol or α-sec-phenethyl alcohol.[4] Photochemical reaction of BF_2Pt_2 with 1,2-dichloropropane[5] produced only about 30% apparent conversion to the dichloride. Irradiation of BF_2Pt_2 in the presence of 1,2-dibromopropane produced fast conversion to a species that appeared to be the dibromide and one that corresponded to the intermediate (271 nm absorption) observed in the thermal reaction with Br_2. Over time or continued irradiation, the original photogenerated spectrum changed to one with bands only at 336 and 300 nm, corresponding to the thermally prepared $BF_2Pt_2Br_2$.

UV-Vis spectra

The comparative UV-Vis data in Table 5.1 illustrates the changes in absorption bands of $BF_2Pt_2X_2$ compounds relative to the analogous bands in Pt_2X_2 (Figures 5.1-5.4). A comparison of the bis(acetonitrile) adduct of Pt_2 (λmax=211 nm) with the other Pt_2X_2 complexes led Che *et al.* to conclude that the electronic transition in the dihalide complexes originally assigned as $d\sigma \rightarrow d\sigma^*$ contains a significant amount of ligand-to-metal charge transfer (LMCT) character.[2, 6] Assuming that the interaction between the metal centers (i.e., the splitting of the $d\sigma$ and $d\sigma^*$ levels) is unperturbed by substitution of BF_2^+ groups on the ligands, LMCT bands should redshift as the metal orbitals are lowered by the electron withdrawing BF_2^+ substituents (Figure 5.5). Observation of the opposite trend for the dibromide, dichloride and dihydride complexes is consistent with a larger splitting between $d\sigma$ and $d\sigma^*$ in the BF_2Pt_2, caused by

stronger metal-metal interactions. Better overlap of the lower energy metal orbitals in BF_2Pt_2 with the axial ligand sigma orbitals would also raise the (d)σ^* orbital and produce the observed shifts to higher energy. The latter departure from the simple LMCT picture is supported by the shift in Pt-H IR stretch from 1830 cm^{-1} in Pt_2H_2 to 1940 cm^{-1} in $BF_2Pt_2H_2$, which indicates a stronger Pt-H bond in the BF_2^+-substituted complex.

Table 5.1 Electronic absorption spectra of axial dihalide and dihydride complexes of $[TBA]_4[Pt_2(P_2O_5H_2)_4]$ and $[TBA]_4[Pt_2(P_2O_5)_4H_2(BF_2)_6]$

X_2	Pt_2X_2 λmax (nm)	BF_2Pt_2 λmax (nm)	ΔE (cm^{-1})	ΔE (eV)
H_2	314	294	+2166	+0.27
Cl_2	285	276	+1144	+0.14
	349	321	+2499	+0.31
Br_2	308	301	+755	+0.094
	349	336	+1109	+0.14
I_2	338	364	-2113	-0.26
	438	455	-853	-0.11

Low-temperature spectroscopy on the series of new compounds should shed some light (hehheh) into the nature of the structural changes introduced by the BF_2^+ substituents. Low-temperature absorption and emission spectroscopy in combination with Raman studies will provide valuable information on the Pt-Pt stretching frequency, and by inference, the length and strength of the metal-metal bond in these Pt(III) complexes.

Figure 5.1 Electronic absorption spectra of a) $[TBA]_4[Pt_2(P_2O_5H_2)_4Cl_2]$ and b) $[TBA]_4[Pt_2(P_2O_5)_4H_2(BF_2)_6Cl_2]$

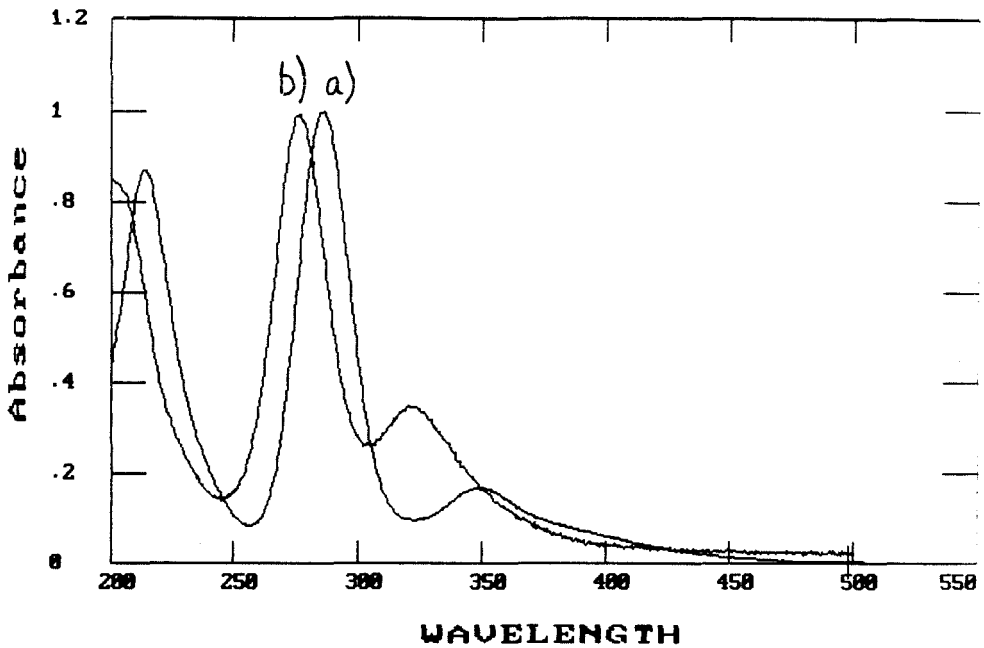

Figure 5.2 Electronic absorption spectra of a) $[TBA]_4[Pt_2(P_2O_5H_2)_4Br_2]$ and b) $[TBA]_4[Pt_2(P_2O_5)_4H_2(BF_2)_6Br_2]$

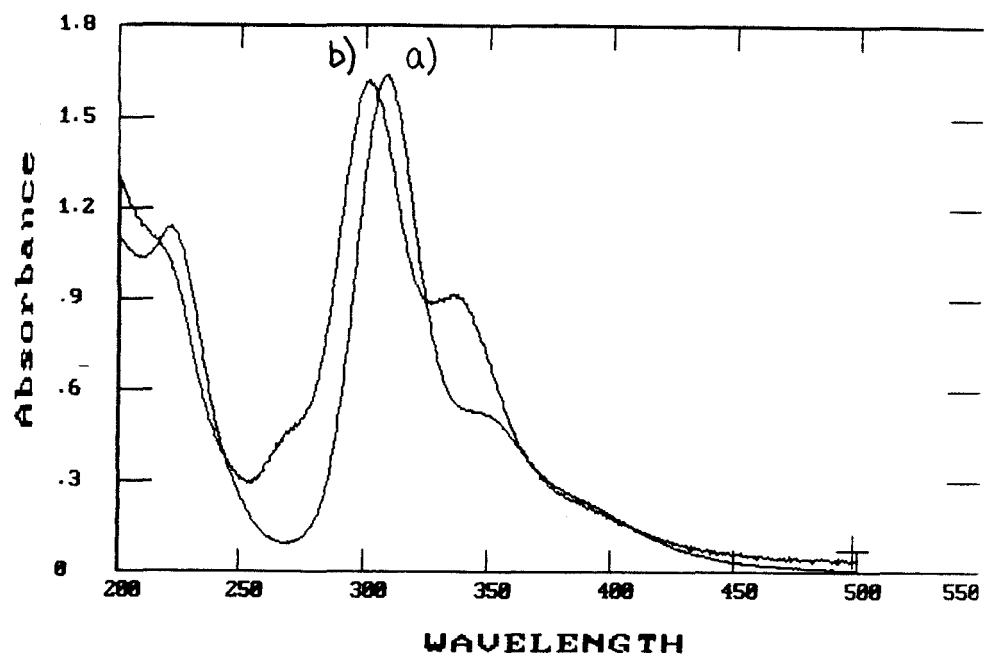

Figure 5.3 Electronic absorption spectra of a) $[TBA]_4[Pt_2(P_2O_5H_2)_4I_2]$ and b) $[TBA]_4[Pt_2(P_2O_5)_4H_2(BF_2)_6I_2]$

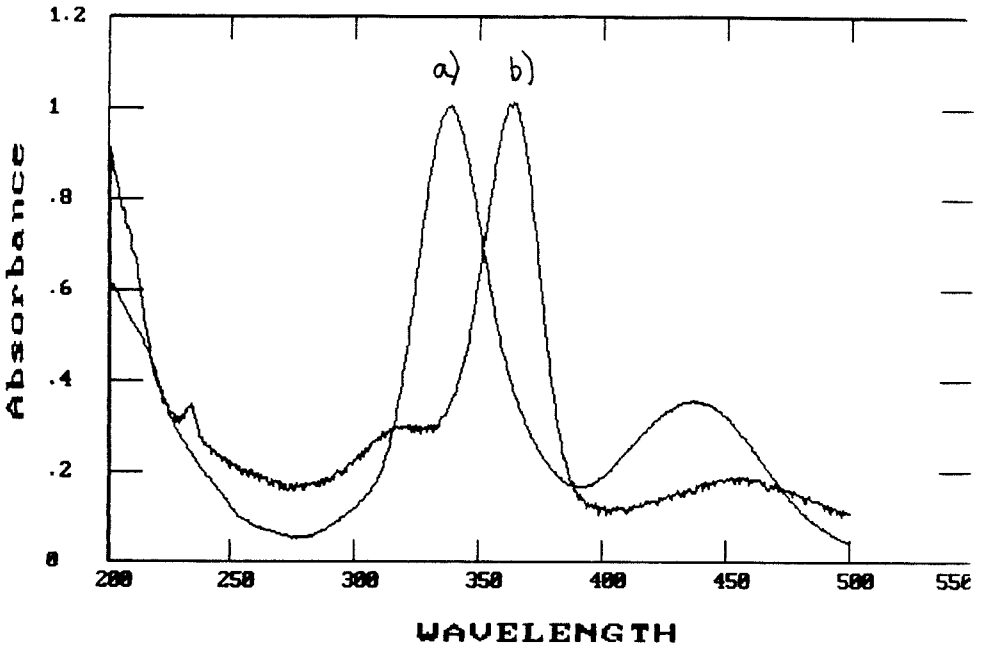

Figure 5.4 Electronic absorption spectra of a) $[TBA]_4[Pt_2(P_2O_5H_2)_4H_2]$ and b) $[TBA]_4[Pt_2(P_2O_5)_4H_2(BF_2)_6H_2]$

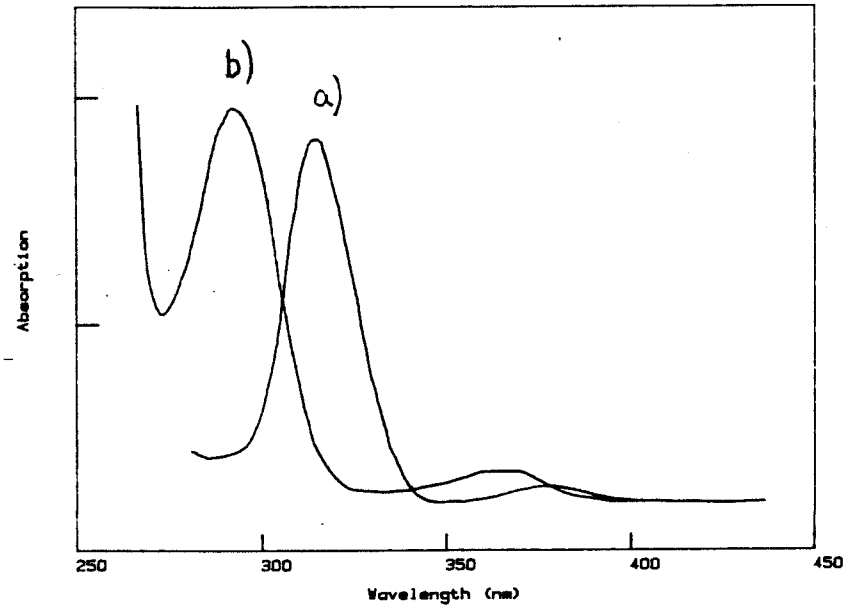

Figure 5.5 Molecular orbital picture of electronic transitions in axial dihalide and dihydride complexes of $[TBA]_4[Pt_2(P_2O_5H_2)_4]$ and $[TBA]_4[Pt_2(P_2O_5)_4H_2(BF_2)_6]$

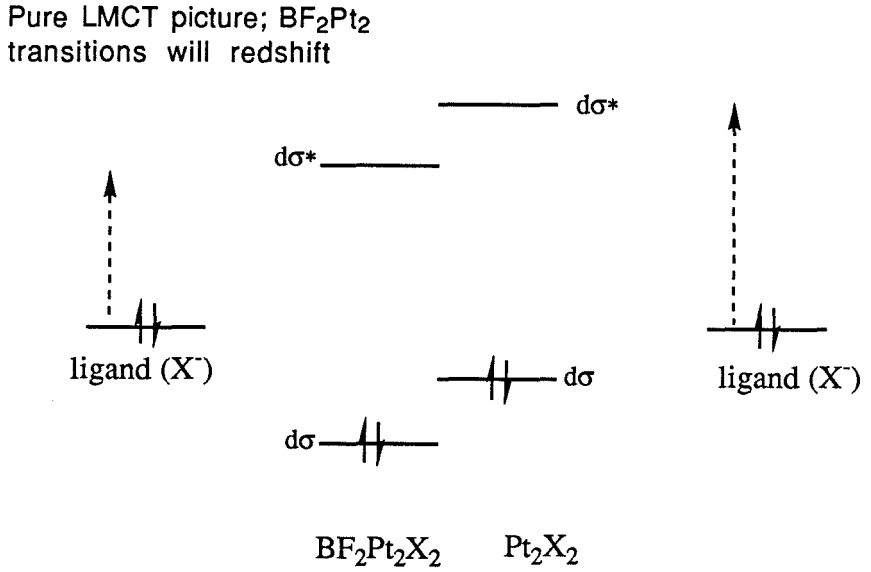

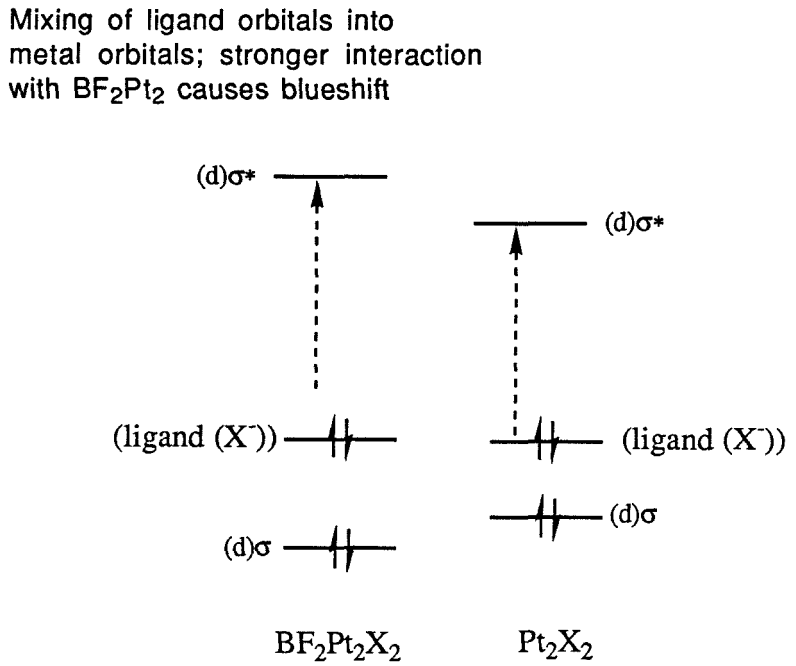

NMR

The ^{31}P NMR spectrum of $BF_2Pt_2Cl_2$ (Figure 5.6) is similar to that of Pt_2Cl_2,[1] but shifted upfield by a slightly greater amount (~15 ppm) than BF_2Pt_2 is shifted from Pt_2 (~10 ppm). The spacing of the platinum satellites (an approximation of $^1J_{Pt\text{-}P}$) is reduced from 3100 Hz in BF_2Pt_2 to 2200 Hz in $BF_2Pt_2Cl_2$; the same effect is observed for Pt_2 (δ=68 ppm, $^1J_{Pt\text{-}P}$ = 3075 Hz) and Pt_2Cl_2 (δ=28 ppm, $^1J_{Pt\text{-}P}$ = 2085 Hz). Three sets of Pt_2Cl_2-like signals separated by 2.5 ppm appear in the $BF_2Pt_2Cl_2$ spectrum, consistent with the three less well-resolved signals observed in the ^{31}P NMR of the parent BF_2Pt_2. (See Chapter 4.)

The ^{19}F NMR spectra of $BF_2Pt_2Cl_2$ and BF_2Pt_2 are shown for comparison in Figure 5.7. One set of fluorine residues in $BF_2Pt_2Cl_2$ shifts upfield relative to its position in the BF_2Pt_2 molecule, remains sharp, and displays a new set of peaks separated by 60 Hz. The other signal becomes less well resolved, but its chemical shift range does not change from that of BF_2Pt_2. The fluorine NMR spectrum of $BF_2Pt_2Cl_2$ provides support for the interpretation of the fluorine NMR of BF_2Pt_2. The fluorine that points toward the axial sites, defined as F_a, is expected to be sensitive to the occupation of the axial sites by chlorine atoms; hence its chemical shift changes more dramatically than that of F_b, which points out toward the P-O-P bridge.

Figure 5.6 ^{31}P NMR spectra of a) $[TBA]_4[Pt_2(P_2O_5)_4H_2(BF_2)_6]$ and b) $[TBA]_4[Pt_2(P_2O_5)_4H_2(BF_2)_6Cl_2]$ in CD_3CN solution at 36 MHz

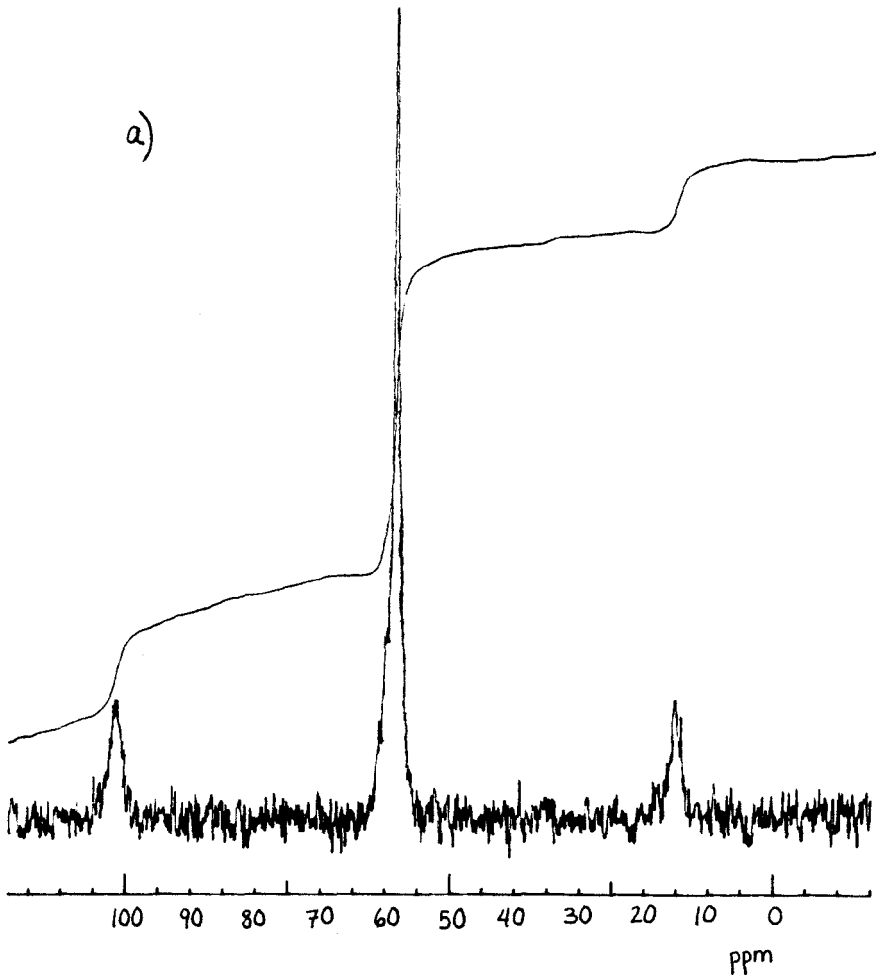

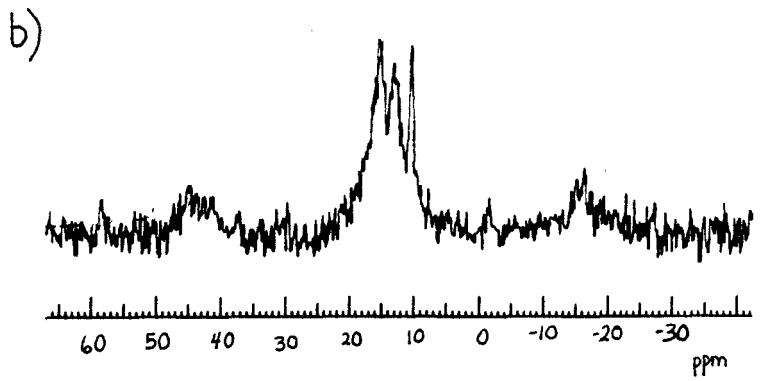

Figure 5.7 ^{19}F NMR spectra of a) $[TBA]_4[Pt_2(P_2O_5)_4H_2(BF_2)_6]$ and b) $[TBA]_4[Pt_2(P_2O_5)_4H_2(BF_2)_6Cl_2]$ in CD_3CN solution at 84 MHz

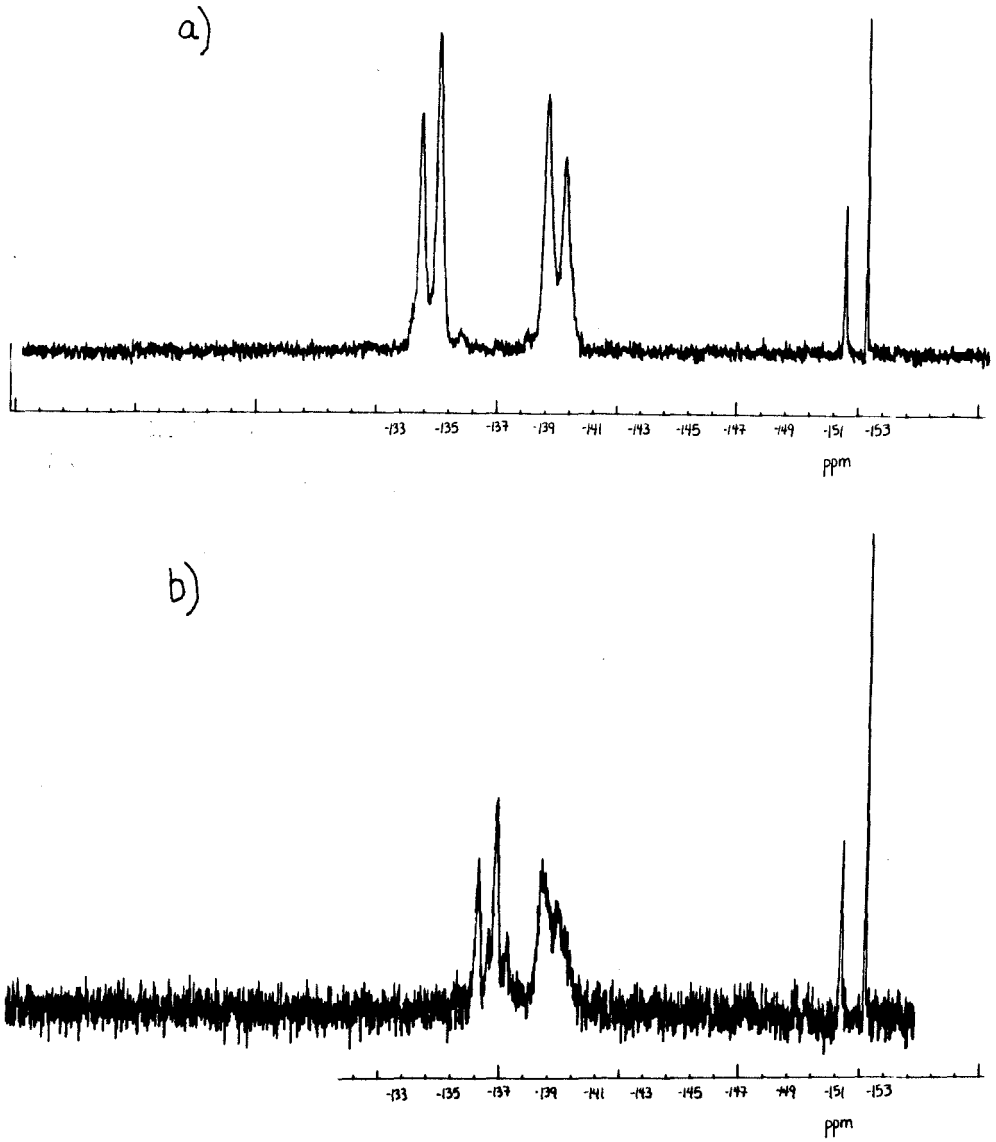

Axial Ligand Loss

UV-Vis spectra of $BF_2Pt_2Cl_2$ taken immediately after synthesis, after four weeks in a closed vial, after dissolution in CD_3CN and 2 hours in the nmr tube, and after sitting on glass wool in air and room light are shown in Figure 5.8. The relative magnitudes of the spectral changes indicate that some decomposition takes place over time even in the solid, but that the process is accelerated by dissolution and exposure to air and/or light. The decomposition apparently involves loss of Cl and also loss of BF_2^+, with at least partial return to Pt_2. More work to discover the nature of the instability is clearly warranted. Photolysis of Pt_2X_2 in methanol regenerates Pt_2,[7] and photochemical release of the axial ligands is well known;[5, 8] perhaps a similar mechanism applies here.

Figure 5.8 Electronic absorption spectra showing decomposition of $[TBA]_4[Pt_2(P_2O_5)_4H_2(BF_2)_6Cl_2]$ over time

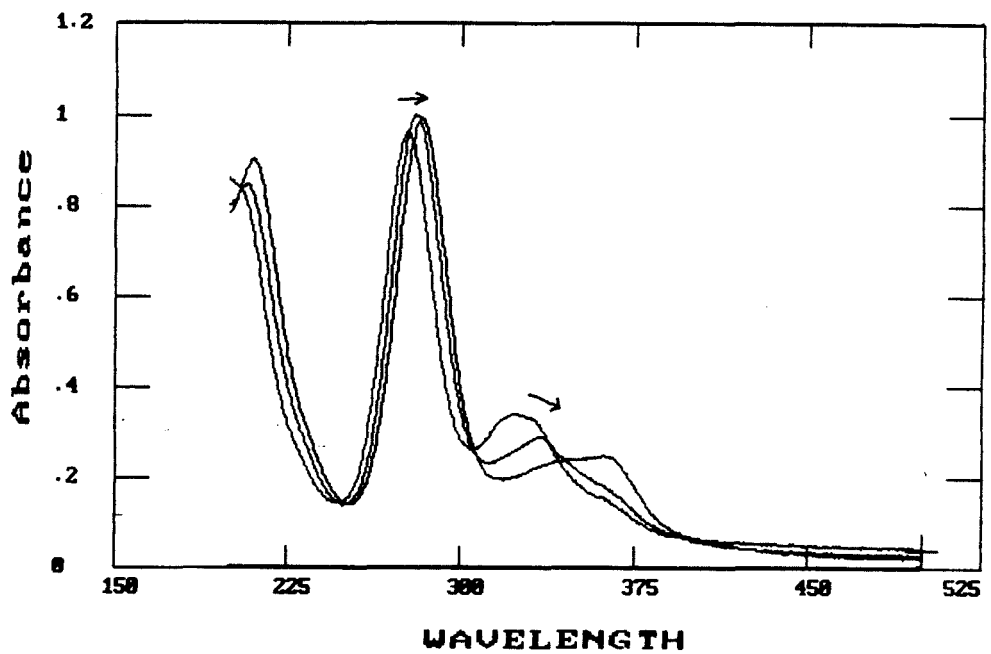

II. Excited State Reactivity

Reductive Quenching

BF_2Pt_2 is expected to be easier to reduce than Pt_2 by extrapolation from the observed oxidation behavior; no ground-state reduction wave is observed for either complex in acetonitrile. Since previous work indicates that $^3Pt_2^*$ is a relatively good excited-state oxidant, $^3BF_2Pt_2^*$ should be a sensational excited-state oxidant! Reductive quenching of $^3Pt_2^*$ has been measured using aromatic amine quenchers with oxidation potentials spanning the range 0.3 to 1.2V vs NHE. Separate quenching rate measurements in methanol[9, 10] agree well, but Vogler[11] reports that no quenching is observed in acetonitrile using even the readily oxidized compound N,N,N',N'-tetramethlyphenylenediamine (TMPD). Partly in an attempt to resolve this discrepancy, and partly because both the quencher oxidation potentials[9, 12, 13] and the Pt_2 and BF_2Pt_2 measurements are reported in acetonitrile, comparative reductive quenching of BF_2Pt_2 and Pt_2 has been investigated in acetonitrile. The present work uses a series of uncharged aromatic amines similar to that used by the previous workers. Experimental difficulties are discussed at some length, followed by experimental results in Table 5.2 and Figure 5.10, and a discussion of the results.

Stern-Volmer plots for lifetime quenching of $^3Pt_2^*$ with TMPD and TMBD curve downward at high quencher concentrations; i.e., the lifetime does not decrease as rapidly as expected (Figure 5.9). In fact, the lifetime of Pt_2^* actually increases as the "quencher" 10-methylphenothiazine is added! Relatively bad fits of the supposedly exponential decay of the emission signal with time were also observed, especially at high quencher concentrations. All three amines exhibit absorbance tails in the 350 nm region that can be excited by the 355 nm laser line.[14, 15] Raman shifting of the 355 nm laser line to 400 nm allows selective excitation of only the Pt_2 absorption. Two points obtained with different 10-methylphenothiazine concentrations using 400 nm excitation show the expected decrease in lifetime, with a calculated quenching rate of

roughly $10^6\ M^{-1}s^{-1}$. Unfortunately, the homemade Raman shifter proved to be self-destructive, so the 400 nm laser excitation was not available for use with any of the other quenchers.

Figure 5.9 Stern-Volmer plot for quenching of the triplet excited state of $[TBA]_4[Pt_2(P_2O_5H_2)_4]$ with TMPD

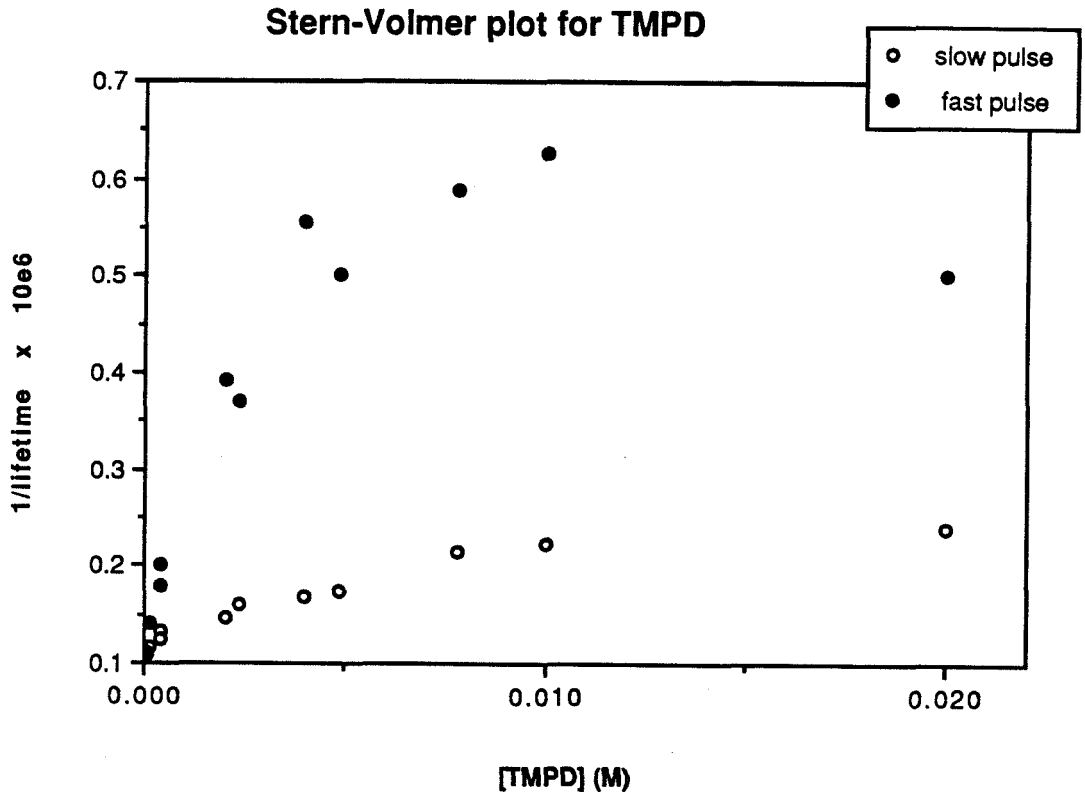

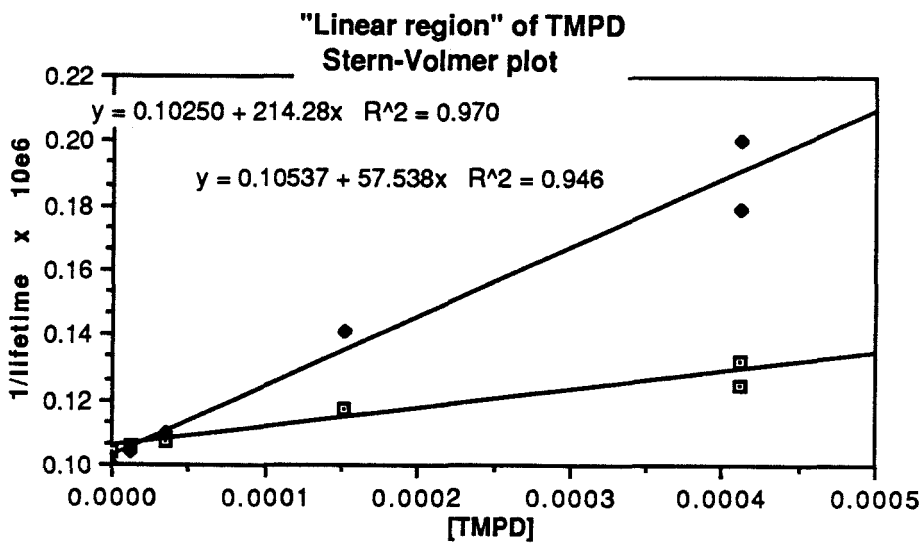

The triplet energies of the amines chosen for the study are above the triplet energy of Pt_2, so energy transfer quenching of $^3Pt_2^*$ by the amines is expected to be negligible.[16] Energy transfer in the reverse direction could be a problem, however. Phosphorescence lifetimes on the order of milliseconds have been observed for aromatic amines.[17] Formation of Pt_2^* by energy transfer from the excited organic triplet state to ground state Pt_2 would artificially increase the apparent lifetime of the triplet excited state of the metal dimer, thereby decreasing the apparent quenching rate. When the quencher is in low concentrations, the absorption tail at 355 nm has negligible intensity, and the lifetime decreases linearly with quencher concentration, as expected. However, as the quencher concentration increases, the lifetime appears to stop decreasing, presumably because the quencher is being excited and replenishing $^3Pt_2^*$ by energy transfer at the same time it is quenching $^3Pt_2^*$ by electron transfer. No experimental details are reported in Vogler's paper[11], but it is possible that if only a single, high concentration of TMPD was used to measure the quenching, the lifetime and/or emission intensity of Pt_2^* would not appear to be quenched!

A second complication in the studies is that $^3Pt_2^*$ lifetimes measured in the presence of amine quencher change significantly as the pulse repetition rate of the laser is varied from 1 to 10 Hz. Slower quenching rates are observed when the pulse repetition rate of the laser is decreased. In addition to decreasing the power and stability of the laser, lowering the pulse repetition rate allows the sample a longer time to relax between pulses. (Although the effects on the lifetime did not seem to be levelling off, repetition rates slower than 1 Hz were not employed because of the very great laser instability at the low repetition rates.) If the reduced Pt_2 and oxidized amine species (abbreviated R_3N^+) generated by reductive quenching do not recombine before the next laser pulse, $^3Pt_2^*$ created in the second pulse will rapidly reduce R_3N^+. Even if very small amounts of R_3N^+ persist in solution,[18] the combination of reductive and oxidative quenching of the metal excited state could result in an observed quenching rate much

faster than that expected for reductive quenching alone. Although a fast recombination rate is expected for the oppositely charged Pt_2^{5-} and R_3N^+ species, flash experiments[10] indicate that decay of the absorption attributed to R_3N^+ (R3N+ = N,N-dimethylaniline, TMBD, TMPD) can take up to milliseconds after the flash.

While the first problem discussed can be readily avoided in emission intensity quenching experiments by exciting into the triplet absorption at 436 nm, the second problem is impossible to avoid in intensity-quenching measurements, since continuous excitation will produce a steady-state concentration of R_3N^+. Observation of R_3N^+ in the flash experiment indicates that Pt_2 does oxidize aromatic amines. The previously observed rates[9, 10] for reductive quenching of the metal excited state, however, and by extrapolation the previously calculated excited-state reduction potential of 1.3 V for Pt_2, may be artificially high.

Because of the experimental difficulties detailed above, few well-determined electron transfer rates have been obtained in the present study. The points in parentheses in Figure 5.10 denote rates that are based on changes in $^3Pt_2^*$ or $^3BF_2Pt_2^*$ lifetime using only one or two different quencher concentrations. Nevertheless, two important observations can be made. For $^3Pt_2^*$, reductive quenching rates for which experimental complications have been partially eradicated are generally slower than those previously observed. The change of solvent from methanol to acetonitrile may be an important factor in this difference;[10] alternatively, the interference from R_3N^+ discussed above may be important. The very slow quenching rate of $^3Pt_2^*$ with diphenylamine -- essentially no quenching observed -- remains a mystery.

The second observation is that $^3BF_2Pt_2^*$ does react much faster than $^3Pt_2^*$ with quenchers expected to undergo oxidation. The greater excited-state oxidizing power of BF_2Pt_2 is consistent with the presence of electron-withdrawing substituents. The

observed differences in reductive quenching rates measured in the two systems are roughly consistent with the expected 750 mV shift in ground-state reduction potential. Thus, for any Pt_2 reduction potential >-2.75 V, the ground-state reduction wave of BF_2Pt_2 should be within the solvent window of acetonitrile. The conspicuous absence of such a wave may indicate that the difference in excited-state reduction potentials is actually less than 750 mV, so that both reduction potentials are hidden behind the solvent window. Another possibility is that electron transfer to BF_2Pt_2 and/or Pt_2 across the electrode surface is kinetically impeded in some way, perhaps by the repulsion between a tetraanion and a negatively biased electrode surface, so neither wave is observed at the thermodynamically expected potential. The latter observation is the easiest to reconcile with Nagle's estimate of the reduction potential of $^3Pt_2^*$ as 1.3 V, which suggests that the ground state reduction wave should be observed at ~-1.2 V vs NHE, a value well within the solvent window of acetonitrile.

Figure 5.10 Quenching rate constants versus oxidation potentials for aromatic amine quenchers with the triplet excited states of $[TBA]_4[Pt_2(P_2O_5H_2)_4]$ and $[TBA]_4[Pt_2(P_2O_5)_4H_2(BF_2)_6]$

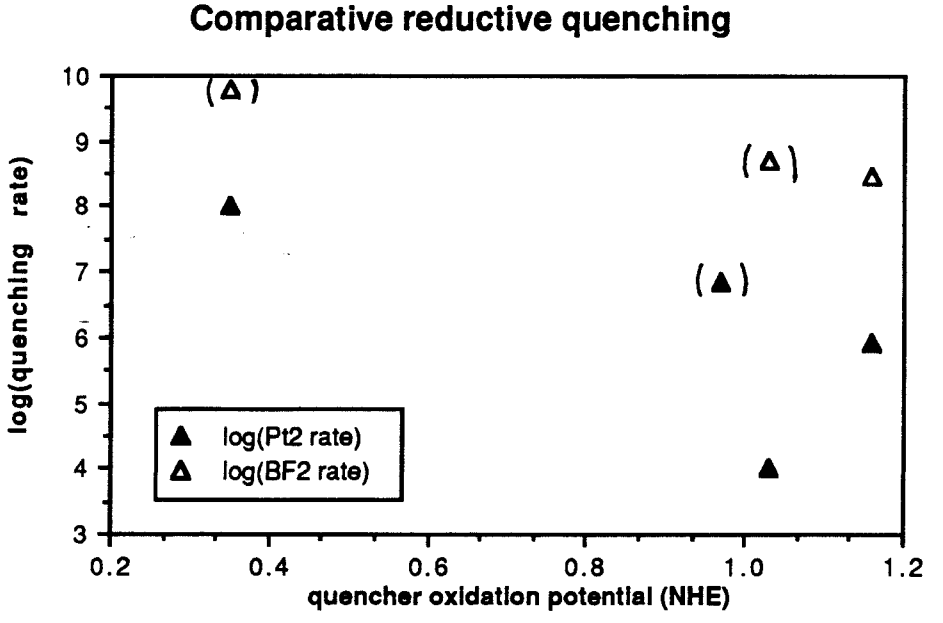

Table 5.2 Rates of reductive quenching of the triplet excited states of $[TBA]_4[Pt_2(P_2O_5H_2)_4]$ and $[TBA]_4[Pt_2(P_2O_5)_4H_2(BF_2)_6]$ correlated with quencher oxidation potentials

Quencher	Oxidation Potential (vs. NHE)	BF_2Pt_2 Quenching Rate ($M^{-1}s^{-1}$)	Pt_2 Quenching Rate ($M^{-1}s^{-1}$)	Nagle's Pt_2 Quenching Rate ($M^{-1}s^{-1}$)
TMPD	0.35	($6x10^9$ a)	$1x10^8$	$1.2x10^{10}$
TMBD	0.60			$3.0x10^9$
DMT	0.95			$3.9x10^7$
10-MPTZ	0.97		($7x10^6$)	
DMA	1.02			$1.2x10^7$
DPA	1.03	($5x10^8$)	$\sim10^4$	
TPA	1.16	$3x10^8$	$8x10^5$	$1.5x10^6$

parentheses ≡ rate was determined by two or three point lines

a ≡ intensity quenching, 436 nm excitation

TMPD=N,N,N',N'-tetramethyl-phenylenediamine

TMBD=N,N,N',N'-tetramethyl-benzidine

DMT=dimethyltoluidine

10-MPTZ=10-methylphenothiazine

DMA=dimethylaniline

DPA=diphenylamine

TPA=triphenylamine

H-atom Transfer

In contrast to the large differences observed in electron transfer reactivity, quenching rates for $^3Pt_2^*$ and $^3BF_2Pt_2^*$ with a given H-atom donor are almost all within a factor of 5 (Table 5.4, Figure 5.11).[3] Neither metal complex reacts consistently faster than the other with the H-atom donors studied. $^3Pt_2^*$ exhibits faster quenching rates with the benzylic alcohols. With the hydrocarbons and small aliphatic alcohols, $^3BF_2Pt_2^*$ is quenched faster.

The overarching similarity of H-atom transfer rates in the two systems supports the postulation of a relatively pure H-atom abstraction mechanism. As described in Chapter 2, the initial stages of atom transfer reactions may involve orbital interactions similar to those involved in electron transfers. The relative reactivity of BF_2Pt_2 and Pt_2 with H-atom donors provides a sensitive probe of this first interaction. Because of the differences in excited-state redox properties of the two metal complexes, comparisons of their H-atom transfer quenching rates allow a qualitative assessment of how much electron transfer character is involved in the transition state for H-atom abstraction with a given type of substrate. The strength of the Pt-H bond being formed may also influence relative reaction rates with the two metal systems. The fact that the metal hydride stretch in the IR is at higher energy for the BF_2Pt_2 complex indicates that removing a hydrogen atom from the dihydride is more difficult for $BF_2Pt_2H_2$ than for Pt_2H_2. This does not necessarily mean that it will be more difficult to remove an H-atom from the monohydride $BF_2Pt_2H\cdot$ than from $Pt_2H\cdot$, but it is a reasonable postulate. A third possible source of differences in reactivity is the altered steric situation around the axial site.

Table 5.3 Rates of H-atom transfer quenching of the triplet excited states of $[TBA]_4[Pt_2(P_2O_5H_2)_4]$ and $[TBA]_4[Pt_2(P_2O_5)_4H_2(BF_2)_6]$, correlated with the C-H bond strengths for the H-atom donor quenchers

Substrate	Bond Strength (kcal/mole)	Reference	Pt_2 Quenching Rate ($M^{-1}s^{-1}$)	BF_2Pt_2 Quenching Rate ($M^{-1}s^{-1}$)
cumene	84.4±1.5	31	$5x10^3$	$9x10^3$
ethylbenzene	85.4±1.5	31	$1.4x10^4$	$3.7x10^4$
toluene	88.0±1	31	$4x10^3$	$1.4x10^4$
α-secphenethyl alcohol $PhC\underline{H}(OH)CH_3$	82.4±3	31	$1.8x10^6$	$2.3x10^5$
benzyl alcohol	85±3	31	$4x10^6$	$2.2x10^6$
sec-butanol	91±1	33	$9x10^3$	$4x10^4$
isopropanol	91±1	31	$4x10^3$	$9x10^4$

Figure 5.11 Quenching rate constants versus C-H bond strengths for H-atom donor quenchers with the triplet excited states of $[TBA]_4[Pt_2(P_2O_5H_2)_4]$ and $[TBA]_4[Pt_2(P_2O_5)_4H_2(BF_2)_6]$

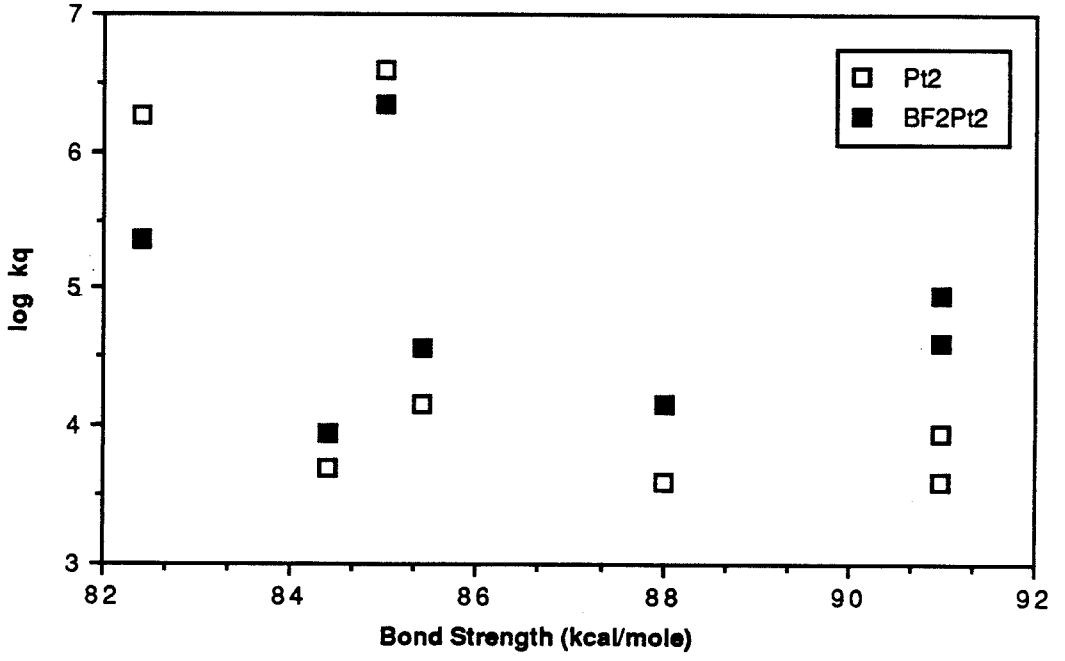

For the alcohol substrates, the oxidation and reduction potentials are expected to be too high and low, respectively, for the metal excited states to oxidize or reduce.[19] Observation of the large isotope effect (k_H/k_D=4) with α-secphenethyl alcohol and $^3Pt_2^*$ also indicates that the abstraction process for the benzylic alcohols involves a relatively pure H-atom transfer. In the absence of polar factors, a second possible reason for the differences in reactivity with alcohols is the strength of the bond being formed in the transition state. Since the Pt-H bond in BF_2Pt_2 is assumed to be stronger than the analogous bond in Pt_2, however, the faster reactivity of Pt_2 with the benzyl alcohols is apparently not due to the strength of the bond being formed.

In view of the H-atom transfer reactivity trends discussed in Chapter 3, the most likely reason for the slower reactivity of the benzyl alcohols with $^3BF_2Pt_2^*$ is the loss of hydrophilicity and increased steric bulk from BF_2^+ substitution around the axial site. The fast rates and correspondingly small entropies of activation for benzyl alcohol and α-secphenethyl alcohol suggest that the steric situation for those two alcohols with $^3Pt_2^*$ is very close to ideal; any perturbations will increase the entropic contribution to the transition-state barrier and slow the rate, as observed.

$^3BF_2Pt_2^*$ reacts faster with isopropanol than with sec-butanol, and $^3Pt_2^*$ reacts faster with sec-butanol than with isopropanol. This trend also makes sense in light of the discussions in Chapter 2. Addition of some steric bulk to the axial site in BF_2Pt_2 should help guide even the small isopropanol substrate toward the Pt center with the orientation necessary for efficient abstraction. As the alcohol gets larger, however, the combination of steric bulk on the substrate and on the metal complex results in a hindered approach of the substrate to the axial site, and thus a slower rate.

The faster quenching of $^3BF_2Pt_2^*$ relative to $^3Pt_2^*$ with the hydrocarbon quenchers is consistent with an initial interaction involving filled orbitals on the quencher and the low-lying hole in the dσ* orbital of the excited metal complex. Faster quenching of a better excited state oxidant by substrates that are easier to oxidize

suggests that electron transfer to the metal complex is a component of the quenching process for those substrates, and the hydrocarbons are known to have relatively low ionization potentials.[20] An isotope effect would be a useful probe of how much electron transfer character is actually involved; a larger effect would be expected for $^3Pt_2^*$ than for $^3BF_2Pt_2^*$, since the quenching process with the latter complex presumably involves more electron transfer character. The observed difference in rates between the two metal complexes for the hydrocarbon substrates is also consistent with the assumed differences in Pt-H bond strength. The effectively "teflon-coated" axial site of BF_2Pt_2 should be more appealing to the less polar substrates as well, although the increased steric bulk may hinder the approach of the more substituted hydrocarbons.

Conclusion

A Pt_2 complex modified by substitution of 6 electron-withdrawing BF_2^+ groups for 6 H^+ moieties in the ligands exhibits a variety of thermal and photochemical reactivity analogous to that observed with Pt_2. Reductive quenching measurements with a series of aromatic amines demonstrate that $^3BF_2Pt_2^*$ is a much better excited state oxidant than $^3Pt_2^*$, as expected from the observed shift in peak potential for oxidation of the ground state. The new complex exhibits the same reactivity with H-atom donor substrates as the parent complex, including formation of an axial dihydride complex. H-atom transfer rates with the two metal complexes are similar overall, but $^3BF_2Pt_2^*$ is more active toward hydrocarbons and small aliphatic alcohols than $^3Pt_2^*$. Both steric and electronic factors are important in determining the rates of reaction with the two complexes. An ability to predict the relative reactivities of the two complexes is rapidly developing, and a firm basis has been set from which detailed mechanistic work on H-atom transfer in this novel inorganic system can be launched.

References

1. Che, Chi-Ming; Schaefer, William P.; Gray, Harry B.; Dickson, Mark K.; Stein, Paul B. and Roundhill, D. Max *J. Am. Chem. Soc.* **104**, 4253 (1982). "Novel Binuclear Platinum (III) Diphosphite Complexes."

2. Che, Chi-Ming; Butler, Leslie G.; Grunthaner, Paula J. and Gray, Harry B. *Inorg. Chem.* **24**, 4662 (1985). "Chemistry and Spectroscopy of Binuclear Platinum Diphosphite Complexes."

3. The thermal syntheses and UV-Vis absorption spectra of the dihalide complexes were performed jointly with Bob Sweeney; he also measured the quenching rates for cumene, ethylbenzene, and sec-butanol.

4. Harvey, Erica L.; Stiegman, Albert E.; Vlcek, Antonin, Jr. and Gray, Harry B. *J. Am. Chem. Soc.* **109**, 5233 (1987). "Dihydridotetrakis(pyrophosphito(2-))-diplatinate(III).

5. Marshall, Janet L.; Steigman, Albert E. and Gray, Harry B. in *Excited States and Reactive Intermediates* (ed. Lever, A.B.P.) (American Chemical Society, Washington, D.C., 1986), pp.166-176.

6. Che, Chi-Ming; Mak, Thomas C. W.; Miskowski, Vincent M. and Gray, Harry B. *J. Am. Chem. Soc* **108**, 7840 (1986). "Binuclear Platinum (III) Complexes. Preparation, Structure, and $d\sigma d\sigma^*$ Spectrum of $[Bu_4N]_2[Pt_2(P_2O_5H_2)_4(CH_3CN)_2]$."

7. Che, Chi-Ming; Lee, Wai-Man and Cho, Kar-Cheong *J. Am. Chem. Soc.* **110**, 5407 (1988). "Photochemistry of Platinum(III,III) Pyrophosphite Complexes. Efficient Photochemical Reduction of $[Pt_2(pop)_4X_2]^{4-}$ to $[Pt_2(pop)_4]^{4-}$ in Methanol."

8. Bryan, Samuel A.; Dickson, Mark K. and Roundhill, D. Max *Inorg. Chem.* **26**, 3878 (1987). "Synthesis, Reactivity, Kinetics, and Photochemical Studies on Tetrakis(μ-pyrophosphito)diplatinate(II) and Dihalotetrakis(μ-pyrophosphito)diplatinate(III) Complexes. Comparison of the Substitution Mechanisms of the Diplatinum(III) Complexes with those of Monomeric Platinum(II) and Platinum(IV) Compounds."

9. Heuer, William B.; Totten, Mark D.; Rodman, Gary S.; Hebert, Eric J.; Tracy, Henry J. and Nagle, Jeffrey K. *J. Am. Chem. Soc.* **106**, 1163 (1984). "Electron-Transfer Reactions and Luminescent Quantum Yield of the Triplet Excited State of Tetrakis[μ-diphosphito(2-)-P,P']diplatinate(II)."

10. Peterson, John R. and Kalyanasundaram, K. *J. Phys. Chem.* **89**, 2486 (1985). "Energy and Electron Transfer Processes of the Lowest Triplet Excited State of Tetrakis(diphosphito)diplatinate(II)."

11. Vogler, Arnd and Kunkely, Horst *Agnew.Chem.Int.Ed.Engl.* **23**, 316 (1984). "Electrochemiluminescence of Tetrakis(diphosphonato)diplatinate(II)."

12. Nocera, Daniel G.; Gray, Harry B. *J. Am. Chem. Soc.* **103**, 7349 (1981). "Electron-Transfer Chemistry of the Luminescent Excited State of Octachlorodirhenate(III)"

13. Bock, C. R.; Connor, J. A.; Gutierrez, A. R.; Meyer, Thomas J.; Whitten, D. G.; Sullivan, B. P. and Nagle, J. K. *J. Am. Chem. Soc.* **101**, 4815 (1979). "Estimation of Excited-State Redox Potentials by Electron-Transfer Quenching. Application of Electron-transfer Theory to Excited-State Redox Processes."

14. *The Sadtler Handbook of Ultraviolet Spectra* (1979). pp. 104, 218, 352

15. Berlman, Isadore B. *Handbook of Fluorescence Spectra of Aromatic Molecules* (Academic Press, New York, 1965). pp. 100

16. Measured quenching rates should be significantly increased by energy transfer contributions only when the electron transfer rates are also slow; potential problems should be minimized because the quenchers expected to have the slowest electron transfer rates also have the highest triplet energies. (See Ref. 12.)

17. Adams, J. Elaine; Mantulin, W. W. and Huber, J. Robert. *J. Am. Chem. Soc.* **95**, 5477 (1973). "Effect of Molecular Geometry on Spin-Orbit Coupling of Aromatic Amines in Solution. Diphenylamine, Iminobibenzyl, Acridan, and Carbazole."

18. Kalyanasundaram points out that photoionization of the triplets of TMPD and TMBD produces some $TMPD^+$ and $TMBD^+$ in methanol solution (Ref. 10).

19. Bard, A. J., ed. Encyclopedia of Electrochemistry of the Elements (Marcel Dekker, New York, 1982). (See Chapter 2, Ref. 35.)

20. Turro, N. J. *Modern Molecular Photochemistry* (Benjamin/Cummings, Menlo Park, NJ, 1978).